Master Thesis

Optically Transparent Flax Fiber Reinforced Composite Materials

Ioannis Zygouris

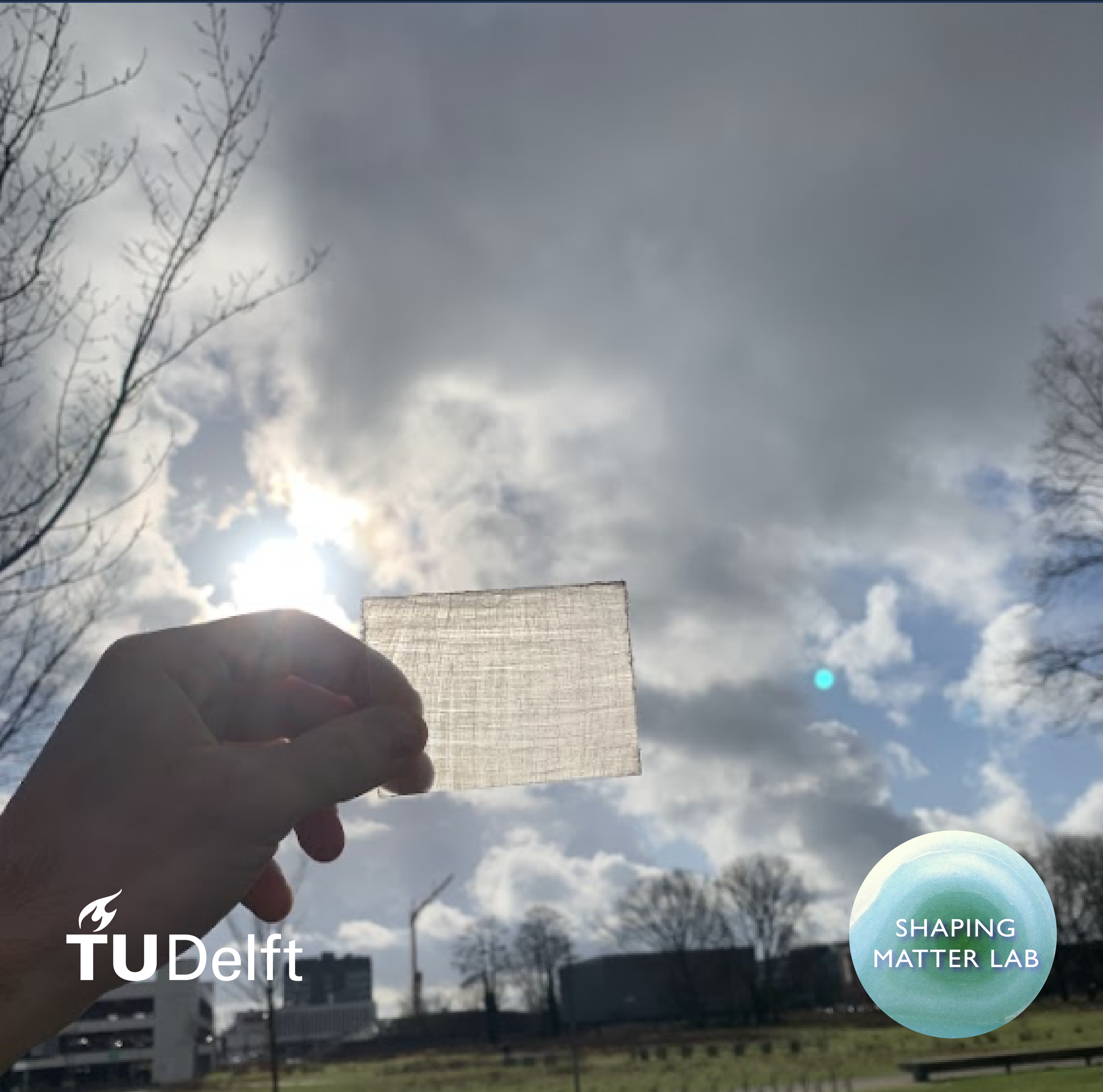

Master Thesis

Optically Transparent Flax Fiber Reinforced Composite Materials

by

Ioannis Zygouris

to obtain the degree of MSc in Materials Science and Engineering
at the Delft University of Technology
to be presented publicly in April, 2024

Thesis committee:

Supervisors:	Prof. Georgy Filonenko
	Prof. Kunal Masania
Place:	3me Faculty and AE faculty, Delft
Project Duration:	April, 2023 - April, 2024
Student number:	5508061

3me Faculty · Delft University of Technology

Abstract

Transparent Natural Fiber Composite Materials may pose a more environmentally friendly alternative regarding energy efficiency and low CO_2 emissions in contrast to traditional composites, exhibiting transparency for future smart building or photovoltaic applications. The present study involved a research effort for the development of a lightweight flax fiber-reinforced composite material, which will exemplify high optical transparency. A detailed focus is conducted, on minimizing light absorption phenomena with delignification methods of flax fibers, eliminating light scattering via a *Refractive Index Matching* procedure between the reinforcement and the polymer matrix and via fiber modifications which tackle several issues such as enhancing the imperfect interphase between the hydrophilic reinforcement and the hydrophobic matrix, or providing finer polymer impregnation of the fibers. Acetylation, nitric acid, or TEMPO-oxidation treatments that modify the fiber's nature and morphology are implemented to tackle these obstacles. *Transparent Flax Fiber Reinforced Composites* of 35-45 % fiber volume fraction were fabricated with wet-lamination and hot press forming techniques, indicating a maximum total light transmittance of approximately 70% (at low thickness) and 56-58% (at high thickness), depending on the fiber modification implemented. Regarding mechanical properties, a maximum specific flexural strength of 153 $MPa/(g/(cm^3))$ and a specific flexural stiffness of 11.95 $GPa/(g/(cm^3))$ was achieved for these materials. The transparent FFCMs showed comparable values of total light transmission correlated to reference materials like GFRPs or other natural fiber-reinforced composite materials, with similar volume fractions, signifying the success of achieving high optical transparency.

Contents

Nomenclature

List of Abbreviations

H_2O_2	Hydrogen Peroxide
HNO_3	Nitric Acid
$NaClO$	Sodium Hypochlorite
$NaOH$	Sodium Hydroxide
ABPE	Ethoxylated Bisphenol A Diacrylate
AM	Additive-Manufacturing
BB	Benzyl Benzoate
BMC	Bulk Moulding Compound
DASML	Delft's Aerospace Structure and Materials Laboratory
DI	Deionized
DL	Delignified
EC	Ethyl Cinnamate
EM	Electro Magnetic
EP	Epoxy
ES	Ethyl Salicylate
ESEM	Enviromental Scanning Electron Microscopy
FF	Flax Fiber
FFCM	Flax Fiber Composite Materials
FRC	Fiber Reinforced Composites
FTIR	Fourier Transform Infrared Spectroscopy
GaAs	Gallium Arsenide
GFRP	Glass Fiber Reinforced Polymers
HPF	Hot Press Forming
InGaAs	Indium, Gallium, Arsenide
IR	Infrared
MC	Merocyanine
NF	Natural Fiber
NFCM	Natural Fiber Composite Materials
NL	Natural
OM	Optical Microscopy
PB	Probe Sonication
PDMS	Polydimethylsiloxane
PEEK	Polyether Ether Ketone
PMA	Polymethacrylate
PMMA	Polymethylmethacrylate
PP	Polypropylene
PVC	Polyvinylochloride
PVP	Polyvinylpyrrolidone
R1200/1204	Resoltech 1200/1204
RI	Refractive Index
RIM	Refractive Index Matching
RTM	Resin Transfer Molding
SEM	Scanning Electron Miscroscopy
SMC	Sheet Moulding Compound
SP	Spiropyran
TEMPO	2,2,6,6- tetramethylpiperidine-1-oxyl radical
TTP	Time, Temperature, Pressure
UD	Uni-Directional
USD	United States Dollars
Uv/Vis	Ultraviolet/Visible
vf	volume fraction
VI	Vacuum Infusion
VP	Vacuum Pressing
WC/W300	"Water-Clear"/W300 epoxy casting resin system

List of Figures

List of Tables

1

Introduction

Composite materials are a class of materials that obtain major importance day by day, in contrast to other categories of materials such as metals, ceramics, and polymers. Mankind started using composite materials especially *Fiber Reinforced Composites* (FRC) since ancient eras. For example, the shield of the Greek hero Achilles, in which he fought in the Troyan War is constructed based on a composite laminate design. [1] As time and periods pass, the applications of these materials are expanding and the development of those becomes a crucial part of the material research field. Today, composite materials are a pivotal part of many aircrafts, such as the famous ”Dreamliner 787” model of Boeing or the Airbus A380. [1] They are also used in the transportation industry, like the Cobra tram in Zurich or ships like the Royal Danish Navy Flex 300 Corvette. [1] Categorizing the composite materials based on multiple parameters like the reinforcement type or the matrix’s origin, as well as determining which is most effective for a specific purpose and the advantages they offer, will provide a deeper understanding to the utilization of these materials.

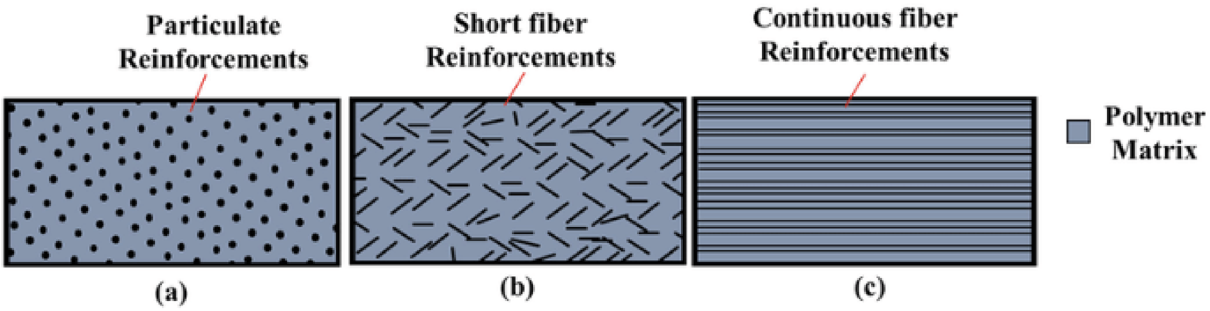

Figure 1.1: Composite material as a combination of a reinforcement and a polymeric matrix. a) Particulate reinforcements, b) Short fiber reinforcements, c) Continuous fiber reinforcement [2]

But what are composite materials? A combination of two or more chemically and/or physically distinguishable phases via a distinct interphase can be classified as a composite material. With this combination of these two constituents, a material with superior properties and lightweightness can be achieved. [3] The ratio of a mechanical property (i.e. tensile strength, stiffness) to the density of the material is defined as a specific property and is possibly the most crucial parameter for designing a composite material. For example, when merging a material that exhibits high tensile strength or stiffness, with an additional one that has low density, will demonstrate a high specific strength or stiffness. [3] Paraphrasing the previous sentence in simpler words, a reinforcement can provide high stiffness or strength to a softer/lighter material which can be described as a matrix. These properties are highly valuable to sectors such as aviation or aerospace, where fuel efficiency plays a pivotal role. Reinforcement phases provide the mechanical properties which transform a composite material into an advanced material with high structural capabilities. [3] Several common reinforcement materials can be carbon, glass, natural fibers (wood, flax), or particles, depending on the performance that is required. On the other hand, the matrix is the material that ensures protection of the reinforcement from its surrounding environment as also it is vital for transferring the loads into the stiffer and stronger phase. [3] Usually, it is lighter than the reinforcement (lower density) and its mechanical properties are inferior. Some examples of matrices can be polymer (PEEK, epoxy) metallic, or ceramic matrices. Fiber-reinforced composites are probably the most popular and important category of these materials, due to the high specific properties (i.e. high stiffness and high strength combined with very low density) they possess. There are various applications in which this type of materials can be utilized, such as the aviation, automotive, marine industry, etc. [1] For this reason in this report, the focus will be directly on fiber-reinforced polymer composites and for that reason every time referring to *composite materials*, it intends to point out *fiber reinforced polymer composite materials*. Some of the advantages of the fiber reinforced polymer composites are: [3]

1. High specific strength
2. High specific stiffness
3. High fracture resistance
4. Good impact resistance
5. Good fatigue resistance
6. Good corrosion resistance

A big research field which emerges focuses on the sustainability and eco-character of these materials. In the case of fiber-reinforced polymers (polymeric matrix), the end of life of the material or the origin of the raw materials should be carefully assessed. Some polymers, such as thermosets cannot be re-used after the end of their life due to the inability to melt at high temperatures (they degrade) and thus to be reformed. [4] The production of some constituents such as carbon or glass fibers emit colossal amounts of gases that influence the global warming phenomenon, like CO_2 or require excruciating amounts of energy for their production. [4] In addition, burning the constituents of those materials can be extremely toxic and hazardous for the earth's atmosphere because the majority of them are petroleum-based materials (epoxy resins, carbon fibers etc). Landfill disposal is a potentially environment-harmful solution for the end-of life of a material due to the excessive period of time (usually several decades to centuries) that petroleum-based materials require to degrade. [4] Studies have shown that these landfills can leak hazardous substances to water sources. [4] Petroleum-dependent materials (i.e. carbon fibers) have a particular usage span due to the limited amount of petroleum on the planet and the unimaginable consumption rate of it (100.000 times quicker than its production rate). [4] Alternative solutions for the development of composite materials are inevitable for their smooth sustainable transition in the future. [4] Some of the actions that are being implemented to follow this sustainable path in the field of these materials is the substitution of petroleum-based constituents (fibers or matrix) with bio-based components. Lignocellulosic materials such as flax, wood, or bamboo are abundant in Nature and can be utilized as reinforcement in composite materials providing a natural aroma for this scope. [4] These composite materials can be named as *Natural Fiber Reinforced Composite Material* (NFCM).

The functionality of the materials is a further interesting topic, providing an innovative flair to them, and categorizing them into the tier of smart materials. In contrast to structural materials, which are the materials that are used for their load-bearing capabilities (i.e. FRC), functional materials are designed to fulfill one pre-specified function having special properties, such as semiconductors, nanoparticles, etc. [6] Optical transparency can be described as a functional property in materials and is getting progressively more important for the research society, as this category shows promise as a candidate which can replace ordinary panels in smart buildings, used as energy providers or light trappers, etc. [7],[8] The applications can be various from parts in electronic devices to transparent windows in smart buildings, depending on the optical properties which are altered (light transmission or haze). Moreover, a transparent material can be used as a fracture tracker, like a tracker for crack tip propagation in the interior of it, which wouldn't be possible in an opaque material. There are numerous examples in the literature on materials that exhibit transparency, such as the occasion of a transparent composite material in Figure 1.2. However, these materials usually consist of non-sustainable constituents such as glass

Figure 1.2: An example of a functional transparent glass-fiber reinforced epoxy composite. [5]

fibers and polymer epoxy in this case. Combining the functional properties of optical transparency with bio-based composite materials, a particular type of material can be created which can show high specific structural capability (high stiffness and strength with low density) with extremely valuable functionality, like high optical transmittance. [7],[8] Sustainability will be also addressed as the fibers will be bio-based, reducing the embodied energy and emissions during production (as will be explained in Chapter 2), making this eco-friendly material an intriguing prospect. There is tremendous progress in the current research about bio-based composites which exhibit functional properties, like transparent wood composite or a cotton-based composite material with a high optical transmittance. There are still remaining challenges in the development of a transparent bio-composite material with flax fibers acting as reinforcement, principally due to incompatibility issues between the flax fiber and the matrix.

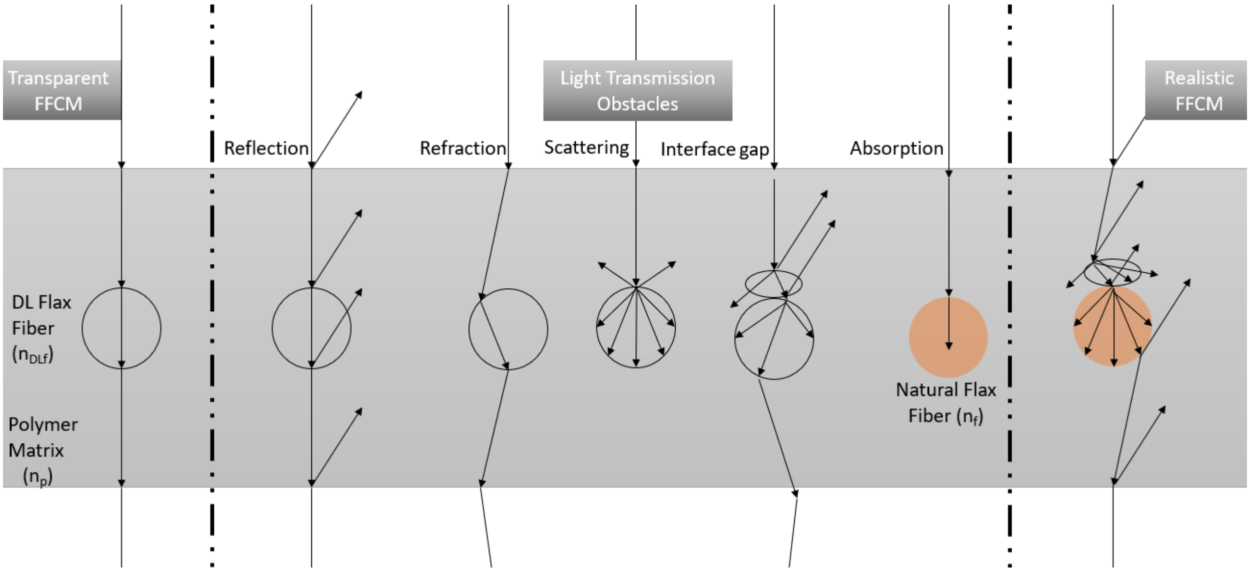

Figure 1.3: Light scattering and absorption phenomena on a non-transparent FFCM. The light path is shown on a transparent FFCM ($n_{DLF} = n_{n_p}$) in comparison to a realistic FFCM on which there are multiple light-hindering issues. These light hindering issues will be explained in later Chapters.

The two main challenges facing the development of a transparent *Flax Fiber Composite Material* (FFCM), is the difference between the hygroscopic character of natural-based materials and polymer-based materials and the minimization of the light scattering and absorption phenomena. Obviously, these two issues connect with each other, as the incompatibility of flax fibers and polymer matrices can lead to light scattering. Flax fibers contain high percentages of cellulose which is hydrophilic, while polymers are highly hydrophobic. [9] This can lead to incompatibility issues in the interphase of the fiber/matrix composite and therefore light scattering. They also contain the light-absorptive substance lignin, which has to be removed from the fibers for them to be transparent. Additionally, the selection of a polymer has to be consistent with the fiber on the aspect of the refractive index and it will reduce the light scattering effect, by achieving *Refractive Index Matching* (RIM). To fill this challenging gap, the recommendations and actions that would be made in this report to accomplish the highest optical transparency on an FFCM, will revolve around fiber modifications with chemical treatments which will adjust the structure, hygroscopic nature, and wetting ability of the fiber, achieving compatibility and high optical transmittance. These treatments were based on issues that were identified from the literature as obstacles that were required to be surpassed to achieve the appropriate result. The identified obstacles to ensuring high light transmittance in a flax fiber-reinforced composite material can lead to the following fiber treatments being categorized into the following types:

- **Delignification**: Removes the light-absorptive substance of lignin, thus eliminating the obstacle of light absorption at the visible spectrum. Transforms the opaque brown flax fibers into a distinct white color. One of the two most important processes of transparent NFCMs is identified from the literature. [10], [11], [12], [13], [14]

- **Nitric Acid/Probe Sonication**: Removes pectin which acts like a glue material between the elementary flax fibers in the structure of technical fibers, improving dispersion and hindering cellulose fiber aggregations, which can scatter light due to the fiber boundaries. The hydrophilic character of cellulose fibers due to the presence of polar hydroxyl groups on their surface can lead to the formation of hydrogen bonds between them, accumulating them, and can act as light scattering sources as well. This treatment was discovered from the research of Jiang et al., developing a printable transparent FFCM which showed great results in low fiber weight concentrations. [14]
- **Acetylation**: This treatment transforms a hydrophilic natural fiber like flax to a hydrophobic one by replacing the $OH-$ groups into CH_3CO-, improving the interphasial properties by better bonding of the fiber with the polymer, and decreasing the air light scattering sources in the interior of the material. Bad wettability and permeability of the hydrophilic character of flax fibers can lead to the hindering of a suitable bond formation between the fiber/matrix, which will lead to the formation of air gaps in their interphase. These air gaps will scatter and refract light severely in various locations due to RI mismatch between air and the other two constituents, reducing light transmittance. Li et al., showed that acetylation could assist in improving the optical transmittance of transparent wood. [13]
- **TEMPO-oxidation**: TEMPO oxidation occurs as a carboxylation of the $-OH$ groups present on the surface of the flax fibers, with the negative carboxyl groups to repel each other and create wider spaces which could be impregnated thoroughly with a refractive index matching polymer and lowering the refractive index mismatch between the fiber/polymer. This treatment was implemented on a cotton fiber-reinforced polymer material, by Abe et al. increasing the maximum light transmittance of the sample. [15]
- **Sodium Hydroxide**: Sodium hydroxide treatment can swell the cellulose lattice, increasing the space in the crystalline structure by changing the cellulose structure from cellulose I into cellulose II, and allowing light particles to pass through without major scattering on the molecules. Light can be stopped due to the compacted structure of the crystalline structure of cellulose-I. The tight space in the crystallites can scatter or reflect light, resulting in low optical transparency. Abe et al. conducted this treatment again on the transparent cotton NFCM. [15]

From all these fiber treatments, delignification was implemented on all occasions due to the significance of eliminating light absorption which transforms FFCM into opaque materials, while the last three treatments were decided to be conducted all on the same flax fibers because the combination of them seemed to tackle several issues investigated and also due to the result of the transparent cotton based NFCM. Delignified flax fiber immersion testing in organic compounds or liquid polymers are implemented, together with techniques that can estimate the *Refractive Index* of the delignified fiber and can lead to selections of appropriate polymers for polymer infusion and therefore to RIM in a composite material.

Figure 1.4: Plan of accomplishing optical transparency on a flax fiber reinforced composite material, with a stepwise procedure of delignification, fiber modification, polymer infusion, and composite manufacturing.

Merging this exact ability of a transparent partially bio-based composite material can give immense interest to the research community as sustainability, lightweigthness, and functionality can all be accomplished. In this report a research study is conducted, to develop a flax fiber-reinforced composite material that will exemplify these special functional properties.

1.1. Motivation of Thesis Project

The aim of the report focuses around a special pre-specified topic which is:

Research Objective

Development of an optically transparent flax fiber reinforced composite material

The concepts of transparent delignified wood, polymer infiltration, or fiber modification are adopted and adjusted for flax fiber reinforced composite material, with a desire to accomplish optical transparency in a composite. Based on the goal of the thesis project and some observations which were made from the literature review the research questions which are pivotal to answer for the accomplishment of the objective of the report are:

Research Question 1

What is the exact refractive index of a delignified flax fiber?

Research Question 2

Which is the optimum surface modification of flax fibers, ensuring that their compatibility with the matrix will be the highest possible and therefore light scattering will be minimized?

Research Question 3

Which polymer is the most suitable for a complete flax fiber impregnation, leading to RIM and therefore to high optical transmittance?

Research Question 4

Which is the best composite production technique for fabricating a transparent flax fiber composite material?

These are the research fields in which this report and project will focus on. Having all the appropriate information about these questions will light up gaps in the research and future recommendations about the research actions which can be implemented to develop a flax fiber-reinforced composite material that will demonstrate excellent optical transparency.

1.2. Structure of the Report

This report consists of seven chapters and three main parts. The parts are composed of the Literature Review, the Analysis, and the Summarization parts. These parts are structured as:

Chapter 1: Introduction of the master thesis project, its motivation, and the research questions which are raised.

Chapter 2: A depiction of some NFs and why are they used in the industry. A detailed explanation of the flax structure and composition. Tensile and compressive mechanical properties of flax fibers are presented. Also, fiber modifications for flax-reinforced composites and numerous manufacturing techniques are shown.

Chapter 3: Description of some fundamental optical properties like refractive index and light interaction with a solid. A reference on measurement techniques in fiber's RI is being made, along with ways of measuring transmittance and haze in a material. A small review is made on optical transparency in NFCM, such as wood, flax, and cotton fiber-reinforced composites.

Chapter 4: An explanation of the materials, and the methodologies (like fiber modifications, immersion testing, or composite production) that were implemented during the project. Also, the composite materials' recipes which are followed to create the appropriate materials, are presented.

Chapter 5: All the results which are generated from the analysis of the transparent flax fiber composite material, are presented and discussed. How fiber modifications affect light transmittance and mechanical properties, immersion tests for the estimation of the DL flax fiber's refractive index, which polymers are suitable for fiber impregnation, and the fabrication of the composite materials are explained thoroughly in this section. Comparison graphs between the FFCMs materials developed during this project, the GFRP samples, and materials/values extracted from the literature (transparent wood or cotton, etc) are presented.

Chapter 6: Conclusion of the report, with a precise summarization of all the valuable details and knowledge established from the development of the transparent FFCM.

Chapter 7: Ideas and discussion topics about future research on this particular theme, which can light up new actions and potentially could solve some issues that are identified in this report.

Part I

Literature Review

2

Flax in Composite Materials

2.1. Natural Fibers in Composite Materials

Fibers in composite materials are possibly the most significant component of the material, due to the reinforcement they provide on the mechanical performance. These can be distinguished into four main classes of materials; fossil-fuel-based or bio-based and non-biodegradable and biodegradable. A material can be both bio-based and non-biodegradable. Concerning these types of materials, environmental issues are transforming petroleum-dependent materials into unattractive materials for both fibers and matrix, due to the limited availability and environmental concerns. [4] This implies a sustainable transition from high-performance but petroleum-based fibers, such as carbon fibers into bio-based natural fibers.

Natural Fibers (NFs) can be extracted from many different non-petroleum-based sources such as animals, plants, or minerals. [16] A vast categorization of NFs are depicted in Figure 2.2. As seen from the following figure plant fibers can be extracted from seeds, stems, leafs, or even fruits. Many important NFs that are valuable for composite manufacturing are flax, hemp, jute, kenaf, bamboo, etc. These can easily substitute the widely used glass fibers in the industry as they present positive properties when combined with a matrix to form a composite material. [9] NFs can offer high specific properties such as high specific tensile strength or high specific stiffness, while maintaining their environmentally friendly character. [17]

The usage of natural fibers has expanded in the past years showing how crucial they are for the sustainable transition of many industries. In Europe, an estimation depicted that the usage of bio-based fibers in composite applications reached up to 315.000 tones and 13% of all reinforcing material in 2010, having an enormous increase from 2003 which was 49.000 tones. [9] It is estimated, that the market of Natural Fiber Composite materials is going to increase to 10.89 billion $ USD dollars by 2024 from 4.46 billion $ USD in 2016. [18] Only in the automotive industry, there was a huge increase in the usage of NFs, from 19.000 tones in 2005 to 30.000 tones in 2012. Flax was half of the volume percentage in those numbers, while kenaf was one-fifth and jute 12%. [16]

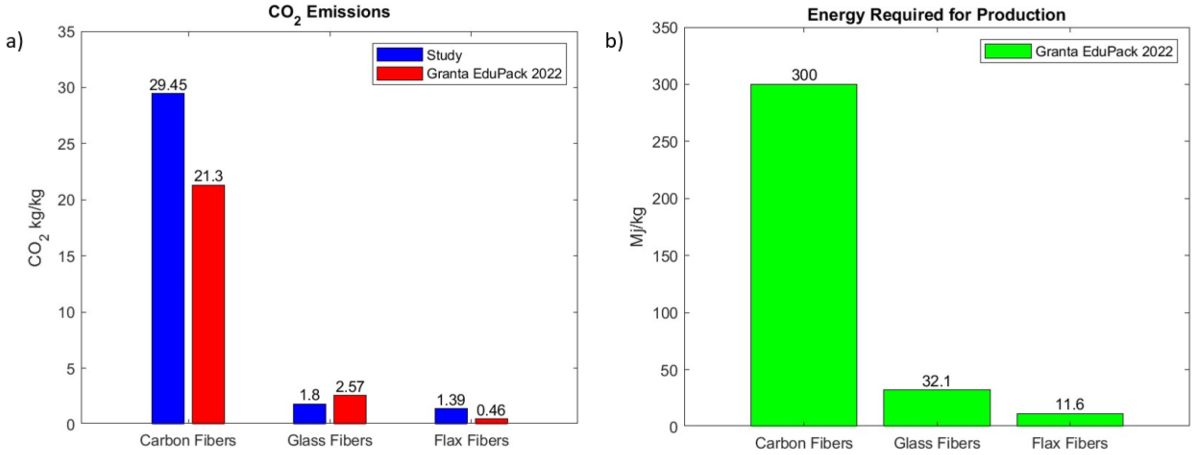

Figure 2.1: a) CO_2 emissions, b) Required energy for the production of one kg of carbon/glass/flax fibers, according to Barth's study and Granta EduPack database. [16], [19]

NFs are demonstrating a desirable carbon footprint when being produced in comparison to petroleum-based fibers. Carbon emissions are a very significant concern for our environment as carbon dioxide increases the temperature of the planet, creating climate change. According to a study, the production of flax and hemp fibers emits 1.39 $kg\ CO_2/kg$ in comparison to 1.80 $kg\ CO_2/kg$ for glass fibers and 29.45 $kg\ CO_2/kg$ for virgin carbon fibers. [16] According to the Granta EduPack 2022 database developed from Ansys, the production of virgin high modulus carbon fibers seems to have a carbon footprint of 19.3-21.3kg CO_2/kg and requires energy of 272-300 MJ/kg, while E-glass fibers emit 2.33-2.57 $kg\ CO_2/kg$ and require 29-32.1MJ/kg energy for production. [19] Flax fibers have significantly lower CO_2 emissions in 0.42-0.46 $kg\ CO_2/kg$ and required energy 10.5-11.6MJ/kg for their production. [19] Carbon and glass fibers are not biodegradable (they do not decompose naturally) in comparison to the NFs (like flax and hemp) and sometimes landfill deposition is the only solution for their end-of-life. [19]

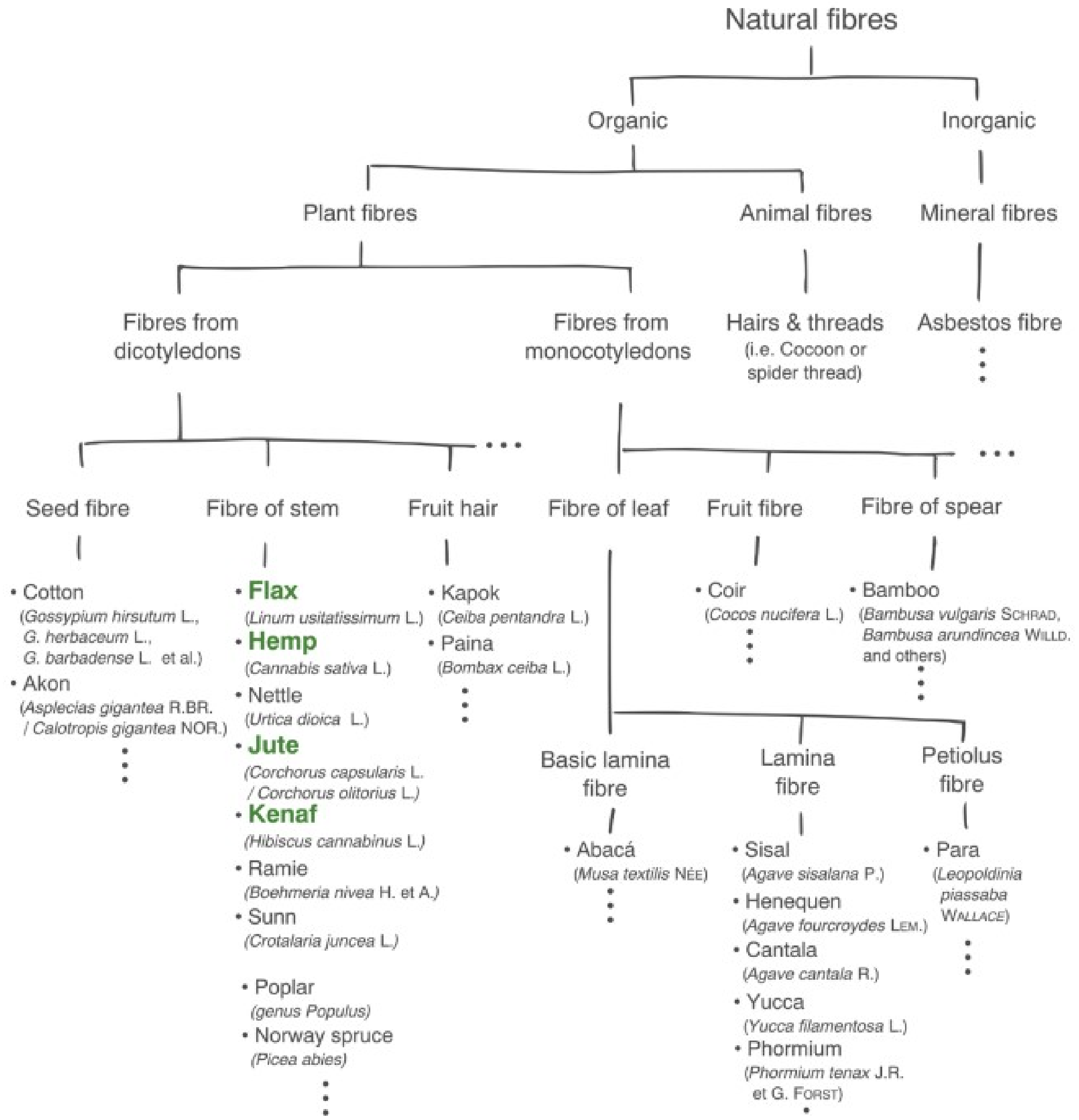

Figure 2.2: A vast categorization of Natural Fibers based on their origin, chemical composition, etc. [16]

Observing Table 2.1, it is clear that natural fibers are mechanically comparable to one of the most used types of reinforcing fibers in composites in the world, E-Glass, when the comparison is made on the specific properties of these fibers. Figure 2.3a shows that NFs are not only comparable to E-glass fibers but a big proportion of them outperform them. [9] Flax fibers can reach up to a median value of 45 $GPa/(g/cm^3)$ for the specific Young's modulus compared to the E-glass' value of approximately 29 $GPa/(g/cm^3)$. All of this is attributed to the relatively lower density of flax fibers (1.4-1.5 (g/cm^3)) in contrast to glass fibers (2.5-2.6 (g/cm^3)). This is valuable when lightweight and circular composites are desired and it shows that both of these requirements are achieved with NFs. Additionally, the cost per kg is shown in Figure 2.3b and it clearly highlights that NFs are extremely affordable (0.30-1.50 $ USD) in comparison to glass fibers (1.60-3.25 $ USD), making them appealing for low-cost applications.

Table 2.1: Mechanical properties and density of glass fibers and NFs. [9]

Fiber	***Density*** (g/cm^3)	***Tensile Strength*** (MPa)	***Young's Modulus*** (GPa)	***Specific Young's Modulus*** (GPa/(g/cm^3))	***Elongation at break*** (%)
E-Glass	2.5-2.6	2000-3500	70-76	29	1.8-4.8
Flax	1.4-1.5	343-2000	27.6-103	45	1.2-3.3
Hemp	1.4-1.5	270-900	23.5-90	40	1-3.5
Jute	1.3-1.49	320-800	30	30	1-1.8
Kenaf	1.4	223-930	38	24	1.7

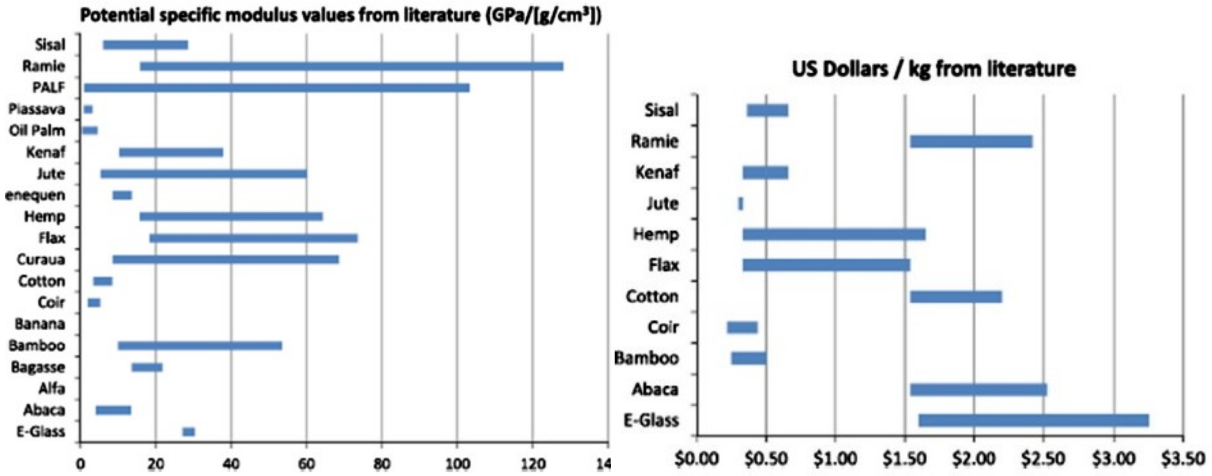

(a) Specific Young's Modulus

(b) Price per kg in USD

Figure 2.3: Specific properties and cost for various NFs and glass fibers. [9]

Summarizing Table 2.1 and the previous graphs, it is safe to say that *Flax Fibers* (FFs) can be classified as the category of the most promising fibers regarding the performance-to-density ratio they can provide as a reinforcement in composite materials, while they are relatively economical too. Also, as a plant-based fiber, they can be re-generated sustainably without using petroleum-based materials and their re-growth can be rapid. [9] For these reasons, flax is investigated further as a fiber in composite materials.

2.2. Flax Structure and Composition

Flax or *Linum usitatissimum* is a widely used natural fiber on composites, as stated in the previous sections. If seen in the mesoscopic scale, a fiber bundle or technical fiber can contain up to 40 elementary fibers and it is directly extracted from the stems of the flax plant. [9], [17] *Elementary fibers* are the fibers that have a small diameter of about 10-40 μm and can reach a fiber length of 40 mm. On the other hand, *technical fibers* have a bigger fiber diameter, which approximately is 5-10 times bigger than the diameter of elementary's. [17] Their length can reach up to on 1 m. These elementary fibers are connected via a "composite material" form as pectin or lignin can behave as a matrix to them and thus they form the fiber bundles. Their form is remarkably complex and hierarchical as they are composed from one primary cell wall and three secondary cell walls. The outer primary cell wall is very thin (0.2 μm) in comparison to the other three secondary walls. In more detail, the thickest cell wall (S2) is the one responsible for the strength and stiffness the flax fiber provides. [9] Many cellulose microfibrils are present in the S2 cell wall structure, which are connected with hemicellulose chains. [17] The microfibrils are parallel one to another and form an orientation angle of 10^0 in the hemicellulose-lignin matrix which is the main reason for the high tensile strength of the fibers. [9] This angle could directly affect the strength that the flax fibers possess. [9], [17]

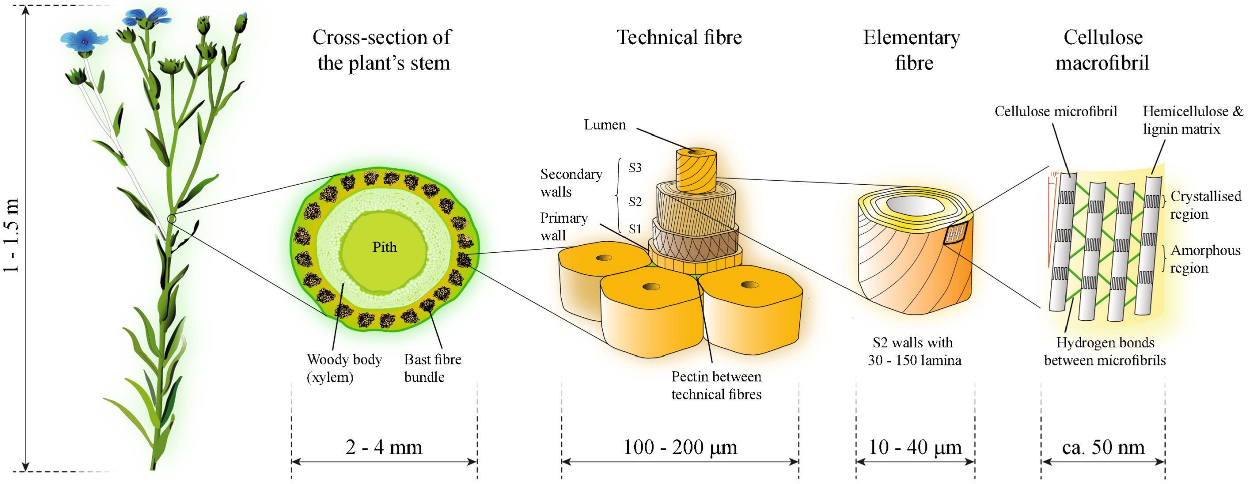

Figure 2.4: The hierarchical structure of flax fibers in multiple scales from macroscale(cross-section of the plant's stem) to nano-scale (cellulose microfibril). The technical fibers consist of multiple elementary fibers which are connected in a pectin matrix. The cellulose micro-fibrils are bonded through hydrogen bonds in a matrix of hemicellulose and lignin in the S2 wall. [17]

Table 2.2: Chemical composition of flax fibers. [9]

	Cellulose (%)	*Hemi-Cellulose (%)*	*Lignin (%)*
Content	62-75	11-20	2-5

The chemical composition of flax is consisted of three main components. These are cellulose, hemicellulose and lignin. [9], [20] Other constituents are low percentages of wax and pectin which deteriorate the mechanical properties of the fibre. Cellulose is the component which has the majority of the concentration of flax, followed by hemicellulose and then lignin. Table 2.2 depicts the previous sentence. *Cellulose* is probably the most significant component of flax due to the strength and stiffness it provides. [9] It is a fibrous and tough unbranched homopolysaccharide which can be found in abundance in plants. [21] It can be formed as a crystalline, amorphous or semi-crystalline structure. Crystalline structure can be distinguished into two sub-forms, the cellulose-Iα and cellulose-Iβ. [20], [21] Due to the many hydroxyl groups present in cellulose, it can be described as a hydrophilic material. [9], [21] Because of the hydrophilicity of cellulose, the fiber component attracts and absorbs water molecules which deteriorate the mechanical performance of a fiber when used in a composite material as a reinforcement. *Hemicellulose* is a heterogeneous polysaccharide which is branched, fully amorphous, and partly soluble in water due to many hydroxyl and acetyl groups. [9], [22] It has a significantly lower molecular weight than cellulose and it is hygroscopic. [22] *Lignin* is the third main constituent of flax fibers. It contributes in the lowest amount to the total biopolymer composition (Table 2.2) but it is particularly crucial due to the bonding of the microfibrils, such as hemicellulose. [17] As a substance it is fully amorphous and aromatic and it is the second most abundant organic material after cellulose consisting of 15-40 % of woody plants. [9], [23] In contrast to cellulose, lignin is hydrophobic. [20], [23] The structure of lignin consists out of three phenylpropane units: coniferyl, sinapyl and p-coumaryl alcohols. Its molecular weight is very big, approximately 80.000 which can be justified by its complicated form. [23] *Pectin* is an heteropolysacharide which can be found in the outer layer together with lignin as it connects the elementary fibers together forming fiber bundles and reduce the interphasial properties between the fiber and a matrix. [24] These non-cellulosic substances can demote the mechanical properties of FFs due to the low interphasial adhesion they provide, which eventually will not contribute to the internal load transfer between the constituents (matrix to fiber). [24]

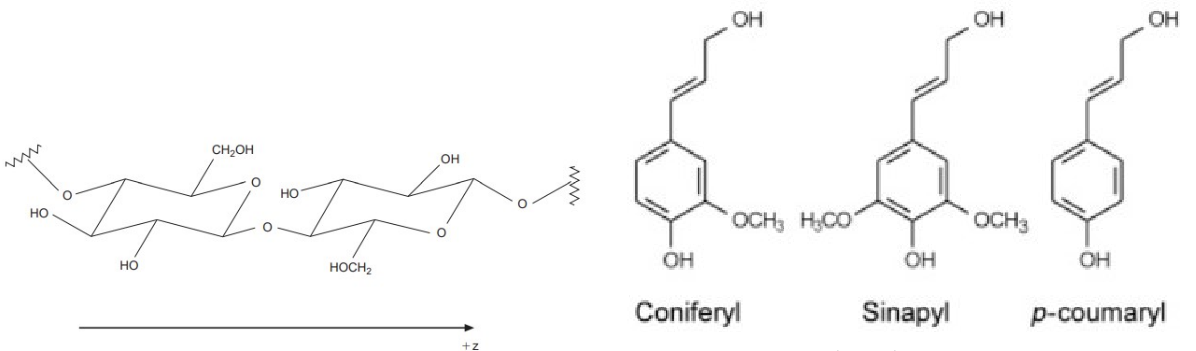

(a) Moleuclar structure of cellulose [21]

(b) Lignin sub-units of coniferyl, sinapyl and p-coumaryl [23]

Figure 2.5: Units of the fundamental components in natural plant-based materials

2.3. Mechanical Properties of Flax Fibers

Table 2.1 gives an overview of the tensile properties of many NFs, in comparison to flax fibers. Flax fibers have excellent tensile properties (tensile strength up to 2000 MPa, Young's modulus up to 103 GPa) while their density is very low. Also, as stated before the specific Young's Modulus of flax fibers is impressive, on a note that evidently outperforms commercial E-glass fibers, as shown in Figure 2.3a. The low price of them with their high specific properties makes them undoubtedly a competitor to glass fibers.

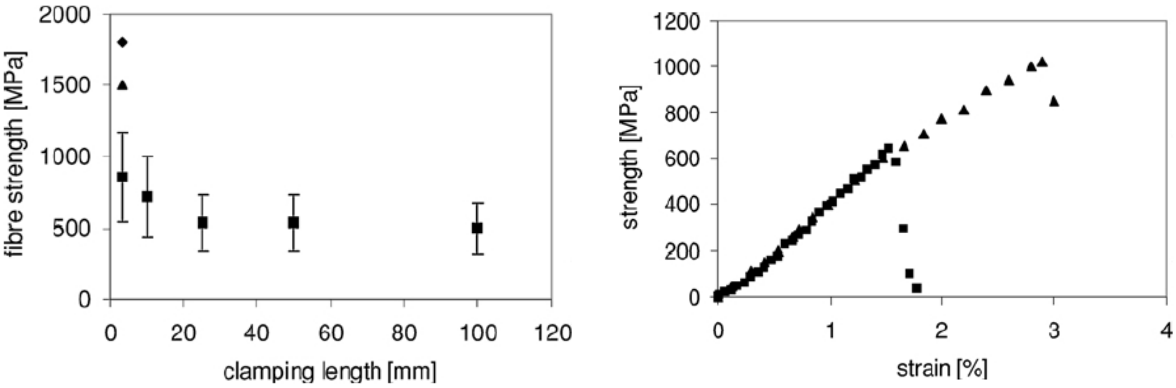

(a) Tensile strength vs clamping length of technical and elementary flax fibers. [25]

(b) Stress-strain curve for the technical and elementary flax fibers. [25]

Figure 2.6: Tensile Properties of flax fibers in relation to their clamping length. Triangular and rhombohedral marker depicts elementary flax fibers, while square marker depicts technical flax fibers.

Additionally, flax fibers' tensile mechanical properties are fully dependent on their fiber length. Bos et al. have shown that the mechanical properties of flax fiber vary in relation to their fiber length. [25] Figure 2.6a shows the tensile strength of flax fibers about the fiber length. The fibers that are below the 3 mm clamping length can be classified as elementary fibers (triangular point) while the fibers up to 100 mm can be classified as technical fibers (square point). The elementary fiber showed a tensile strength of about 1522 ± 400 MPa, while the technical fiber has a range of 500-850 MPa depending on the fiber length. [25] The rhombohedral point shows the tensile strength of elementary fibers which were isolated by hand and they were free of kink bands, which is a form of damage. [25] It is apparent that by reducing the fiber length, the structure of it becomes purer due to the reduction of critical flaws, and thus the tensile strength of the fiber increases. [25] But that is not the only explanation for the high tensile strength of elementary fibers in comparison to technical fibers. There is evidence of alteration of the failure mechanism in flax fibers when increasing the fiber length. In small fiber lengths, the crack mainly has to pass through the strong cellulose walls of the fiber, while in bigger lengths the fiber fails due to shear failure in the pectin interphase. [25]

Compression testing (via elastica loop test) indicates values of 1200 ± 370 MPa for compression strength. [25] The compressive failure of the flax fibers can be attributed to the kink bands which are present in the fibers. Testing on hand-isolated flax fibers (kink-bands free during growing) and standard isolated flax fibers don't show a difference in the compression values between these two, as in the case of tensile strength. [25] This is attributed to the kink-band formation procedure, which indicates that it is identical to these two types of flax fibers. Also, the fracture point of a flax fiber is assumed to happen when kink bands have occurred to the whole fiber.[25] Lastly, there are no differences observed in the stress-strain relation for all of the fiber types, indicating a similar Young's modulus for them. [25]

Naturally, due to the hydrophilic character of cellulose and thus flax fiber, *Relative Humidity* (RH) plays a decisive factor in the deterioration of the mechanical properties of flax fibers. Moisture is easily absorbed in NFs due to the high percentages of hydrophilic cellulose and thus it can degrade the fibers' performance significantly. [9] A relevant study from Davies et al., shows that the static and dynamic moduli of flax fibers decreases significantly when the RH is increasing, as seen in Figure 2.7. [26]

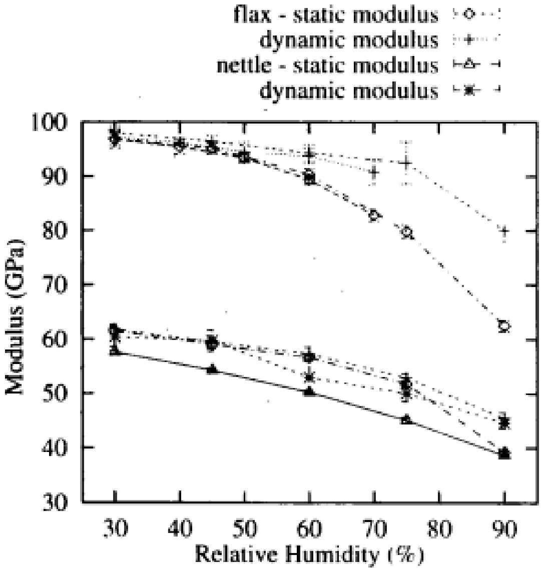

Figure 2.7: Static and dynamic moduli in relation to relative humidity for flax fibers. The graph depicts how the moduli is decreased when the absorbed humidity increases in a flax fiber. [26]

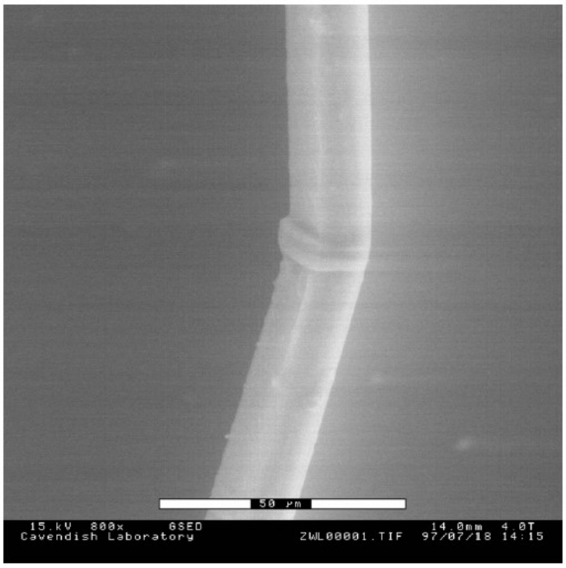

Figure 2.8: ESEM image of a kink band defect developed on a flax fiber. [25]

2.4. Chemical Modification of Flax Fibers

One of the main disadvantages of NFCM, is the incompatibility of the NFs with a polymeric matrix. [9], [27] The main reason for the poor interphase of the fiber/matrix is the hygroscopic character of each constituent. Usually, NFs are hydrophilic due to the high percentage of cellulose, while the majority of the polymeric matrices are hydrophobic, implying a poor interaction between them. [9], [27] Numerous approaches have been available in the literature to make the flax fiber more compatible (less hydrophilic) with the matrix. A list of the most significant of them is presented below.

1. **Alkaline Treatment**: This chemical treatment is based on the usage of sodium hydroxide ($NaOH$), which cleans the surface of the fiber from impurities like pectin, wax, or even a certain amount of lignin, making the interphasial adhesion stronger. The surface morphology of the fibers is totally modified

showing a better fiber/matrix adhesion and thus better mechanical properties. [27], [28] A study from Samyn et al. has showed that flax fibers which were alkalized with sodium hydroxide ($NaOH$), were cleared from lignin, hydroxyl groups ($-OH$) formation on the surface was increased and the surface roughness' was enhanced. This could enable a more successful mechanical interlocking between the fiber and the matrix and thus improve the interphasial properties. [29] This treatment also, provides a swelled crystalline structure, transforming cellulose I into cellulose II with a wider crystalline structure which can allow visible light particles to be transmitted efficiently, without scattering phenomena. Abe et al., implemented this swelling procedure on a cotton-based reinforced composite, achieving high light transmittance (will be discussed in the next Chapter). [15]

2. **Silane Treatment**: Several studies have been implemented on the silane treatment which works with a formation of hydrophobic silanol groups ($Si-OH$) that interact with the hydroxyl groups of the NFs and improve the adhesion between the components. [27] An interesting study from Alix et al., showed that the silane modification implemented in flax fibers increased the tensile properties of the fibers, such as tensile strength and toughness, as seen in Figure 2.10 [30]
3. **Acetylation Treatment**: Acetylation is a popular pre-treatment method of fibers, transforming a hydrophilic fiber into a more hydrophobic and resin-compatible fiber. [22], [27] It works with a reaction that destroys the bond between the hydrophilic hydroxyl groups ($-OH$) and thus replacing them with hydrophobic acetyl groups (CH_3CO-) resulting in the esterification of all the hydroxyl groups. [22] Bledzki et al., showed improvement in the fiber-polymer (PP) interface and flexural properties when the fibers were subjected to acetylation until 18% degree, as seen in Figure 2.9. Surpassing this threshold indicates that the flexural properties of the FFCM deteriorate. Also, there is resistance to moisture absorption thus increasing the mechanical properties of the material, like tensile and flexural strength. [22]
4. **Benzoylation Treatment**: This chemical treatment's principle is to make the fiber less hydrophilic and thus more compatible with the polymer matrix. Sodium Hydroxide ($NaOH$) is applied to the fibers followed by a treatment with benzoyl chloride (C_6H_5COCl). The interphasial properties are improved by this technique. [27]

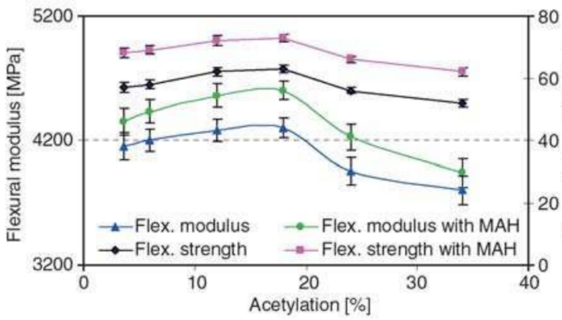

Figure 2.9: Flexural strength (black and purple) and modulus (blue and green) of an FFCM vs acetylation degree of flax fibers. MAH is a coupling agent added to the composite. [22]

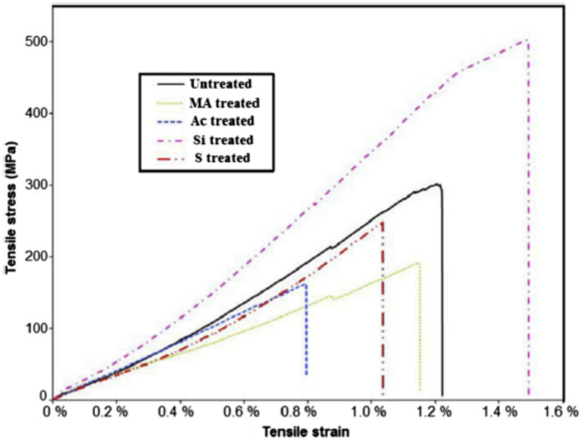

Figure 2.10: Tensile stress-strain curves for various chemical treatments of flax fibers. (Si) is the silane treatment and (Ac) is the acetylation treatment which is of interest. Untreated flax fibers' stress-strain curve is also present. [30]

2.5. Flax Fibers on Composites

2.5.1. Polymer Matrix Selection

Flax fibers combined with a polymer can form a fiber-reinforced composite material with excellent specific properties. These composites can be defined as NFCM. As discussed before, the matrix is very important as well and organic polymers are very attractive due to their low density and cost, ease of processing, and production. [31] The result of the combination of NFs, like flax and a polymer matrix can be a composite material that is lightweight, cheap, and more environmentally friendly.

The usage of a matrix can help in the connection and protection of the fibers from the environment and can contribute to the effective transfer of the load to the fibers. [31] The two different types of polymer matrices that are found to be the most suitable for a polymeric matrix in a composite material are: i) thermoset polymer ii) thermoplastic polymer. Both types of thermoset and thermoplastic polymer matrices can be merged together with NFs to form a composite material. Thermoplastic polymer matrices are more common as a polymer matrix due to the fact that they provide affordability, good impact resistance, and excellent chemical resistance. [9], [31] On the other hand, thermoset polymers are more durable, have superior mechanical properties, and are easily processable (low viscosity, low required pressures). [9] A list of the most common polymer matrices used as a matrix in NFCM with some of their properties is depicted in Table 2.3.

Table 2.3: Density and tensile properties (together with the melting temperature) of thermoset and thermoplastic polymers used as matrices in NFCM. [31]

Thermoplastic Polymers

Material	*Density (g/cm^3)*	*Young's Modulus (GPa)*	*Tensile strength (MPa)*	*Melting Temperature (^0C)*
Polypropylene	0.90-0.91	1.1-1.6	20-40	175
Polyethylene	0.91-0.95	0.3-0.5	25-45	115
Polystyrene	1.04-1.05	2.5-3.5	35-60	240
PVC	1.38	3.0	53	212

Thermoset Polymers

Material	*Density (g/cm^3)*	*Young's Modulus (GPa)*	*Tensile strength (MPa)*	*Melting Temperature (^0C)*
Phenolic	1.29	2.8-4.8	35-62	210-360
Epoxy	1.1-1.6	3.0-6.0	28-100	100-200
Polyester	1.0-1.5	2.0-4.5	40-90	90-250
Vinylester	1.2-1.4	3.1-3.8	69-86	86

An impressive study from K Van de Velde et al. compares many different thermoplastic polymers as suitable candidates for a matrix on an FFCM. [32] In this study, PP showed the most promising characteristics as a polymeric matrix on flax fibers, like low density, low moisture absorption, low cost, and great thermal properties. [32] The only concern is the incompatibility between the flax fibers and the PP matrix. A fiber surface modification is suggested by the author. [32]

2.5.2. Manufacturing Process

There are plenty of manufacturing production processes for composite materials available in the literature. A categorization of these processes can be done based on some parameters such as the type of the polymer matrix, the fiber size, the size and shape of the composite, the production quantity etc. [3] Some of the most basic manufacturing processes of composite materials are:

- **Hand Lamination**: One of the most fundamental and simplest methods of creating a composite material. It is extremely affordable and can work if a prototype is desired. It works by applying the release agents, the resin and the reinforcing materials with a handheld roller/brushes, in an open one-sided mold. It works mainly on thermoset composites. [3]
- **Spray-Up**: In this technique a spray gun, sprays mostly thermoset resin mixed with chopped fibers into a mold. Rovings can be used as an import to the gun where they are chopped to fiber lengths as 10-40 mm. This method can be controlled by human hand or by automation techniques. Curing is done in room temperature. [3]
- **Pre-preg lay-up**: Can work both on thermoset and thermoplastic composites. This method works by stacking pre-impregnated layers of material on the top of a one-sided mold. It usually is implemented by hand but recently some other automatic methods have been available. [3]
- **Resin Transfer Molding**: This method is probably the most popular method of producing structural composites. The reinforcement (usually fabrics) is stacked altogether and placed to the lower part

of the closed-mold formation with some extra components (release film, peel ply material etc). Not only closed mold can be used for this method but also one-sided mold covered with a vacuum bag. Then the mold is closed and the resin is injected into it, flooding the reinforcement. Vacuum can also be applied if desired (Vacuum-assisted resin transfer molding), in a vacuum bag which is perfectly sealed and air is eliminated from the set-up. Afterward, the resin is cross-linked with or without the assistance of heat and lastly, it is removed from the mold. The most common combinations which are used for RTM are glass fibre/unsaturated polyester and carbon fiber/epoxy. It is also very suitable for large-size applications. [3],

- **Compression molding**: This method works with a closed-mold formation and a heated-hydraulic press applies pressure and heat into this mold and cures/consolidates the composite. It is available both for thermoplastics and thermosets. Some pressure profiles used are 10-20 MPa for thermoplastic composites and 3-20 MPa for thermoset composites. The flow of the resin can play a huge role on this process. In thermoplastics, if the resin flow is not high then the method is called hot stamping. In thermosets, this method is also called BMC or SMC, depending on the form of the material (sheet or bulk) prior processing. The applications for compression molding composites can be numerous, i.e. lightweight automotive parts. [3]
- **Filament Winding**: Filament winding is very popular when cylindrical shapes like pressure vessels are required. Rovings or yarns are used for reinforcement. These are immersed into a resin and then they cover a rotating mandrel. The viscosity of the resin has to be low to impregnate the fiber with ease. [3], [9]
- **Pultrusion**: This method is very efficient when constant cross-sectional composite parts are desired. Rovings are used for direct impregnation into a resin and they are drawn through a die of required shape. Afterwards, it is cured/consolidated (via heated and cooling dies) and cut to appropriate lengths. The viscosity of the resin should be low to allow impregnation. High fiber volume fractions can be achieved by this method. The applications for pultruted products can be transport or building materials. [3]

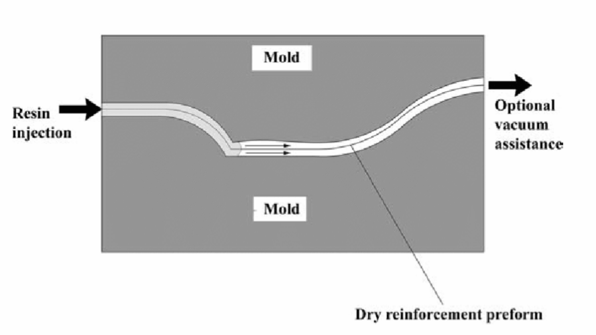

Figure 2.11: RTM or VARTM processes for composite production. [3]

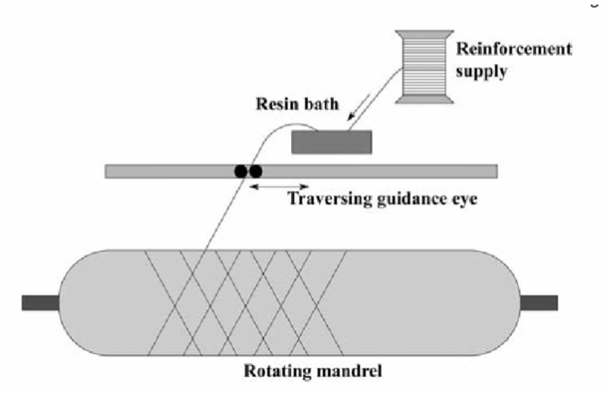

Figure 2.12: Filament winding process for composite production. [3]

2.5.3. Mechanical Properties of Flax Fiber Composite Materials

Here, the advantages of FFCM are presented in comparison to other FRC as well as metallic materials like aluminum or steel. [33] From the Figures 2.13a-2.13c, it is comprehensible that the specific stiffness in tension of flax fibers combined with PP (as a UD FRC) outperforms glass/PP composite and is comparable with aluminum and steel in high fiber volume fractions (>50%). Additionally, the specific bending stiffness' graph of the same materials shows that flax/PP outperforms all the aforementioned materials and it is slightly lower than the advanced composite material of carbon/PP (15-25%) for some values of fiber volume fractions. [33]

Kong et al., developed two types of FFCMs with VI, one with UD plies and one with woven fabric reinforcement. [34] The materials consisted of a vinyl-ester matrix, with approximately 35% fiber vf% for both laminates. The results indicated a flexural strength of 188 MPa and flexural stiffness of 9.7 GPa of the UD composite material, while the woven fabric reinforcement provided a flexural strength of 108.70 MPa and a flexural modulus of 6.7 GPa. [34]

Additionally, Goutianos et al. developed a UD epoxy-based FFCM with hand-lay up and consolidation under vacuum (-1 bar). [35] The fiber vf% was estimated at 28%, despite the thickness being at higher levels (2.5 mm) possibly due to lower pressure during consolidation. The results indicated a longitudinal flexural strength at 190 MPa and a longitudinal flexural modulus at 16 GPa. [35] Moreover, for the woven plain weave $(0^0/90^0)$ composites created with an RTM process and a vinyl ester matrix (lower matrix properties than epoxy), the flexural properties showed a maximum value of 140 MPa for flexural strength and 10 GPa for flexural stiffness on a 29% fiber vf material.

Based on the technical datasheet of ampliTex no 5025 280gsm flax fibers from Bcomp, a composite material on 54% fiber volume fraction with Epoxy resin Araldite LY 8615/XB 5173 was created for demonstration issues. This material presented a longitudinal flexural strength of 377 MPa and longitudinal flexural stiffness of 32.6 GPa, while presenting a transverse flexural modulus of 4.6 GPa and transverse strength of 39 MPa. [36]

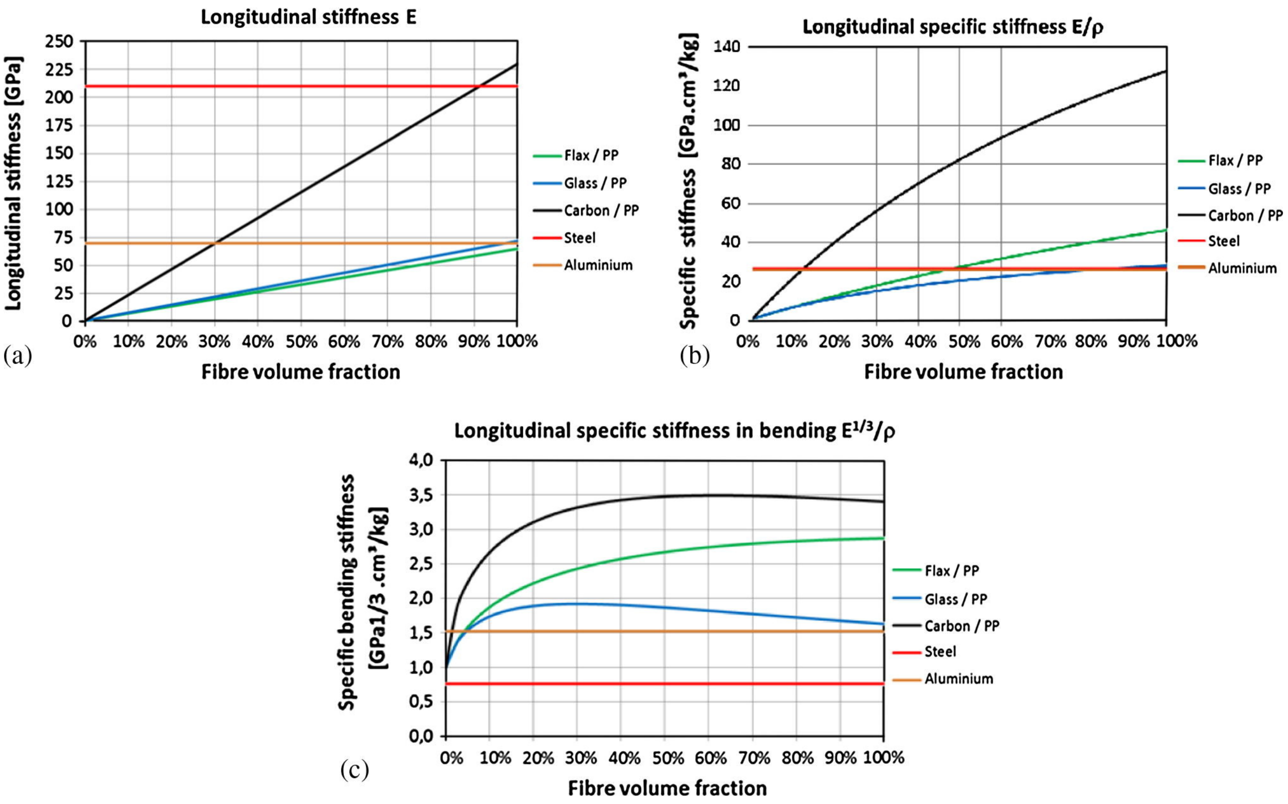

Figure 2.13: a) Longitudinal modulus, b) Specific longitudinal modulus in tension, and c) Specific longitudinal modulus in bending for fiber reinforced UD composites of flax/PP, glass/PP, carbon/PP as well as for aluminum and steel in relation to their fiber volume fraction. [33]

2.6. Applications of Flax Fiber Composite Materials

Flax fiber reinforced composites are desirable and attractive materials, because of all the mechanical/specific properties discussed earlier as well as the sustainability and eco-friendly character they offer. For these reasons, multiple applications are suitable for FFCM.

A field, which NFCM can be utilized and being exploited is the sports industry. A nice paradigm is given by the use of these natural based composites on this industry. *Notox*, is a French company, located in the Basque country, who manufactures surfboards based on flax fiber reinforced composites. [37] It produces surfboards from FFCM which are 20% lighter, very elastic and impact resistant. [37] A second example, can be the *Pure Aero* tennis racquets manufactured from the french company *Babolat* which utilize the usage of flax fibers for vibration-damping purposes and are incorporated in the head and handle of the racquet. [38]

Furthermore, *NPSP B.V.* is a Dutch company, located in Amsterdam, which develops NFCM and gives massive focus on FFCM. The materials which are generated from NPSP B.V. can be used in interior and exterior applications such as traffic signs, furniture and building panels. [39] An example, is the material *Nabasco 8010*, which can be produced with flax fibers and partially bio-based resin, utilized in bio-based generated traffic signs and offers excellent specific properties (E = 8 GPa, σ_f = 40 MPa, density = 1.7 g/cm^3) and environmental properties. [39]

Another popular and emerging field where natural fiber composites and especially flax fiber composites can be employed, is the automotive industry. Many automotive companies are trying to transition to sustainable and energy-efficient alternatives. An instance can be the Swiss company *Bcomp*, which offers many sustainable product alternatives in materials, from sports and biking equipment to automotive parts. [40] Automotive parts such as door panels, seat backs etc, manufactured from powerRibs^{TM} can reduce the weight up to 50% in cars and uses 70% less plastic, providing the natural aroma of flax fibers. [40]

Figure 2.14: Interior part of an automobile produced from poweRibs^{TM}, which contain flax fibers. [40]

Figure 2.15: Pure Aero tennis racquet with flax fibers, from Babolat. [38]

3

Transparency in Natural Fiber Composite Materials

3.1. Definition of Fundamental Optical Terms

3.1.1. Light

Light has a double character, as it can be described as both an electromagnetic (EM) wave or a quantized photon. The electromagnetic spectrum of light is not only the visible part of light that a human eye can catch, but additional spectrums which are invisible to it. [41] These are distinguished based on the wavelength (λ) of the EM character of light. Some examples can be x-rays, gamma-rays, infrared (IR) radiation, Ultra-Violet (UV) radiation etc. [41] The smaller the wavelength of a light EM wave, the higher the energy they possess. An example can be the harmful gamma-rays which have the lowest wavelength and thus the higher energy. [41] Visible light is usually characterised by wavelengths of 400-700 nm. The visible light spectrum is characterized by many different colors, which can be distinguished by seven wavelength ranges. Violet is the color with the lowest wavelength (400-420 nm) and the highest energy, while red color has the highest wavelength (620-700 nm) with the lowest energy. [41] Figure 3.1 gives a detailed description of the light EM regions based on their wavelength and energy.

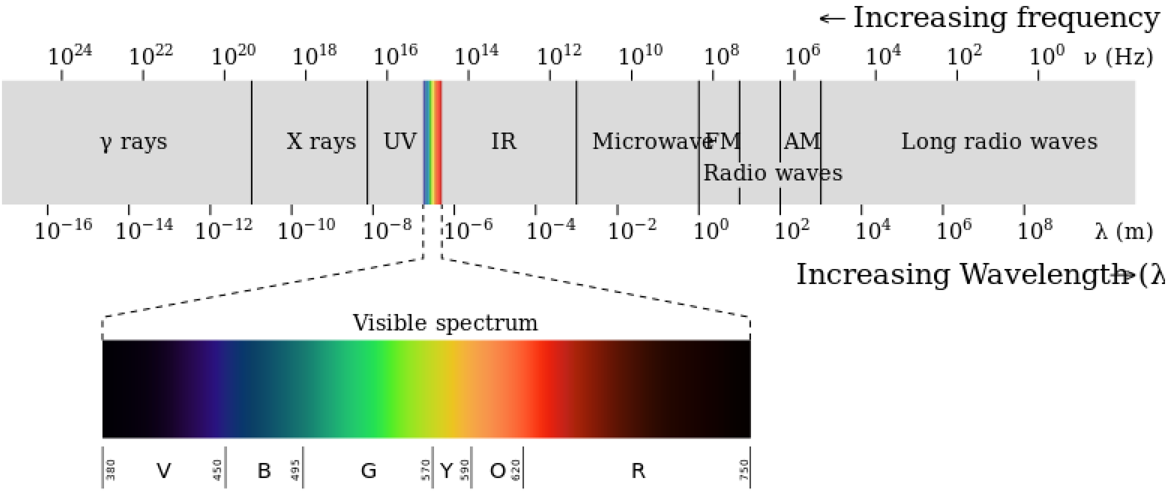

Figure 3.1: Electromagnetic spectrum of light. The light's wavelength varies from the biggest to the smallest, from left to right (γ rays to long radio waves). The visible spectrum is maximized for observation, while the chromatic aberration of visible light in relation to the wavelength is also depicted.[41]

The way light is absorbed, reflected, or transmitted can give an insight of the behavior and structure of a material. The two most crucial factors for the optical behavior of a material to light stimuli are the

Refractive Index (RI) *n* and the *Optical Light Transmittance* (T). [42]

3.1.2. Refractive Index

The most fundamental concept to start with is the refractive index of a medium, which can be defined as: [20], [42], [43],

$$n = \frac{c}{v} \tag{3.1}$$

In equation 3.1, *c* describes the velocity of light in vacuum ($c = 299.792.456.2$ m/s), in comparison to *v* which is the velocity of light in the medium. Light will always travel slower and change direction due to this change of speed, in a medium than in vacuum, and that has consequences for it. Reflection or refraction phenomena could occur for light due to this velocity mismatch. An EM wave such as light, which is trying to pass through a solid is subjected to dispersion and attenuation. [42] Dispersion is defined as the dependence of *n* on the wavelength of light and the split of visible light into its various constituent colors, while attenuation is described as the loss of energy due to various forms of scattering or absorption of the EM wave, as mentioned earlier. [42] This will be explained thoroughly in section 3.2. For these terms, light can be assumed as an EM wave.

The refractive index in anisotropic materials (such as textile fibers) varies in the longitudinal direction and in the transverse, accordingly. [43] This variation is called the birefringence of the material/fiber. In Table 3.1, examples of refractive indices of various NFs, such as flax but also glass fibers are shown. As seen there is a difference between the longitudinal and the transverse n and this generates the birefringence of the fiber. These values are very sensitive, showing a sensitivity of three decimals, which is required to describe them.

Table 3.1: Refractive indices (in the longitudinal and transverse direction) and birefringence of various NFs and glass fibers. [43]

Fibre	$n_{\|\|}$	$n_{\perp}$	***Birefrigence***
Glass	1.547	1.547	0
Flax	1.596	1.528	0.068
Cotton	1.578	1.532	0.046
Viscose rayon	1.539	1.519	0.020

3.2. Interaction of Light with a Solid

When light tries to propagate from one medium to another it can lead to transmission, absorption, reflection, and refraction/"light bending" due to a refractive index mismatch of the two solids. Refraction is the change of direction of the light in a medium, due to refractive index mismatch. On the other hand, reflection is the reversion of the direction of light when it hits a boundary that does not allow its propagation through it and light scattering is the striking of light with particles in the interior of the material which scatters light in various directions different than the initial. Optical transmittance is the most crucial property for a material to become transparent. A transparent solid allows light to propagate through it, while an opaque solid forbids this relation. This is due to backward (not forward) light scattering, reflection, and absorption. All of them are depicted in Figure 1.3. The optical transmittance can be defined as the ratio of the transmitted light intensity (both the direct transmitted $I_{T,direct}$ and the diffused transmitted intensity $I_{T,diffused}$) to the total initial light intensity I_{IO}. [8] The diffused transmittance can be related to the optical haze of a material, as haze is described by the ratio of it divided by the total transmitted light intensity. These terms are dependable on the refractive indices of the mediums, thickness, porosity, etc. [8] Refraction is happening in the interphase of the two solids when light tries to pass through it and it obeys Snell's law: [20], [43]

$$n_1 sin\theta_1 = n_2 sin\theta_2 \tag{3.2}$$

with n_1, n_2 being the RIs of the two materials, θ_1 being the incident angle and θ_2 being the refraction angle of light. This could work as an extra definition of the refractive index if one of the two different solids is substituted with a vacuum (n_{vac} = 1).

Light scattering reduces light transmittance through a solid, on various occasions i.e. the thickness of one solid overcomes a threshold value, the interfaces between the solids are numerous and not smooth (air gaps), high light absorption is present, RI contrast. [8] A strong example, is the incompatibility between NFs (hydrophilic) with the polymeric resins (hydrophobic) in NFCM. This will create many scattering sites in the material, due to the rough interphase between its constituents, which will lead to many debonding air gaps ($n_{air} \neq n_{fiber}$). A nice alternative could be a chemical treatment of the NFs, which was discussed in section 2.4. In addition, the material may contain some chemical substances with an absorptive character (i.e. lignin). This leads straight to light absorption which reduces the transmittance of light and makes the solid more opaque. Absorbed light can be transformed into a different form of energy, as heat. [8] Refractive index mismatch is a source of various problems for the transmission of light, such as the chromatic dispersion or refraction of the light. The bigger the mismatch of the refractive indices of two solids, the higher the scattering of light and thus the lower the transmittance. This implies that the light will not be able to pass through the solid or it would be distorted due to the difference of the refractive indices of the materials. [8], [20] To the contrary, RIM is a technique which can limit these problems. This method is about, choosing a material which has an identical RI as its surrounding environment (i.e. a liquid, a solid, etc) can result in neither scattering nor refraction of the passing light on its interphase. That will provide a material which will be fully invisible in the surrounding environment as its borders with the environment will not be distinct. [43] The refractive index of the materials is a very sensitive property, in which a small mismatch between the RI of the two different materials (in the third digit) can result in a scattering of the light and thus in a loss of transparency. [44]

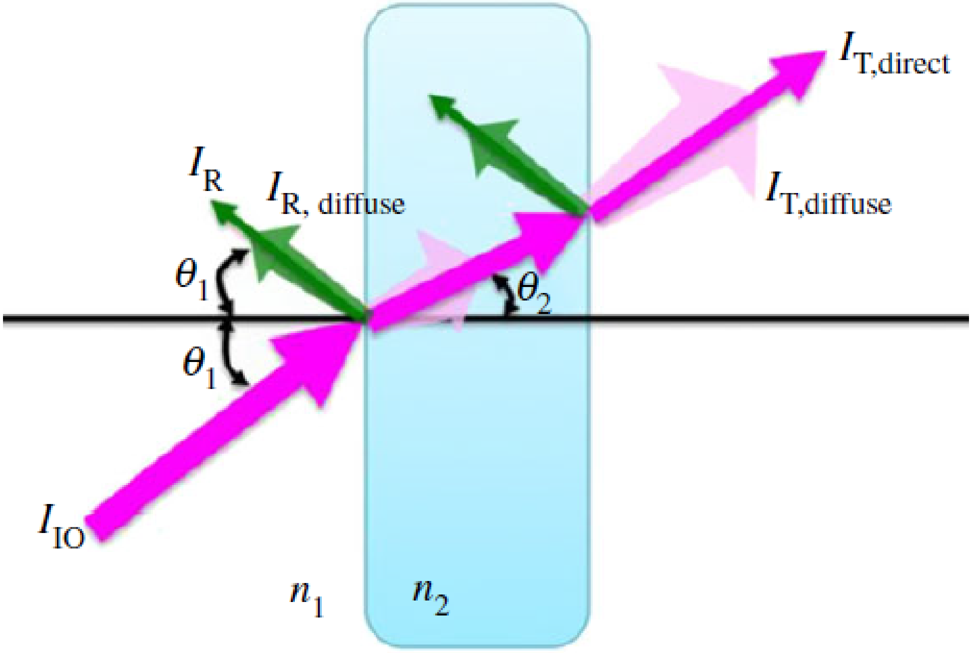

Figure 3.2: Light transmittance in two solids with a refractive index mismatch. Direct transmittance $I_{T,direct}$, diffused transmittance $I_{T,diffused}$, reflection I_R and refraction is shown. $\theta 1$ are the incident angles, while $\theta 2$ are the refraction angles. Refraction obeys Snell's law with the according angles. [8]

Also, particular interest is raised in which wavelengths of visible light, the light transmittance decreases. Based on what wavelength the light transmittance is decreased, implies an absorption of a particular light radiation due to the dispersion of light. This can be interpreted as a change of observed color in the material. When visible light hits a substance, a portion of this light based on its wavelength, can be absorbed from the material. The remaining light radiation will be either transmitted or reflected from the substance leaving a distinct color of the material. The observed color can be estimated from the color wheel, presented in Figure 3.3. Here the different chromatics of the visible light spectrum are presented in a wheel, and the observed color of the material can be assumed to be the *complementary color* (the color opposite) to the wavelength that is absorbed. [45] Only green is a special exemption which can be visible in either high absorption rates close to 700-800 nm or 400 nm. [46]

Light dispersion can also occur, depending on the RI mismatch of the fibers and matrix. [47] RI is dependable on the wavelength of visible light and if the matching of RI occurs at higher wavelengths, then colors of visible light that relate to longer wavelengths (like red) are transmitted, while low wavelength colors (like blue) are refracted due to mismatch and thus light disperses. This can also reduce significantly the transmission of light in the material, at these low wavelengths and reflect these light colors due to inner reflection which can cause this observed chromatic aberration. [47]

Designing a composite material with the pre-condition that its transparency would be the key focus, three decisive issues should be addressed. The refractive index contrast between its constituents should be the minimum possible and light absorption in the interior of the material should be low. [8] Additionally, the interface of its constituents should be smooth enough to lead to compatible interphase and non-light scattering sites.

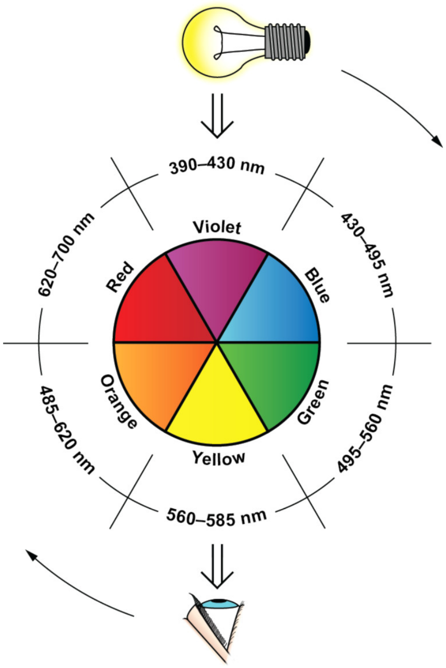

Figure 3.3: Color wheel which demonstrates the relation between the absorbed and observed color to the naked eye based on the wavelength of light . These colors are called complementary colors. [45]

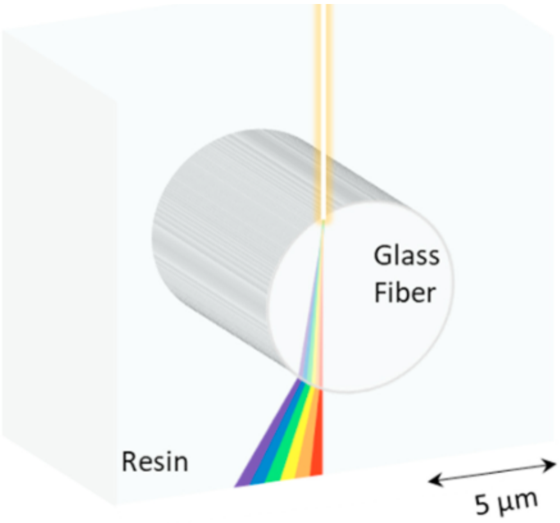

Figure 3.4: Light dispersion/refraction on GFRPs due to RI mismatch on low wavelengths of light. Violet color (low wavelength color) is refracted due to this mismatch while red (high wavelength color) is transmitted undistorted. [47]

3.3. Measurement Techniques

3.3.1. Fiber’s Refractive Index

As explained in the previous section, with eliminating the mismatch of the RIs of two solids the boundaries of those disappear and thus the interphase becomes invisible. The same can be assumed for a composite material with more than one constituents. For this material, if a fiber is impregnated with a resin of the same RI then the fiber/resin interphase becomes not visible and the fiber cannot be distinguished from the matrix. Matching the RI of two different sub-components with a final purpose of transforming it into a transparent composite material, can be achieved if at first there is a clear image about the values of their optical properties.

Testing in order to search for the RI of a fiber is a challenging procedure. Many techniques have been discovered for defining the RI of a fiber. An example is the immersion of a single fiber, such as flax into multiple liquids with a dissimilar but known RI to check for RIM. With a procedure of a trial and error an estimation of the RI of the fiber can be made. [43]

One more technique is the *Becke line* method, which can be accomplished in an optical microscope and it is based on the difference in the RI of a fiber with a liquid. A bright line can be observed in the boundary of the fiber with the liquid if there is a difference in the RI. When increasing the focus of the objective lens of the microscope, then the Becke line can cross the boundary to the solid which has a higher RI. For instance, if $n_{fiber} > n_{liquid}$ then the Becke line will move towards the bulk of the fiber. [43]

Additionally, *Heyn's method* can be utilized for the evaluation of the RI of a fiber. This works with the basis that a fiber will behave like a convex lens and the polarized light will pass through the fiber and the liquid, creating an image (a bright band in the centre of the fiber) above or below the fiber depending on the relation of the RIs between the constituents. If the fiber has a higher RI than the liquid on which is immersed, then the bright band will be visible above the fiber. In contrast, if the RI of the fiber is lower than the liquid's RI, then the image will be formed below.[43]

These methods are very valuable and revolve around the immersion of a fiber into multiple liquids with unknown RI, to estimate its RI. There are alternative methods which don't require this process. To the contrary, a single fiber is immersed into a liquid with a known RI, and a light wavelength from a monochromatic laser is alternated until the boundary of the fiber/liquid is diminished. A graph of the RI vs light wavelength can be discovered for the fiber, if this procedure is repeated for multiple liquids. This method is called the *Frey-Wyssling* method. [43]

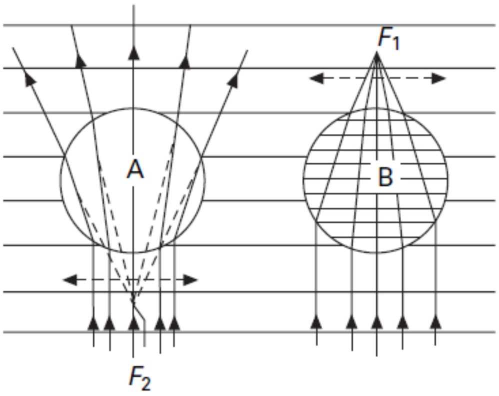

Figure 3.5: Heyn's method of evaluating the RI of a fiber immersed in a liquid when a) $n_{fiber} < n_{liquid}$ b) $n_{fiber} > n_{liquid}$. Light is refracted and passes through a bright point on the second occasion. [43]

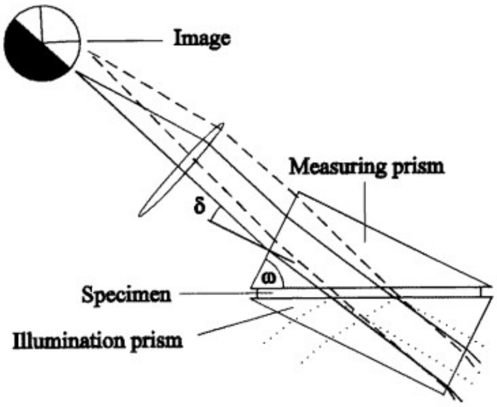

Figure 3.6: Fundamental basis of Abbe's refractometer. [48]

Abbe's Refractometer is one more popular lab instrument which can assist in the estimation of a fiber's RI. It is a simple process which can measure usually a liquid sample's RI, *n*. In this case, it can assist in the measurement of each liquid solution's RI which can be used on immersion testing or other techniques explained before. It is based on the principle of refraction on two prisms and a sample. [48] The sample is placed right between the two prisms, which have a high RI, *N*. Then the light passes through the prism and hits the sample in various angles. The condition is that if the incident angle is bigger than the $arcsin(n/N)$ and if $N > n$, then the total reflection is happening and the light doesn't propagate through the sample. In the other case, the light can pass through the sample into the measuring prism, the lenses of the refractometer, and thus forms a bright image in the eyepiece. [48] There is one angle, δ in which the transition from light propagation to total reflection is happening and a total segregation of the bright and dark ranges of the image is shown. By alternating the observation angle of the refractometer into a point at which the segregation line intersects a reticle, the measured RI, n' can be determined. [48]

3.3.2. Transmittance and Haze

In section 3.2, optical transmittance in a solid is defined. Transmittance is probably the most crucial property for a material to be transparent. All the light hindering issues for its propagation (light absorbance, scattering and reflection) should be minimized in exchange for high optical transmittance. Moreover, optical haze is one more pivotal functional property of a material which is drawing more attention for multiple applications. High optical haze can be utilized in solar cell applications because the light will be trapped for a bigger period of time due to extreme light scattering. [10] Applications of transparent building structures have required a higher optical haze, to ensure that the indoor privacy is preserved. [7]

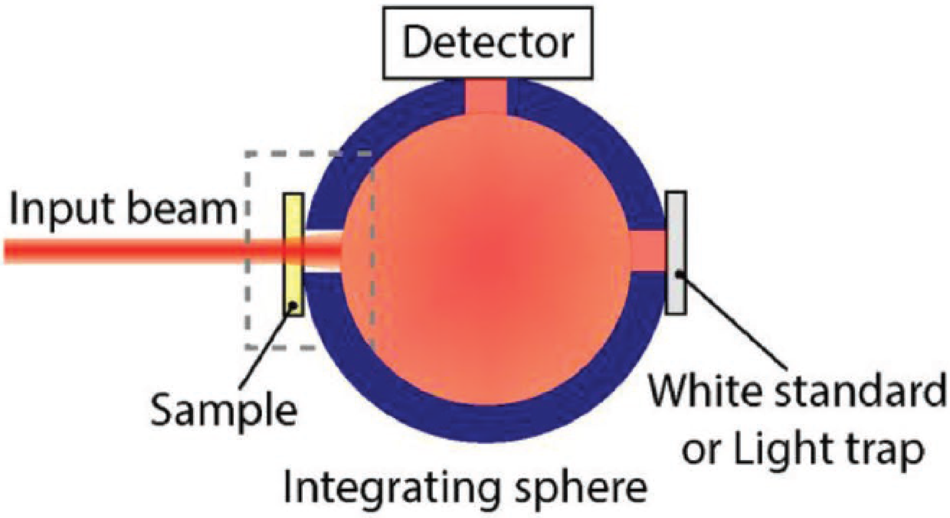

Figure 3.7: Experimental setup of transmittance and haze measurements. The configuration is consisted of the integrating sphere, the incident light beam from a light source, the photo detector, the reflectance (white) standard and the light trap. [7]

A transmittance measurement setup is depicted in Figure 3.7. It includes an integrating sphere, a light source, a photodector, an output filter and a light trap or reflectance standard (depending on measurement), according to ASTM D1003 Standard. [49] The light trap works with the principle that it absorbs all the light beam from the light source when no specimen is present. [49] Extreme care should be taken on the measurements of composite materials like transparent wood because of the high anisotropy of it. Due to the high scattering of light, this configuration can measure scattering light and thus the measured transmittance can be higher than the actual transmittance of the material. [7] More parameters can influence the measurements like the geometry of the sphere, thickness of the specimen, beam size etc. [7] Four different configurations of the experimental setup have to be implemented, for transmittance and haze measurements, according to the ASTM D1003 Standard. [49] These are:

1. T_1 is the measurement of the initial light beam. No sample or light trap is present. Reflectance standard is present and in position.
2. T_2 is the measurement of the total transmittance of the specimen. Sample and reflectance standard are present and in position. No light trap is in the configuration.
3. T_3 is the measurement of the scattered light of the instrument. No sample and reflectance standard are present. Light trap is present to detect the scattered light.
4. T_4 is the measurement of the scattered light of the instrument and sample. No reflectance standard is present. Light trap and sample are present to detect the scattered light.

The total transmittance, diffused transmittance and haze can be calculated based on the following equations: [7], [49]

$$T_t = \frac{T_2}{T_1} \tag{3.3}$$

$$T_d = \frac{T_4 - T_3(\frac{T_2}{T_1})}{T_1} \tag{3.4}$$

$$H = \frac{T_d}{T_t}100\% = (\frac{T_4}{T_2} - \frac{T_3}{T_1})100\% \tag{3.5}$$

, where T_t is the total transmittance of the specimen, T_d is the diffused transmittance of the sample, and H is the haze.

However, there are some restrictions of this methodology. Firstly, this method was designed to work for materials which have values of haze below 30%. [7] The anisotropy behaviour of the composite materials, will account for strong scattering phenomena and thus will give higher values for haze than this threshold which implies that the measurement is not fully accurate. [7] Secondly, the sample thickness and beam size should be monitored to reduce the measurements errors which will lead to incorrect values. [7]

With all of these techniques, an image of the refractive indices of fibers or resins in a composite material, can be detected as well as the optical transmittance and haze of the material. Consequently, RIM theory can be accomplished, implying the elimination of the RI mismatch between the constituents of natural fiber reinforced composites. This will minimize the scattering sites between those components. However, the light absorption issue in NFCM and the harsh interphase between the constituents of the composite material, are not solved with these techniques and other methodologies are available in the literature, such as the chemical modification of NFs presented at section 2.4 and the delignification technique considered in the following section. Next, the transformation of some NFCM into transparent materials is discussed.

3.4. Transparent Wood

There is a lot of research on transforming the traditionally opaque natural wood into transparent wood. Wood as a material is very similar to FRC as it is composed of hollow microfibers (with a big lumen) in its structure resembling a porous structure. [8], [11] This structure of wood can be compared with the structure of a FRP and thus wood can be classified as a composite material, showing remarkable specific properties (high strength, low density, high modulus). [10], [11] However, regarding the optical properties of it, it is clear that it is not transparent as a material. The two main reasons for this are the scattering of light which is present at the interfaces in the microfibers of it and the absorbing character of lignin (approximately 30% mass percentage) which absorbs UV and visible light. [20], [11]

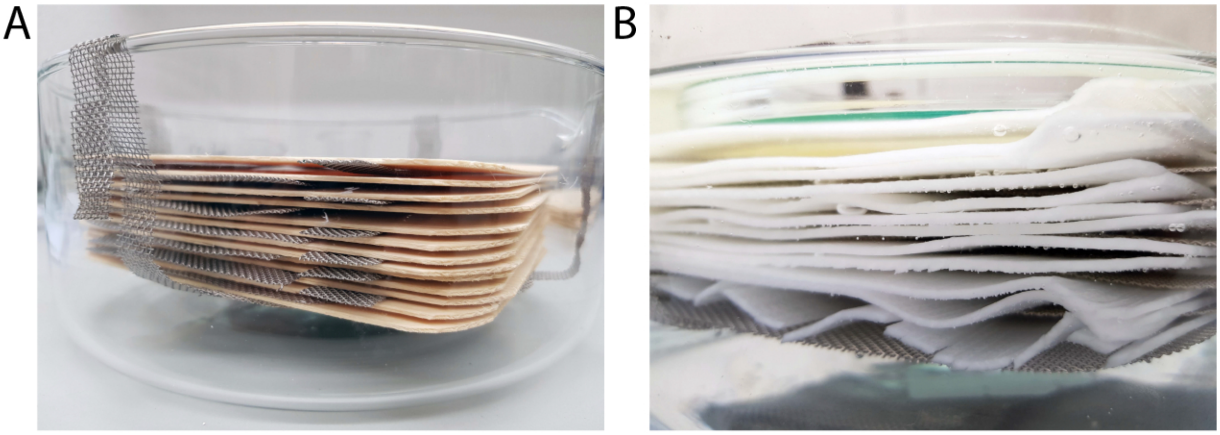

Figure 3.8: Wood veneers A) before and B) after the delignification treatment with hydrogen peroxide and glacial acetic acid. [50]

3.4.1. Manufacturing Procedure

The solution for these problems is based on the removal of the absorptive lignin from wood via a delignification method. [8], [10], [11], [12], [13] Afterwards, a polymer which has a similar refractive index as the delignified wood is infused with the assistance of the ”pipe”-like structure of wood and reduces significantly the scattering of light due to the reduction of mismatch in RI between wood and air, achieving RIM, as seen in Figure 3.9.

Table 3.2: RI of wood’s and other NFs constituents. [8], [20]

	Cellulose	***Hemi-Cellulose***	***Lignin***
Refractive index, n	$n_{\|\|}$ = 1.596, $n_{\perp}$ = 1.525	1.532	1.610

There are many methods found in the literature regarding delignification of a lignin-based material, like wood or flax. One method is via a sodium chlorite ($NaClO_2$) treatment with acetate buffer solution (pH 4.6) in an elevated temperature (80^0C) for a pre-specified period of time (6-12 hours). [10] Another one is the treatment with sodium hydroxide ($NaOH$) and sodium sulphite (Na_2SO_3) for 12 hours, followed by a treatment by hydrogen peroxide (H_2O_2). [11] Nevertheless, these methods are hazardous and unsuitable for some cases (like the degradation of the polyester yarn which holds the flax fibers together) and thus a third method is also introdueced for delignification. [20] This method is used by Frey et al. and it demonstrates a natural wood treatment with a mixture of hydrogen peroxide (H_2O_2) and glacial acetic acid in a temperature of 80^0C for pre-specified period of time depending on the lignin content (0-6 h). [50] This method is less hazardous because hydrogen peroxide produces only water as a by-product. [51] After the procedure the lignin is removed from the wood veneers and the ”brown-ish” colour of wood (due to absorptive lignin and its phenolic nature) becomes white, as seen in Figure 3.8,. [8], [11], [50] The delignification time varies depending on the sample thickness for all the techniques. Higher sample thickness imply higher delignification time periods. [51]

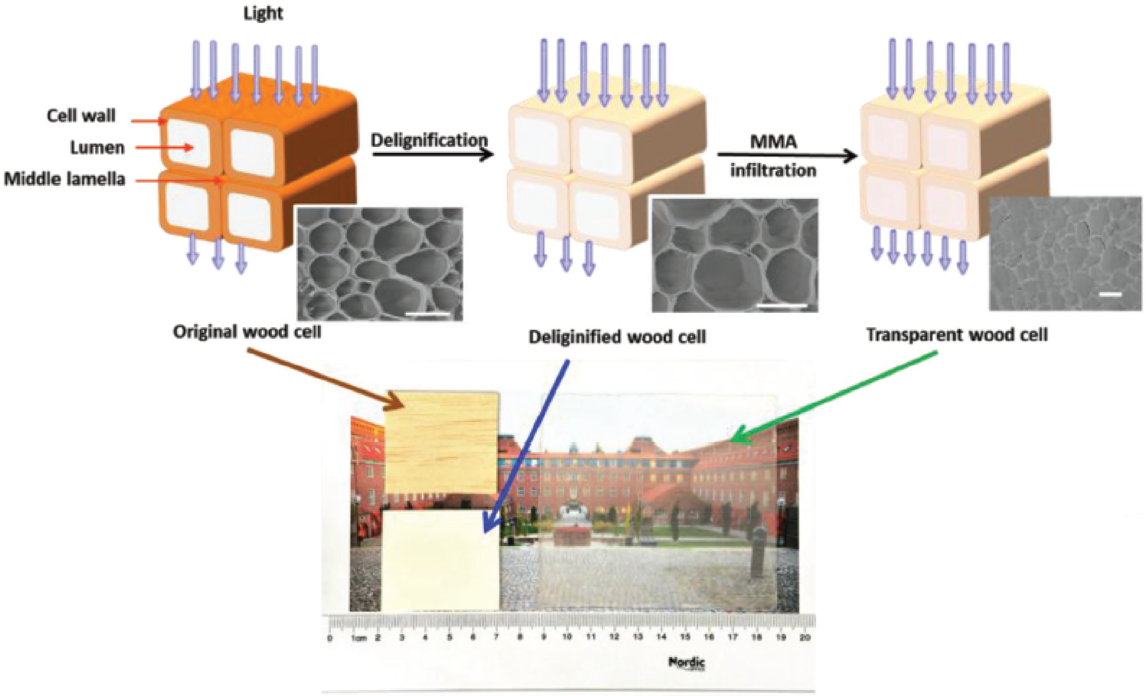

Figure 3.9: Transparent wood fabrication process with delignification of wood and polymer infiltration with PMMA which results in the transparent NFCM. The last image shows the three different wood materials, brown arrow: natural, blue arrow: delignified, green arrow: transparent wood [7]

Polymer infusion is the next step in the transformation of a wood composite into a transparent composite material. The key for this part is to focus on the refractive index matching between the polymer and the delignified wood. To implement that, an overview of the refractive index of the natural wood and delignified wood shall be made. As the majority of natural materials, wood consists of cellulose, hemicellulose, and lignin. From Table 3.2, it is understandable that lignin as an absorptive has a bigger RI than the other components, as well as that cellulose fibers exhibit birefringent properties. [20] Removing it will drop the RI to slightly lower levels (1.53). Air has an RI of 1.00, so light scattering is unavoidable in the lumen between the air and the hollow wood fibers. The bigger the RI mismatch between the two materials, the higher the diffraction angle would be. [11] Thus, an infiltration with a polymer close to RI of 1.50-1.55 would make light scattering significantly lower. Polymers that can be categorized to this could be epoxy resin(RI = 1.50), PMMA (RI = 1.49), polystyrene, PVP (RI = 1.53), etc. [8], [11] Furthermore, the polymer which is selected to impregnate the delignified wood structure plays a major role for the enhancement of the structure regarding the mechanical properties of the material. [51] With this way the delignified wood will transform from a white translucent chromatization to fully transparent, letting the light to pass through its bulk undistorted with minimal scattering based on the mismatch of wood/polymer or the air voids being present on the material.

3.4.2. Transmittance and Haze

Studies have shown that the transmittance of transparent wood with the procedure which was explained previously can reach up to levels of 85-90% in visible and near-IR regions. [10], [11], [12], [52], [13] Besides the transmittance, high haze values can be also acquired from transparent wood. [10], [11], [12], [13] High haze is achieved due to light scattering inside the wood structure due to microcavities, bumps etc. [7], [10]

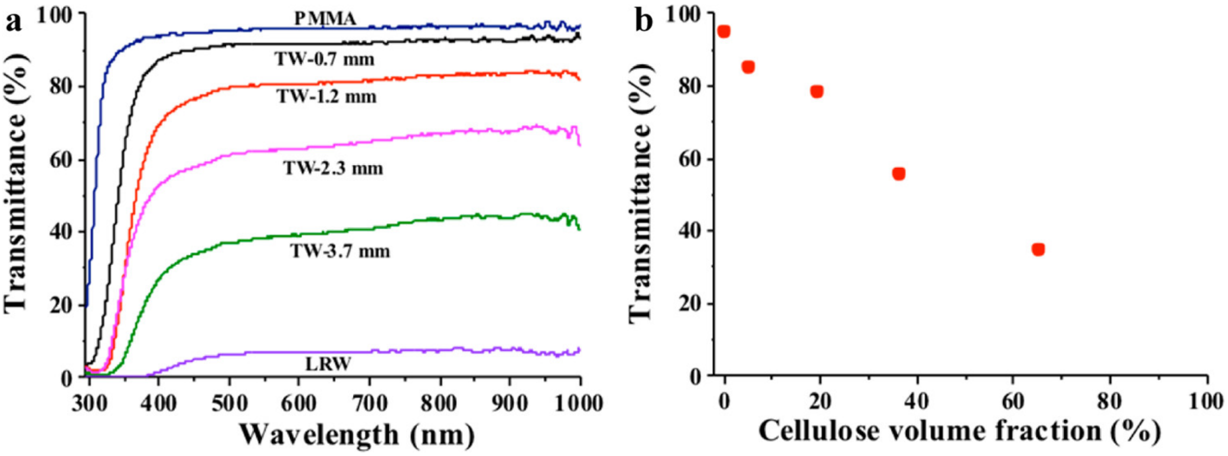

Figure 3.10: Transmittance of optically transparent wood in relation to the a) wavelength of light, the graphs depict various thicknesses of transparent wood as well as the polymer PMMA.and b) cellulose volume fraction in 1.2 mm thick sample. [10]

Figure 3.10-3.11 shows the results of a study from Li et al., for a transparent wood fabrication with a delignification method of sodium chlorite ($NaClO_2$) and a polymer infusion with PMMA, which was described in the former section. [10] It shows that the optical transmittance of the wood composite material is directly influenced by the total thickness of the specimen (thickness ↑ leads to light scattering ↑), with 85% of total light transmittance reported on a 0.7 mm thick transparent wood, while for a 2.3 mm thick material, it drops to 60-65% levels due to a longer pathway of the light. It also reports a direct dependence of both the transmittance and haze properties of the transparent wood, to the cellulose volume fraction of the wood (cellulose ↑, optical transmittance ↓, haze ↑). [10] A high transmittance level of 80-85% can be reached if the thickness of the material is minimal (approximately 1.2 mm) and the cellulose volume fraction is low (5-20%), while for a thickness of 1.2 mm and almost 40% cellulose fiber vf, the transmittance is dropped to below 60%. [10] High haze values, as approximately 80% can also be achieved depending on the thickness of the material, as higher thickness leads to higher haze values, which is reasonable as high haze requires high light scattering in the material.

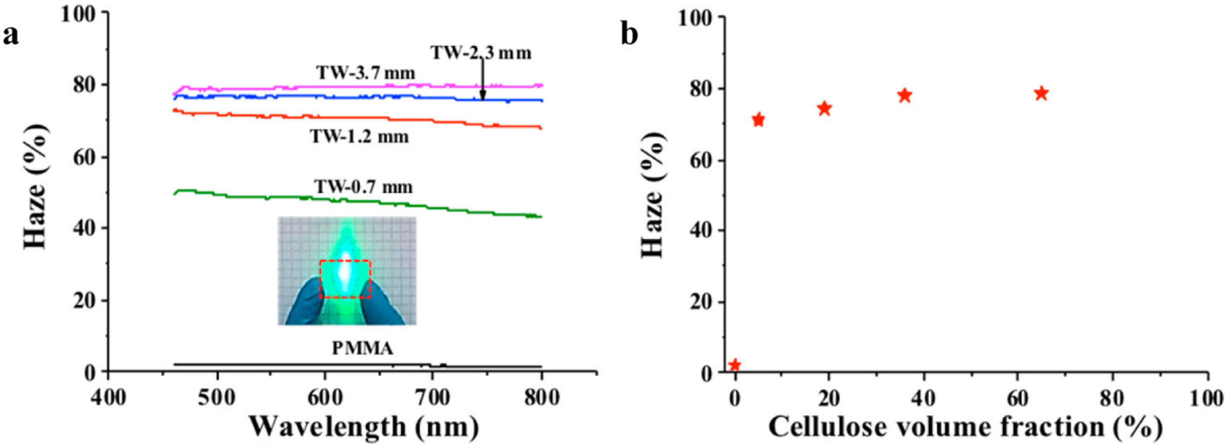

Figure 3.11: Haze of optically transparent wood relating the a) wavelength of light, the graph depict various thicknesses of transparent wood as well as the polymer PMMA. and b) cellulose volume fraction in 1.2 mm thick sample. [10]

Figure 3.12, also shows high transmittance levels, according to Zhu et al., made on transparent wood composite being fabricated with a different delignification method than the previous, concerning sodium hydroxide ($NaOH$) and sodium sulphite (Na_2SO_3) for 12 hours and then bleached by hydrogen peroxide (H_2O_2). The polymer that was used for infiltration was PVP. [11] A small sample is depicted in the same Figure showing that it is indeed see-through as the text can be read underneath it. That verifies the results which were acquainted and show a transmittance of nearly 90% in the spectrum of visible to near-IR light and can be compared to the transparency of glass. [11]

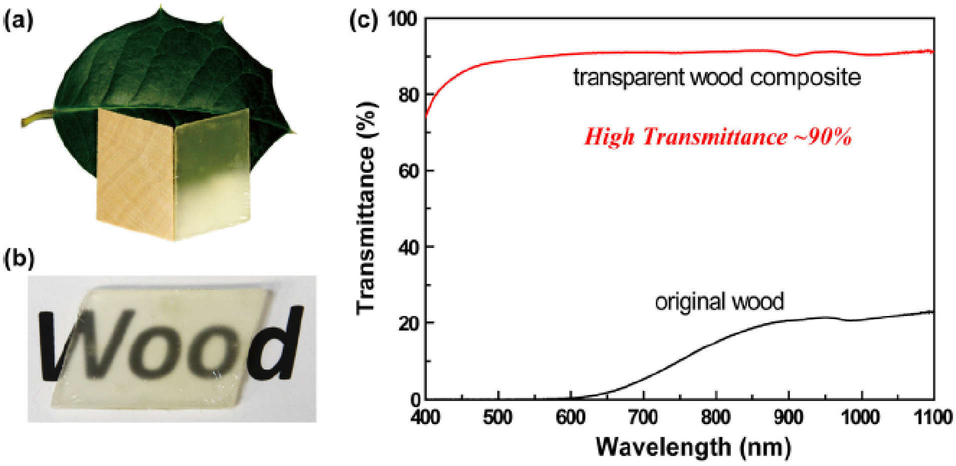

Figure 3.12: a) Transparent wood imaging b) (30 mm × 22 mm × 1 mm) transparent wood sample c) comparison of transmittance levels between transparent and natural wood in [11]

There is an immediate interest in improving the compatibility between the hydrophilic constituents of wood with the hydrophobic polymer matrices. This would assist on the improvement of not only the mechanical properties of transparent wood but also the functional properties. Li et al., improved the optical transmittance of transparent wood composite infiltrated with the polymer PMMA, by conducting surface modification on the structure of the delignified wood by sodium chlorite ($NaClO_2$). The surface modification was acetylation, which as explained in the previous chapter transforms the hydrophilic character of cellulose into hydrophobic, making the compatibility between the surfaces of PMMA (hydrophobic) and delignified wood (hydrophilic) better. [13] The transmittance which was observed in the acetylated transparent wood configurations can reach levels of 92% in low cellulose volume fractions of 5% and thickness of 1.5 mm (which is relatively close to the transmittance level of PMMA), in comparison to non-treated transparent wood's transmission level of 83% in same thickness and volume fraction. [13] Also, for a transparent wood of 30% fiber vf and 1.5 mm thickness, total light transmittance increases from 64 to 90% when acetylation treatment is implemented. Very intriguing, was the improvement of transmittance in acetylated transparent wood specimens, while the thickness of it increased.

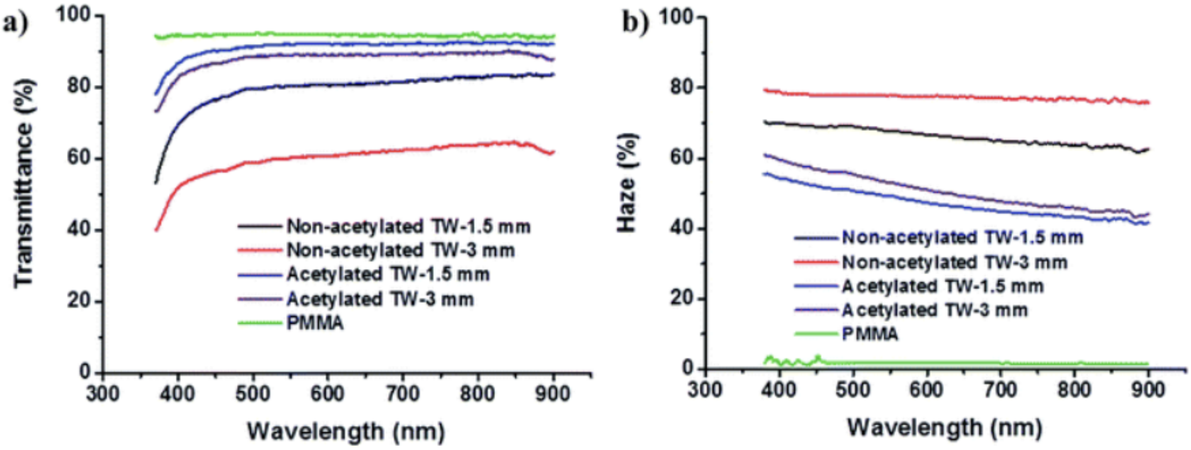

Figure 3.13: a) Transmittance of acetylated and non-acetylated transparent wood composites of 5% fiber vf and various thicknesses (1.5 mm and 3 mm). b) Haze of acetylated and non-acetylated transparent wood composites of 5% fiber vf and various thicknesses (1.5 mm and 3 mm). Light transmittance and haze of polymer PMMA are also depicted. [13]

In more detail, the optical transmittance reached 89% in 3 mm of thickness, while the non-acetylated samples showed 60%, accordingly. [13] These upgrades in the numbers, is the direct result of the boosted compatibility between the constituents, which resulted in lower light scattering. Interface debonding gaps and cellulose aggregation were found on the interphase of non-acetylated wood with the polymer in contrast to the chemically treated wood's case, on which nearly no debonding gaps and cellulose aggregation were present. [13] SEM images confirmed the previous hypothesis. Consequently, acetylation treatment in delignified wood can provide thicker composite materials consisting of transparent wood. [13]

3.4.3. Mechanical Properties

The mechanical properties of transparent wood composite are of interest, too. One of the studies discussed before showed an increased elastic modulus (3.59±0.27 GPa) for a transparent wood formation with 19% cellulose volume fraction in comparison to a transparent wood of 5% of cellulose volume fraction (2.05 ± 0.13 GPa), PMMA (1.80±0.18) and delignified wood (0.22±0.08 GPa). The tensile strength was also improved, reaching nearly double levels (90.1±10 MPa) compared to PMMA (44.1±9.5 MPa). [10] Therefore, a dependence on the cellulose volume fraction was discovered. Increasing the volume fraction of cellulose results in an increase in the mechanical properties of transparent wood composite. [10]

Three-point bending flexural testing was also implemented in the research of acetylated transparent wood. [13] Big improvements were observed both in bending strength and flexural modulus in comparison to plain PMMA polymer and delignified wood. Stress at break increased from 32.8 MPa for delignified wood and 65.9 MPa for PMMA into 78.9 MPa for their combination (transparent composite material), with flexural stiffness of 4 GPa . [13] The acetylated transparent wood reported a 30% cellulose fiber volume fraction. This is associated with better compatibility and thus stronger interlocking between the cellulose microfibers and the matrix. [13] Moreover, acetylated transparent wood with PMMA provided higher work of fracture than glass, exhibiting increased toughness. [13]

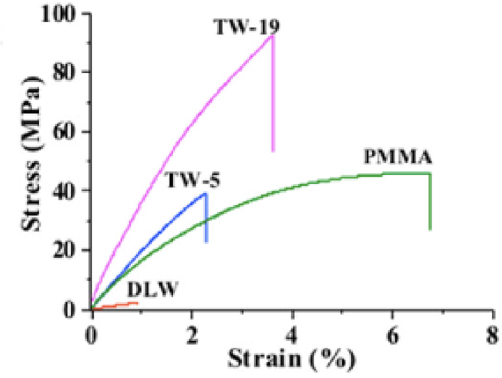

Figure 3.14: Stress-strain curves for transparent wood formations of 5% (TW-5) and 19% (TW-19) cellulose volume fraction. PMMA and delignified wood stress-strain curves are also depicted in the graph. [10]

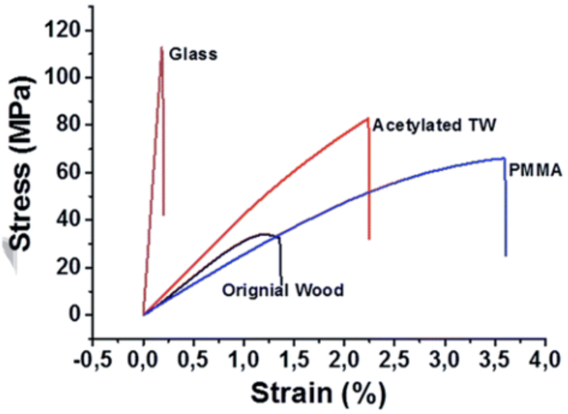

Figure 3.15: Stress-strain curves for three-point bending test of 30% vf acetylated wood along with PMMA, original wood, and glass. [13]

3.5. Other Transparent Natural Fibers

3.5.1. Transparent Flax

Besides wood, there are some studies on other NFs regarding their optical transparency in polymer composite materials. One study from Jiang et al. concerns the usage of chemically modified flax fibers as reinforcement into a polymer (PDMS), which eventually generates a highly transparent composite material that is printable in *Additive Manufacturing* (AM) processes. [14] In this research the author, modifies a natural flax fiber with a three-step chemical treatment procedure, into a transparent fiber: [14]

- Firstly, the flax fibers were soaked in nitric acid (HNO_3) and then to distilled water for sonication, to improve the dispersion and hinder the fiber agglomeration.
- Secondly, the flax fibers were delignified with both of the methods of sodium sulphite (Na_2SO_3) - sodium hydroxide($NaOH$) (Process I) for 6 h and hydrogen peroxide (H_2O_2) (Process II) for 72 h. This produces a lignin-free flax fiber with the perspective to become transparent.
- Lastly, the fibers were immersed into PDMS to generate the flax fiber composite.

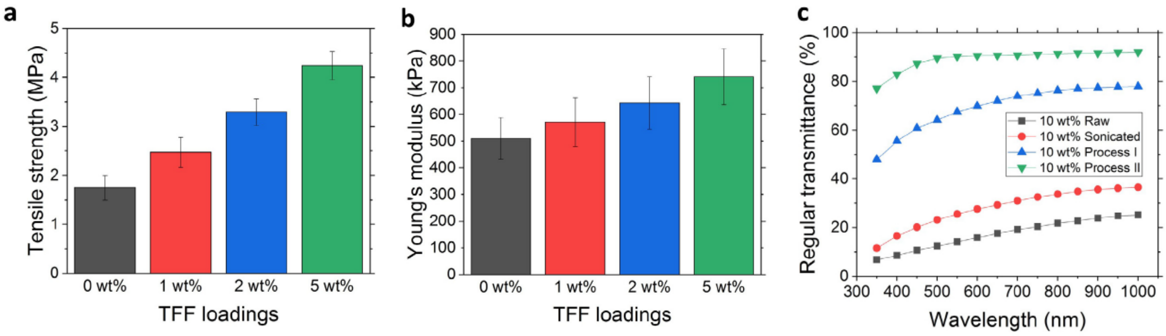

Figure 3.16: a) Tensile strength (0-5 wt%), b) Young's Modulus (0-5 wt%) and c) Transmittance (10 wt%) of light in flax-fiber reinforced PDMS after each step of the procedure explained. [14]

The result of the study was a composite material with enhanced mechanical properties, such as tensile strength, Young's modulus, and high light transmittance. [14] The tensile strength increased as high as 142% (0-5% fiber weight percentage) compared with the pure elastomer, while Young's modulus increased as high as 46%, accordingly. The transmittance was measured after process I and II, for a fiber loading of 10% weight percentage, accordingly. The results show that the transmittance can reach up to 95% levels. They also show that process I is a very important step in the whole procedure as it skyrockets the transmittance. [14] However, the flax fiber weight content is relatively small (0-10%), and for an FFCM which can be used in an industrial application, higher wt% should be achieved.

Osbild researched the RIM of delignified flax fibers into various organic compounds and afterward into polymers with an outmost target to produce a transparent flax fiber reinforced composite material. [20] The FFs were delignified with the method of hydrogen peroxide (H_2O_2) and pure acetic acid for three hours in 80^{0}C and they were immersed into organic compounds (i.e. fluorobenzene, benzene), salt solutions and two polymers for RIM (Topas and Zeonex). The results were unsuccessful as in all cases the fibers were distinguishable in the solutions and therefore no RI matching was present. The author believes that there are three roots of the mismatch between FF and solutions. [20] These are an issue of intrinsic scattering due to cellulose aggregates, light scattering due to leftover air between the microfibrils of the FF and the different hygroscopic character of a natural fiber (hydrophilic) and polymer solution (hydrophobic) which corresponds into an insufficient compatibility between these two components. [20] Also, the polymers were inappropriate for doing immersion testing for RIM due to high viscosity and high melting temperature. [20]

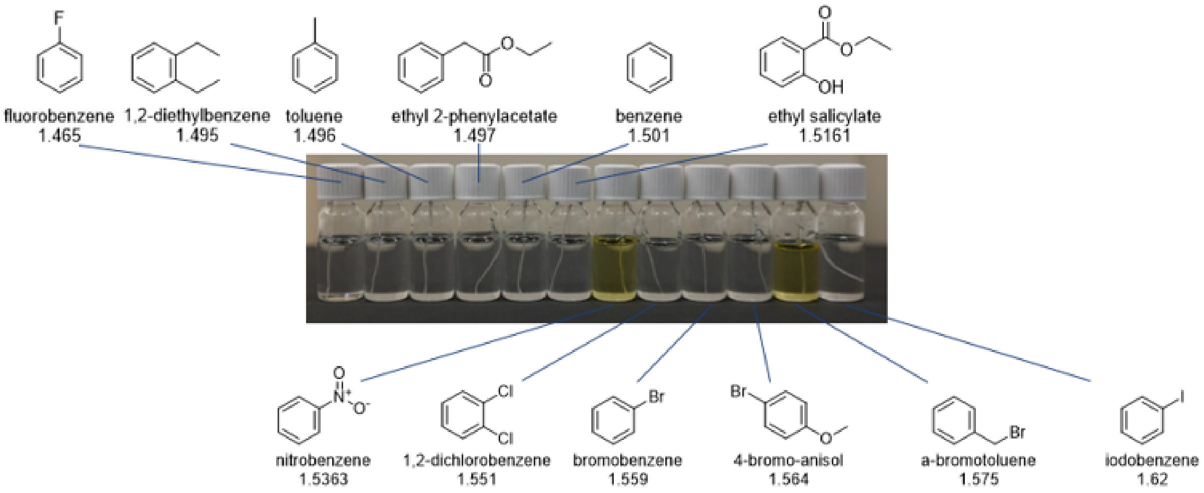

Figure 3.17: Immersion tests of delignified FFs with various organic compounds. The RI varies with each organic compound.[20]

As demonstrated, the fabrication procedure of a transparent FFCM follows the same exact blueprint based on the according process for a transparent wood composite. Delignification and polymer infusion of the fibers are pivotal steps which can not be neglected, for the case of flax fibers if transparency is the outmost target. That is due to the presence of the light-absorptive lignin in FFs (2-5%), even in lower concentrations than wood (25%). [7] Furthermore, RIM of FFs with a matrix (polymer) is another crucial parameter which has to be investigated in depth for a transparent FFCM. Both studies presented, follow this exact plan, which is successful for transparent wood but it might not be enough for the achievement of a RIM for flax fibers, according to the study of Osbild. [20]

There are primary differences between manufacturing transparent wood and FFCM, focusing on the composition and structure of the natural reinforcement of the material. Wood and flax are lignocellulosic materials that can both be used as reinforcement in a composite material. Both of them have high percentages of hydrophilic cellulose which provides great performance in composites but deteriorates the interphasial bonding between the fibers and matrix, which can result in light scattering. In FFs, the cellulose content is nearly 20% higher in composition (62-75%) than in wood fibers (40-50%), which implies a more complicated interphase with more air gaps between fiber/matrix and thus light scattering. [7], [9] These air gaps can create a RI ($n_{air} \neq n_{DL}$) mismatch in the interphase, and therefore light will scatter and transparency will not be accomplished. For this matter, surface modification alters the hydrophilicity of cellulose in a key concept for fabricating a transparent FFCM, in contrast to transparent wood for which there are studies that conclude the achievement of transparency without surface modification (possibly due to a fiber/matrix interphase with fewer defects), as explained in the previous section. Also, there are indications of cellulose aggregations in both wood fibers and flax fibers when used in FRC, which can lead to lower optical transmittance and impose surface modification for more optimal results. [13], [14]

Additionally, a huge factor affecting the RIM of wood fibers with the appropriate polymer is the big lumen they possess (10-70 μm) in comparison to the significantly smaller lumen of the elementary flax fibers (the diameter of fibers is 10-40 μm) which are combined altogether to form the technical fibers that are used in FRC. [17], [20] The porosity of the wood structure also plays a crucial role in the complete impregnation of it with a polymer.[11] After delignification, delignified wood's porosity is increased. [8], [11] This allows the polymer's infusion of the fiber to be more complete and with RIM light is propagated successfully. The smaller lumen and lower porosity of FF, are making polymer infusion and therefore light propagation more difficult in transparent FFCM than in transparent wood's case.

3.5.2. Transparent Cotton

Another very intriguing study from Abe et al., investigated the transparency of cotton fiber-reinforced polymer composite. [15] The steps of producing a transparent cotton fiber-reinforced polymer composite, are similar to the transparent FFCM and wood composite, with the exception that cotton does not contain lignin. This implies that the delignification step was not required. However, the impressive adjustment which was made in this research paper connects with the surface preparation of the cotton fibers with surface acetylation and swelling pre-treatment.

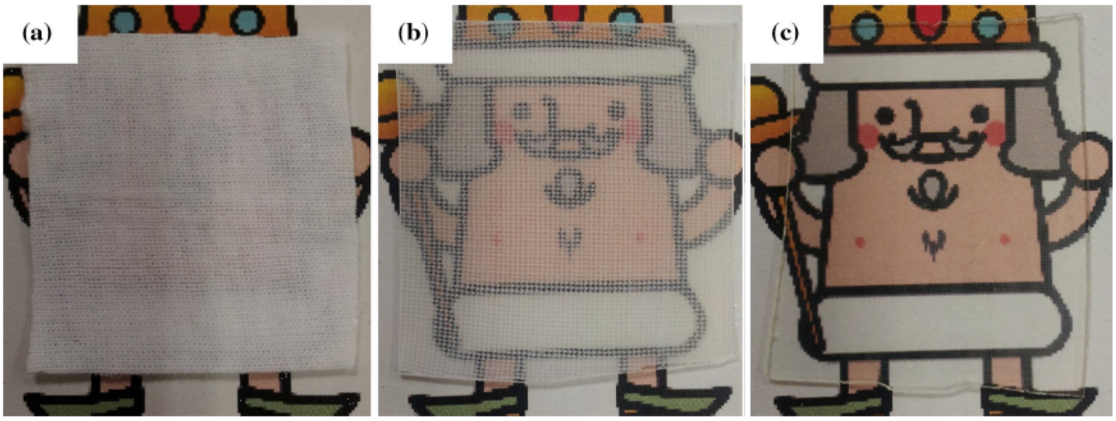

Figure 3.18: a) Image of a single cotton cloth b) Image of an unmodified cotton cloth with resin c) Image of a triple-modified (acetylation and swelling pre-treatment with TEMPO-oxidation and NaOH) cotton cloth with resin [15]

The acetylation procedure was implemented with a solution of toluene, acetic acid, perchloric acid, and acetic anhydride. [15] The swelling pre-treatment was conducted to enhance the resin impregnation between the cotton fibers and the resin, due to the non-presence of lignin which leads to strong cellulose aggregations and therefore poor wettability. [15] This was achieved with a chemical modification by sodium hydroxide ($NaOH$) followed by TEMPO-mediated (2,2,6,6- tetramethylpiperidine-1-oxyl radical) oxidation. [15] The last preparation step of the cotton composite material was the infiltration of the cotton fibers with the acrylic resin ABPE polymer under vacuum conditions. The resin has a RI of $n_{ABPE} = 1.536$. [15]

In more detail, these three treatments ensure that cellulose swells, due to the alkali solution treatment which relaxes its crystalline lattice and spaces out the cellulose molecules, as these spaces are filled firstly with Na^+ which has a big diameter and can diffuse into the empty spaces in the lattice, forming the Na-cellulose I structure and then with water molecules. [53] Next, these hydroxyl groups present in the cellulose structure are transformed into ONa- molecules which swell the molecule and completely transform the cellulose-I structure into cellulose-II. [53] Subsequently, the molecule has a wider space unit, which can allow the light to pass through its structure undistorted, as seen in Figure 3.19. Afterward, a treatment with TEMPO oxidation is implemented. This modification spaces the cellulose fibers due to carboxylation which is happening on the surface of the natural fibers. The carboxyl groups are negatively charged and repel each other, creating space for polymer infusion into deeper areas in the fiber. [15] Next, an acetylation chemical process is conducted to establish acetyl groups on the surface of the hydrophilic fibers. [15] Acetylation transforms the hydrophilic character of the flax fiber to hydrophobic, increasing compatibility between the fibers and the polymer matrix as well as decreasing the fiber aggregations. This is happening due to the hindering of the formation of hydrogen bonds between the fibers (they do not possess any polar OH groups anymore) and encourages a better interphase between the fiber and matrix, by better wettability of the fiber. These treatments settle some of the issues which were raised during this project, like the formation of voids in the interphase of the fiber/matrix due to bad compatibility (light scattering sources), fiber aggregations, or intrinsic scattering of light in the interior structure of cellulose.

The result is depicted in Figure 3.18, a transparent NFCM was yielded. The triple modification (acetylation and swelling pre-treatments) showed excellent results with a light transmittance at 88.5% at a wavelength of 600 nm in comparison to the samples formed with only acetylation of the cotton cloth which showed a transmittance of 64%, accordingly. [15] According to the paper, the high-level transmittance is achieved due to two reasons. Firstly, the fiber becomes more hydrophobic due to the acetylation process of the cotton fibers, improving the compatibility between fiber/polymer and hindering cellulose fiber aggregation. Secondly, the swelling pre-treatment assisted in the avoidance of fiber degradation during acetylation. [15]

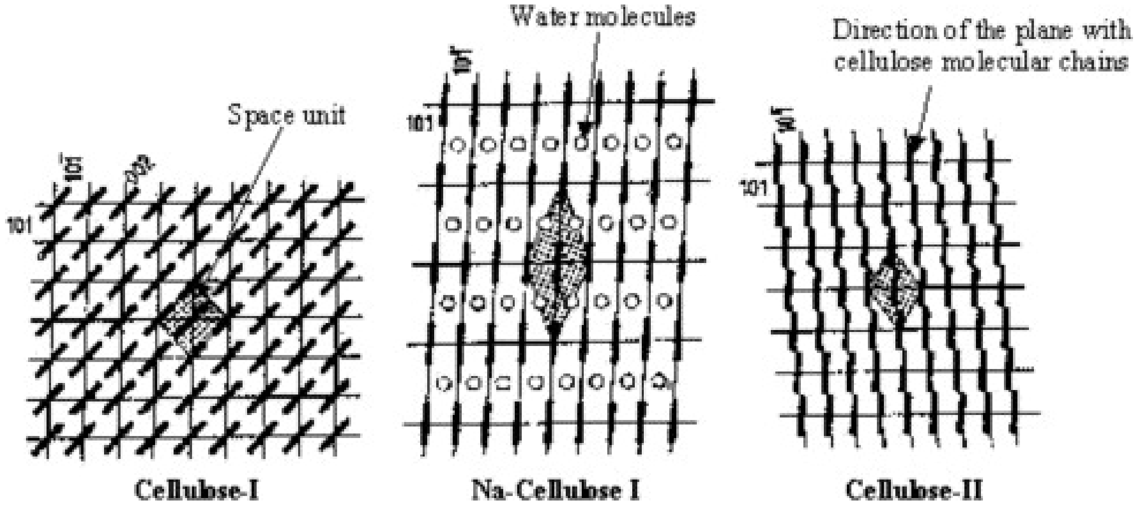

Figure 3.19: Swelling procedure of cellulose I into cellulose II with NaOH. The space unit of the cellulose lattice becomes wider. [53]

3.6. Applications of Transparent Natural Fiber Composite Materials

Transparent NFCM can be deployed in many sectors, as multiple applications can be suitable for these sustainable, functional and engineering materials. The functional (optical) and mechanical properties these materials offer are significantly valuable for the sustainable movement the society is trying to make. One application which can be utilized into are photodetectors and solar cells.

A study discussed earlier by Zhu et al., deploys a transparent wood composite material as a coating substrate in a GaAs solar cell. [11] The high transmittance and haze this material provides, can trap effectively light, which propagates easier due to high transmittance and thus increase the traveling path of the light in the GaAs, increasing the chances of capturing light inside the solar cell. [11] The boost in the conversion efficiency of the solar cell was 18.02±3% with the extra layer of transparent wood in its structure, while with a coating layer of the polymer PVP, it showed a reduced improvement of 10.1.±3%. [11]

Li et al., deployed transparent wood in a rooftop application as an energy-efficient light harvester, as observed from Figure 3.20. [54] Due to high transmittance (approx. 90%) and haze (approx. 95%), transparent wood can provide a more efficient light illumination inside the building guiding the light because of forward scattering. [54] This light scattering happens because of the pipely structure of wood in the axial direction. Transparent wood also provides remarkable thermal properties with thermal conductivity (0.32 $W\ m^{-1}\ K^{-1}$ in the axial direction of the wood fibrils, 0.15 $W\ m^{-1}\ K^{-1}$ in the transverse direction of the wood fibrils), which can provide better thermal insulation inside a building than other material like glass (1 $W\ m^{-1}\ K^{-1}$). [54] Impact toughness is also a very important advantage of transparent wood, showing excellent results (higher fracture strain than glass), due to Van der Walls forces between cellulose and the impregnated polymer. [54]

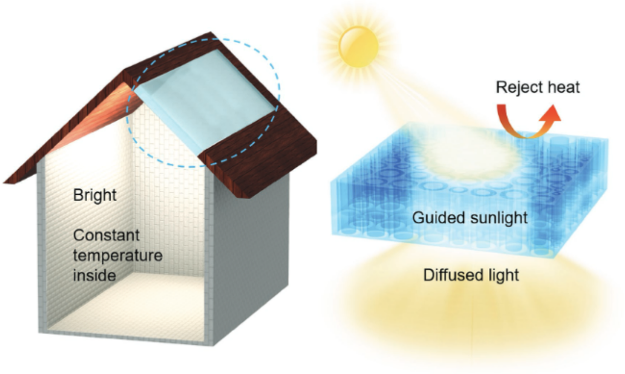

Figure 3.20: Transparent wood as a rooftop application in a smart building. Superior light illumination, thermal insulation, and impact toughness are achieved. [54]

Part II

Analysis

4

Materials and Methodology

4.1. Materials

Bcomp's *ampliTex 5025* twisted flax fiber UD fabric was provided by the *Delft's Aerospace Structure and Materials Laboratory* (DASML). The flax fibers orientation was UD with a fiber angle at 0^o and with a flexural strength/stiffness of 663 MPa/57 GPa. The fibers were connected via a polyester yarn and their areal density is 280 g/m^2. [36]. Each sample's dimensions were 12X12 (LXW) cm. *HexForce 7581* fiberglass woven fabric was provided from DASML, for composite manufacturing of glass fiber reinforced polymer (GFRP) laminates for reference materials, with an areal density of 303 g/m^2 and a layer thickness of 0.229 mm. The glass fibers were oriented both into the warp and weft directions, with the warp being the strong and durable direction. The fabric was cut into specimens of 30X15 (LXW) cm for fabrication.

Figure 4.1: Left: AmpliTex 5025 flax fibers in UD orientation, Right: HexForce 7581 glass fiber woven fabric. Both of these materials were utilized as reinforcement for the composites produced in cut pieces.

All the chemicals and organic compounds for immersion tests or fiber modifications were provided by DASML and the Applied Science faculty of TU Delft (TNW) and are depicted in Table 4.1. The polymer *Resoltech 1200* epoxy resin and hardener *Resoltech 1204*, were used as polymer testing materials for immersion tests and composite production. The resin is a colorless liquid, which has a density of 1.16 g/cm^3 and a viscosity of 6500 $mPa.s$, at room temperature. [55] The hardener is a clear to yellow liquid that has a density of 0.91 g/cm^3 and a viscosity of 18 $mPa.s$, at room temperature. [55] The flexural stiffness lies at 3.09 GPa and the flexural strength at 116 MPa for a specimen of 4 mm, while the density of the polymerized system is 1.18 g/cm^3. [55] The recommended curing cycle for this material is 24 hours at room temperature and 16 hours at 60^0C while the glass transition temperature lies at 75^0C.[55] They were provided by DASML. Moreover, high transparent epoxy casting resin *"Water-Clear", plus the Hardener W300* were provided from the supplier *R&G Faserverbundwerkstoffe GmbH*. This system was also used as a polymer testing material for the infusion of delignified flax fibers and composite production. The resin and hardener were clear transparent liquids. The resin's viscosity is 875 $mPa.s$ with a density of 1.14

g/cm^3, while the hardener's viscosity is approximately 15 $mPa.s$ and its density is 0.948 g/cm^3. [56], [57] The recommended curing cycle is 24-72 hours at room temperature, depending on the thickness and volume of the material. During this project, a 48-hour curing time period is followed.

Table 4.1: Overview of chemical substances used for immersion testing and fiber modifications.

	Immersion Testing			
Chemical	Ethanol	Benzyl Benzoate	Ethyl Salicylate	Ethyl Cinnamate
	Delignification		***Nitric Acid treatment***	
Chemical	Hydrogen Peroxide (30%)	Glacial Acetic Acid	Nitric Acid (65%)	
	Acetylation			
Chemical	Toluene	Acetic Anhydride	Perchloric Acid (60%)	Acetic Acid
	NaOH/TEMPO-oxidation			
Chemical	Sodium Hydroxide (16%)	TEMPO	Sodium Bromide	Sodium Hypochlorite (5%)

4.2. Fiber Modifications

4.2.1. Delignification

As explained in Chapter 3, the delignification method is pivotal for achieving a transparent NFCM. This is due to the elimination of the absorptive substance of lignin which is present in low concentration in FFs. For this project, a delignification procedure which follows the protocol from Frey et al. for wood, was implemented. [50] This involves soaking the flax fibers into a solution of glacial acetic acid (CH_3COOH) with hydrogen peroxide (H_2O_2) (30%). The mix was equal in volume (1:1) and was soaked into the glass beaker until the fibers were fully covered by it. Then they were infiltrated by the solution and were left overnight. Afterward, the solution was heated to 80^0C and let it mixed with the assistance of a magnetic stirrer for 3 hours. When the delignification procedure was over, the fibers were washed with pure fresh water until the pH of the solution was at 4.5. Afterward, they were placed on a metal holder to be able to move around without destroying their integrity. After washing, the fibers were left to dry via air.

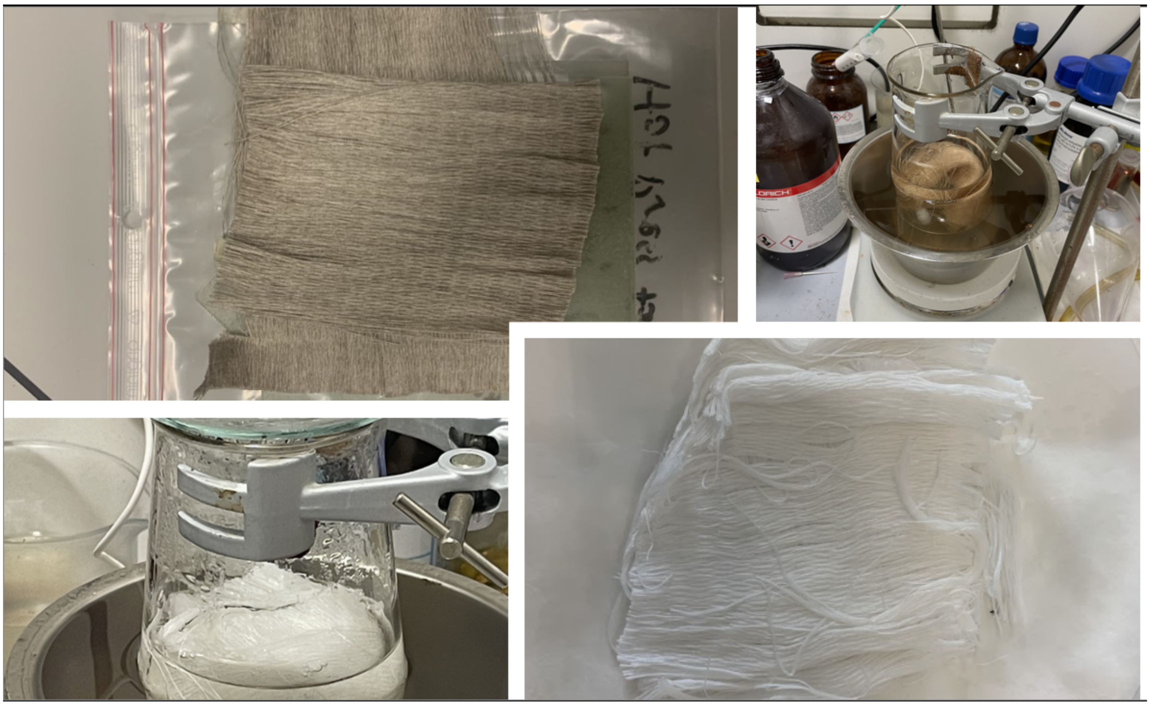

Figure 4.2: Delingification procedure on flax fiber. From top left to bottom right: Natural flax fibers stacked together, soaking the fibers into the solution, solution eliminates lignin and changes brown color into white, delignified flax fibers.

This step is fully certified from the literature in NFCM like wood or other natural fiber composites, and in all of the following treatment cases, the flax fibers had to be first delignified, to increase the chances of better light transmittance and RIM with a polymer, in order to eliminate light absorption. The period of the process is contradictory to the procedure of Frey, who conducts the delignification procedure for 6h on wood veneers. However, delignification for wood should be more aggressive due to the higher percentage of lignin which is present in wood in comparison to flax. The change of color, FTIR analysis, and lignin measurement procedure which are presented in the next Chapter, verify the success of delignification in flax on 3 h. A lignin measurement process was implemented to calculate the lignin percentage before and after delignification and to verify that delignification was successful. This is explained in the first section of the Appendix.

4.2.2. Nitric Acid/Probe Sonication Treatment

The *Nitric Acid treatment (HNO_3) together with probe sonication* was used in the paper of Jiang et al., who developed a printable highly transparent flax fiber reinforced composite. [14] According to the paper as seen in Chapter 3, this treatment improves the dispersion of the flax fibers and reduces the fiber agglomeration, issues that can lead to light scattering sources. Nitric acid treatment dissolves pectin which is crucial for bonding the elementary flax fibers, while probe sonication detaches the primary cell wall which leads to a better dispersion of the fibers and therefore hinders fiber agglomeration. [14] For this case, 2.21 g of delignified fibers were used as a material for nitric acid treatment with probe sonication. The treated fibers were used for immersion tests, to check for RIM. If then RIM was achieved, delignified flax fiber samples would be treated for composite fabrication. For a larger mass of flax fibers (concerning the UD orientation cluster), the volumes and percentages of the chemicals are proportional to the previous quantities.

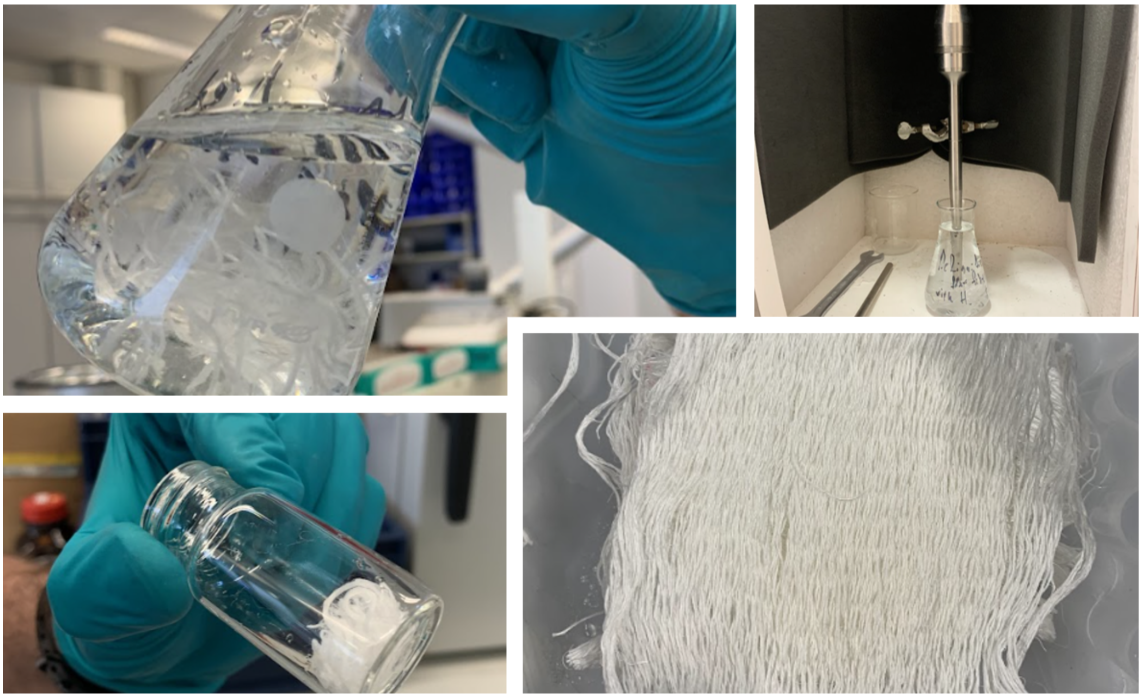

Figure 4.3: Nitric acid/probe sonication fiber treatment procedure on flax fibers. From top left to bottom right: Flax fibers soaked in HNO_3 solution, probe sonication setup, treated delignified fibers after treatment with HNO_3, and final result of treated delignified flax fibers in UD orientation.

The process that was followed during this project about this treatment, involves the following steps:

- Prepare a solution of nitric acid (65%).
- Soak the fibers into the nitric acid.
- Let them stir for 15 minutes at 100 rpm.

- After the treatment, wash with DI water to eliminate any contamination/impurities.
- Place the fibers on the probe sonication setup at 450 W.
- Wash the fibers with ethanol and ether in a solvent exchange to dry them up.

4.2.3. Acetylation Treatment

In Chapter 2, *Acetylation modification* of natural fibers is defined precisely. There are occasions in the literature that show that acetylation assists in the improvement of a material's transparency, due to better interphasial bonding, as seen in Chapter 3. [48], [13] Nevertheless, these instances concerned wood and cotton fibers. Acetylation treatment of delignified flax fibers was implemented in two different series of actions. These procedures involved a mix of toluene (C_7H_8), acetic acid, and acetic anhydride ($C_4H_6O_3$) with a small amount of catalyst of perchloric acid (60%) ($HClO_4$), each one following the papers of Bledzki et al. and Abe et al. [22], [15] The catalyst accelerates the reaction of the mixture with the fibers. However, big amounts of catalyst can lead to hydrolysis of cellulose, which degrades the fibers, especially with powerful oxidizers like perchloric acid (-15.2 pKa). [22] The major difference in the procedures concerns the volume of the chemicals that were added. On the first occasion, a mixture of 100 ml of toluene, 50 ml of acetic anhydride, and 5 ml of perchloric acid was created. [22] The second process, used smaller amounts of aggressive reactive chemicals, with 50 ml of toluene, 10 ml of acetic acid, 10 ml of acetic anhydride, and a tiny amount of perchloric acid (3 drops). The comparison between these two processes can be seen in Appendix A.4 In both cases, 1.2 g of delignified flax fibers were used as a starting investigative point. The treated fibers were then used for immersion tests, to check for RIM and afterward composite manufacturing as UD samples (combined with pre-swelling/TEMPO-oxidation). The results and differences will be discussed in the following Chapter. For a larger mass of flax fibers (concerning the UD orientation samples), the volumes and percentages of the chemicals are proportional to the previous quantities. The methodology acted by the according steps:

- Firstly, prepare the mix of toluene with acetic acid. Soak the mixture into the delignified flax fibers.
- Raise the temperature of the solution to 60^0C.
- Stir the solution with a magnetic stirrer for 5 minutes at 100 rpm.
- Add the acetic anhydride into the mixture.
- Stir for 1.5 hours.
- After the procedure, wash the fibers thoroughly with DI water and ethanol, with a solvent exchange to eliminate any remaining toluene. Let the fibers dry via air.

4.2.4. Pre-swelling/TEMPO/Acetylation Treatment

The last fiber treatment which was used for modifying flax fibers, to develop a transparent flax fiber reinforced composite, relates to pre-swelling the fibers with a $NaOH$ solution (16%) and a *TEMPO-mediated oxidation* followed by an acetylation of the fibers. This method was introduced by Abe et al. for cotton fibers, which ensures that the fibers will have available space for better resin impregnation, the cellulose crystalline structure would be spaced out to allow light to propagate, and the hydroxyl groups will be esterified due to acetylation, transforming the cotton fiber into a hydrophobic material and ensure better compatibility with the resin. [15] This modification is being implemented in the case of flax fibers with the expectation that the same result will be accomplished. The main difference between cotton fibers and flax fibers is that they don't contain any lignin, in contrast to the low percentage of it in flax fibers. [20] Initially, 2.55g of delignified flax fibes were used for this sake. For a larger mass of flax fibers (concerning the UD orientation samples), the volumes and percentages of the chemicals are proportional to the previous quantities.

The series of actions that were followed are:

- Prepare 100 ml of a NaOH solution 16%.
- Soak the delignified fibers in the solution.
- Stir the mixture for 24 hours at 50 rpm.
- After the treatment wash with distilled water and acetic acid to neutralize the fibers from the basic solution.
- Prepare a solution on 100 ml of water, adding 32 mg of TEMPO (2,2,6,6- tetramethylpiperidine-1-oxyl radical), 200mg of sodium bromide ($NaBr$) for TEMPO-mediated oxidation reaction.

- Add 3.4 g of sodium hypochlorite ($NaClO$) in 72 ml of DI water (5%) and add the solution to the mixture.
- Stir for 1h at 100 rpm and check every 20 minutes for pH to be 10, by adding 0.5 M NaOH if the pH drops.
- After the TEMPO treatment wash with distilled water.
- Perform the surface acetylation treatment as it is by the second procedure in the former subsection.

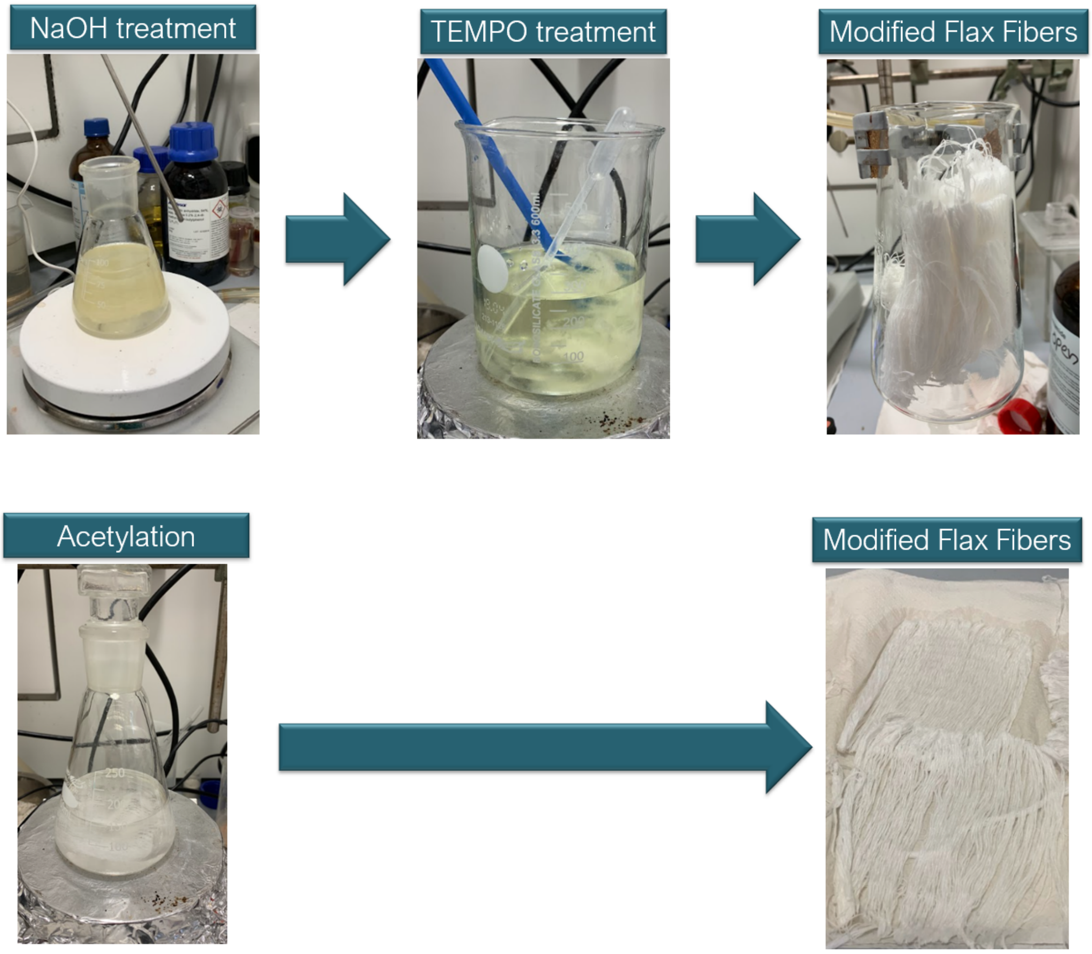

Figure 4.4: NaOH/TEMPO/Acetylation fiber modification procedure. The procedure's steps are depicted clearly and the treated fibers are depicted after each modification.

4.3. Equipment/Measurement Techniques

4.3.1. FTIR Spectroscopy

In this project, a *PerkinElmer Spectrum 100 FTIR* machine was used for FTIR analysis. Different types of flax fibers were put into the diamond holder of the FTIR machine to be analyzed. The equipment was provided by DASML, Physics Lab, and generated a .csv file for data analysis in MATLAB software. The spectra were baseline-corrected. The IR beam's spectrum which hit the sample varied from 500 to 4000 cm^{-1}. Appendix B.1 shows the equipment used and describes the fundamental concepts of FTIR analysis.

4.3.2. Uv/Vis Spectroscopy

A *PerkinElmer model 1050S Uv/vis spectrophotometer*, was used for measuring the light transmittance of various specimens. This setup contains a 150 mm $InGaAs$ integrating sphere in its interior, making it easy to measure the direct, diffused, and total light transmittance. [58] The integrating sphere's principles were described in Chapter 3, following ASTM D1003. [58] Before placing the specimen inside the holder an auto-scan for the correction/reference of 100% transmittance, was conducted. Afterward, the sample was placed inside the machine on the sample holder which was on the front side of the sphere's port and then the process was implemented, producing a .csv file for data analysis in MATLAB software. The beam's spectrum which hit the sample varied from 340 to 800 nm. The sample holder had an elliptical hole (28X17 mm) which let the light pass through the sphere's port. Appendix B.2 shows the equipment used and describes the fundamental concepts of Uv/Vis analysis.

4.3.3. Scanning Electron Microscopy/Optical Microscopy

A *JSM-7500F Scanning Electron Microscope* was used for capturing images of high resolution of various flax fibers under vacuum, with different modifications to identify how their surface structure was. Additionally, a *Keyence Laser Scanning Confocal Optical Microscope* was used provided by DASML, which assisted in the imaging of flax fibers and cross-sections of composite samples on lower magnification but was quicker. The magnification lenses that were used for the optical microscope were 2.5X, 5X, 10X, and 20X. The captured images were analyzed based on the software Analyzer LK. Appendix B.3 shows the equipment and describes the fundamental concepts of SEM and OM.

4.3.4. Refractive Index Measurements

To have an image of the optical properties of each organic compound or polymer that was used for immersion tests and to achieve RIM, the refractive index of each of the solutions was measured. This was achieved with the help of an *Abbe's Refractometer*, which was provided by the Applied Science's faculty (TNW) of TU Delft. The refractometer's fundamental concepts are explained in full detail, in Chapter 3. All the measurements were conducted at room temperature at the yellow sodium D-line of 589 nm.

4.3.5. Mechanical Testing

For mechanical properties, a 3-point bending test was conducted, to investigate the flexural strength, and flexural modulus. The test was performed on a *Zwick Roell 10 kN Tensile Testing Machine*, with a 1 kN load cell. The support span was set at 30 mm and each cylindrical support's diameter was 10 mm. The samples which were generated from the production techniques, were cut into (LXW) 65X17 (±3X3) mm. The thickness varied between the samples due to the variation of plies between the specimens but overall stayed around 0.8-1.3 mm. The span-to-thickness ratio stayed around 32:1 levels, as ASTM D7264/D7264M denotes. [59] The crosshead velocity was defined at 1 mm/min. Three specimens were created from each composite sample, to be tested. Appendix B.4 shows the equipment images and describes the fundamental concepts of 3-point bending testing and how to calculate the flexural strength and stiffness.

4.4. Immersion Testing

4.4.1. Organic Compounds

For immersion testing, organic compounds with already known refractive indices can be operated. Compounds that are commercially available and nontoxic/safe, should be used for this purpose. The idea was to mix two different compounds that are miscible and will not produce any hazardous by-products. The reason behind that is that many different ranges of refractive indices should be achieved and tested with a delignified or modified flax fiber. Figure 4.5 shows an immersion of a solid PMMA tube into water and an immersion testing solution, achieving RIM between the components in the latter case and eliminating the borders of the tube in the interior of the liquid. The same goal is targeted for a transparent FFCM, with the tube being the fiber and the matrix being the liquid. For example, if compound A has a refractive index of 1.520 and compound B has a refractive index of 1.540, the mixture of them would have an RI which will be in the range of 1.52-1.54, depending on the concentration of

Figure 4.5: An example of RIM between a solid PMMA tube that is immersed into a 300 ml glass beaker of water (left) and a solution of 72.2% tetralin 27.8 % ethyl alcohol (right). [44]

the compounds. An 80% of compound A (and therefore a 20% of compound B) mixture, is assumed to have a RI closer to 1.520 (which is the RI of compound A), while the exact opposite's index is believed to be closer to 1.540 (which is the RI of compound A). With this method, a substance with a tunable RI can be created which is very efficient for immersion tests about estimating another RI.

Benzyl Benzoate/Ethanol

Another very significant action is to narrow down the available range of substances with different refractive indices. Vacuum has the lowest refractive index of 1, while air has a RI very close to 1 and water's is 1.332. [20] On the other hand, diamond has the highest refractive index of 2.418. [20] This range is quite big so substances with RI close to certain limits have to be selected. At the beginning of this procedure, *ethanol* (CH_3CH_2OH) and *benzyl benzoate* ($C_6H_5CH_2O_2CC_6H_5$) were selected for immersion tests, to verify the assumption that DL flax fibers' RI is close to 1.53 levels. This assumption is based on the theoretical RIs of cellulose, hemicellulose (not lignin) which are the main constituents of DL FFs, as seen in Chapter 2.

Table 4.2: Refractive indices of tunable solutions of a mixture between Benzyl Benzoate with Ethanol.

No	1	2	3	4	5	6	7	8	9	10	11
Benzyl Benzoate (vf%)	0	10	20	30	40	50	60	70	80	85	100
Ethanol(vf%)	100	90	80	70	60	50	40	30	20	15	0
RI	1.361	1.390	1.411	1.434	1.438	1.473	1.501	1.511	1.530	1.540	1.568

All the measurements of refractive indices were made with the assistance of Abbe's Refractometer. All the mixtures were properly degassed before the immersion testing to remove any remaining air that could be present in the vials. The results of immersion and RIM will be discussed in Chapter 5. Table 4.2 shows the refractive index vs the volume percentage of benzyl benzoate (and accordingly ethanol). The procedure involves pouring the compounds into glass vials of 5 mL, with 5% of a volume fraction being 100μL. After that, a small chopped DL flax fiber is immersed into each vial and the result is observed carefully.

Ethyl Cinnamate/Ethyl Salicylate

Another solution that was used in immersion tests was composed of *ethyl cinnamate ($C_{11}H_{12}O_2$) and ethyl salicylate ($C_9H_{10}O_3$)*. These solutions were created and used to decrease even further the range of the refractive index, due to the results of immersion testing with the previous tunable solution which will be discussed in the following Chapter. These two substances have an RI that is closer to each other and also nearer to the theoretical RI of DL flax fibers. The span of these solutions starts from 1.52 and finishes at 1.56.

Table 4.3: Refractive indices of tunable solutions of a mixture between Ethyl Cinnamate with Ethyl Salicylate.

No	1	2	3	4	5	6	7	8	9	10	11
Ethyl Cinnamate (vf%)	0	10	20	30	40	50	60	70	80	90	100
Ethyl Salicylate(vf%)	100	90	80	70	60	50	40	30	20	10	0
RI	1.521	1.525	1.529	1.531	1.535	1.539	1.542	1.546	1.550	1.555	1.558

The procedure of merging these two substances together is the same as before. They are miscible and colorless after mixing, so the results of immersing the DL flax fiber can be easily detected. All the mixtures were properly degassed before the immersion testing to remove any remaining air that could be present in the vials. As well, the measurements of the RI of each solution is measured with an Abbe's Refractometer at room temperature. Again the plot of refractive index vs the volume of ethyl cinnamate is presented to give an indication of the RI which are detected in these series of immersion tests. The procedure involves pouring the compounds into glass vials of 5 mL, with 5% of a volume fraction being 50μL.

4.4.2. Polymers

The immersion tests with tunable solutions composed of organic compounds are the first and quickest way of estimating the RI of a fiber, however, the outmost target of this procedure is to match this property between the flax fiber and a polymer to merge a transparent composite material. So the most crucial test to implement and judge if a RIM is achieved is between the constituents of the composite material. As explained in Chapter 3, the second deciding step in developing a transparent NFCM is polymer infusion. That means that the reinforcement should be impregnated with a polymer matrix which would desirably have the same RI and therefore let light pass through its bulk undistorted. Two polymers plus their hardeners were composed and used for this scope. Resoltech 1200 is a laminating epoxy resin which can be used for the fabrication of structural parts due to its excellent specific properties and nice wettability. On the other hand, the epoxy casting resin ”Water Clear”, together with the hardener W300 is an epoxy casting system that is highly transparent, and can be used in aircraft panel fabrication, wood finishing, etc.

For the mixing of Resoltech 1200 and Resoltech 1204, the mixing ratio should be taken into account, which is $\frac{R1200}{R1204} : \frac{100}{35}$. The same exact ratio is utilized for the second polymer with its hardener. The polymer is weighted on an electronic scale and prepared/mixed in a fumehood under safety protocols. About 50 grams of polymer and 17.5 grams of hardener were used for the three immersion tests (with different types of fiber) in each polymer's case. After mixing thoroughly for 3-4 minutes, the mix is placed in a degassing chamber under a vacuum pump to remove any air from it. For mixing the more viscous Resoltech 1200/1204 an automatic mixer which mixes at 1000-2000 rpm under a vacuum is used. This is completed after approximately 1-2 hours depending if there are still air bubbles present optically in the mix. Then the mixed polymer is casted into 5 mL glass vials and a DL or modified flax fiber is immersed into the non-cured polymer which is left to cure for 24-48 hours. The refractive index of each uncured polymer and its hardener was measured at room temperature. Finally, the result is observed which is going to be discussed in the next Chapter.

Table 4.4: Refractive indices of the uncured/cured polymers, hardeners, and their mix (100:35, weight ratio) used for immersion testing.

no	1	2	3	4	5	6	Cured	
Polymer	Resoltech 1200	-	Resoltech 1200	Water Clear	-	Water Clear	R1200	WC
Hardener	-	Resoltech 1204	Resoltech 1204	-	Hardener W300	Hardener W300	R1204	W300
RI	1.577	1.452	1.539	1.549	1.446	1.520	1.560	1.538

However, the refractive index is a material property that is directly influenced and dependent by light wavelength and the curing/polymerization process of thermoset resins. [47] This means that there would be differences in the refractive index of the uncured and cured polymers. The RI of the cured epoxy resins can be calculated based on Cauchy's transmission equation: [47]

$$n_{cured} = \alpha(A + \frac{B}{\lambda^2} + \frac{C}{\lambda^4})(w_r n^r_{uncured} + w_h n^h_{uncured}) \tag{4.1}$$

with n_{cured} to be the RI of the cured mixed polymer system, α being the degree parameter of the degree cure, λ is the wavelength of light, A, B, C being the parameters of the Cauchy's equation and w_i being the weight fraction of the resin or hardener while $n^i_{uncured}$ being the measured RI of the uncured resin or hardener. Plugging the fitting parameters of $\alpha = 1.02$, A = 0.99 and B = -4146.8 and C = $1.5490X10^9$ and $\lambda = 589nm$ on which the endured resin and hardener RI were calculated, an estimation about the cured polymer system can be implemented. The results are depicted in the Table 4.4.

4.5. Composite Preparation

For composite manufacturing, Chapter 2 presented numerous production techniques. Each technique has its own special requirements and works only when a preferable outcome is wished. For instance, in this case filament winding production technique would not be recommended, as it works only when cylindrical shapes are required, its production equipment is not cost-friendly and was not available for this project. The same applies to pultrusion which is usually used for a large industrial production line and would not be very efficient for an early research project. On the other hand, compression moulding, hand lamination, or resin transfer moulding under vacuum are very efficient and quick processes that do not require advanced and expensive equipment and are easily implemented for non-complex shapes (rectangular with no thickness variation or complex edges). Moreover, the required equipment for these processes was available in the DASML lab. However, not all the techniques mentioned were implemented in this project, due to time limitations.

The technique which will be effective for the development of the transparent FFCM will be based on multiple parameters, which have to be taken into account. Firstly, mixing the polymer with its hardener will introduce air bubbles inside the material which might be not removed fully with degassing. Therefore, it is crucial to select a method that will reach the consolidation pressure and minimize (due to pressure difference) these air bubbles inside the polymer, because they can lead to light scattering due to refractive index mismatch between the air and the polymer or reflection between light and these particles. There are three main types of void formation in a polymer composite: [60]

1. Entrapped air which is introduced during impregnation.
2. Solvents which can be present in the polymer.
3. Chemical reactions which produce volatiles.

Apart from being light scattering sources which will contribute to the material's transparency in a negative way, these voids/air bubbles deteriorate the mechanical properties of a structural composite. [60] Some studies showed that a critical pressure exists, which dissolves the air and volatiles inside the liquid resin. [60] Also, this critical pressure has to be applied before the gelation point to avoid the formation of voids after it. [60] This critical pressure is defined as *consolidation pressure* of the material.

Studies have shown that the maximum amount of air bubbles that can be dissolved inside a material, is directly dependent on the pressure applied in the mold, due to Henry's law. [61] Henry's law states: [61]

$$G_s = HP \tag{4.2}$$

,

in which G_s is the gas concentration at saturation level, H is Henry's constant which is different for each resin and varies with temperature and P is the pressure applied.

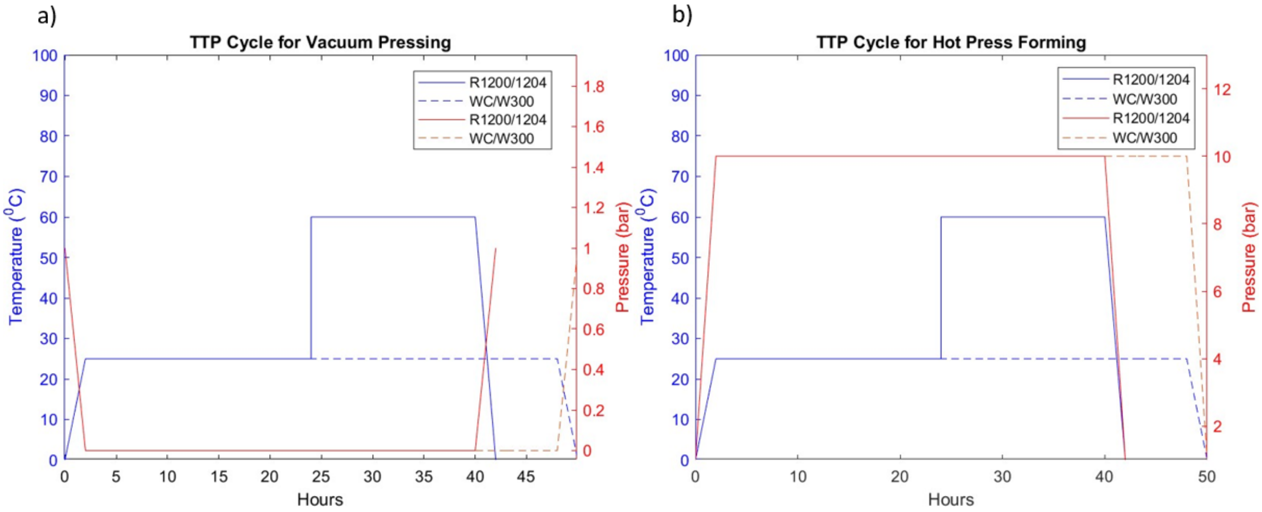

Figure 4.6: Time Temperature and Pressure (TTP) cycles based on the curing procedure of the two resins used for a) wet-lamination/vacuum pressing and b) wet-lamination/hot press forming.

Also, the thickness of the laminate will affect the optical properties of the material at a high level. Thicker laminates will scatter more light inside their structure, because of more incompatible interphases between the two constituents, refractive index contrast, and longer way for the light to pass through, as in transparent wood cases reported from the literature.[11] In this project, three different lay-ups for composite materials were fabricated to verify this exact expectation. The fiber orientation that was selected was in 0^0 and 90^0 directions for UD flax fibers. Regarding the glass woven fabric, the 0^0 relates to the warp direction. The three types of stacking sequences which were designed for composite fabrication are:

- 2 layers of alternating the fiber orientation from $0^0 \Rightarrow 90$. $[0/90]$
- 4 layers of a symmetrical laminate with alternating the fiber orientation from $0^0 \Rightarrow 90$ for the first two layers. $[0/90]_s$
- 8 layers of a symmetrical laminate with alternating the fiber orientation from $0^0 \Rightarrow 90$ for the first four layers. $[0/90]_{2s}$

However, due to some errors in handling the flax fiber samples, when they were placed into a stacked pre-impregnating material before curing, there were some slight fiber missalagnimenets and some samples presented a small difference in the fiber orientation, which can influence the mechanical properties discussed later. These errors can occur by several actions. One of them is related to the fiber modifications which can oxidize the fibers and crumble them affecting their direction (the fibers may present a slight waviness), the technician's ability to place the fibers into the correct angle and apply the resin via wet-lamination which can affect the position of them, the pressure which is applied from the machines which can slightly disorientate the fiber's direction, the weak polyester yarn which holds together the flax fibers as UD which can deform, etc. Therefore, these fiber directions on the plies are a rough evaluation that was intended to be as precise as possible.

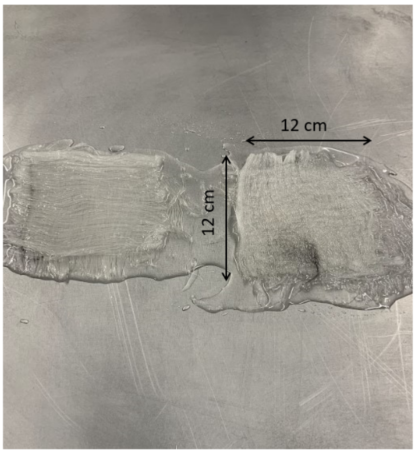

Figure 4.7: Impregnated flax fibers of $[0/90]$ (left) and $[0/90]_s$ (right) stacking sequence, placed on an aluminum mold. The fiber's samples are 12X12 (LXW) cm.

The viscosity of the resin will also play a major role in the void formation and air entrapment inside the material, as well as wetting sufficiently the fibers with the polymer increasing the chances of forming a strong bond. [62] Polymers with higher viscosity are usually harder to impregnate, due to slow impregnation velocity because of the viscous forces. Air is entrapped in the interphase of the fiber and the polymer matrix continuing to the curing of the material after a while and therefore leading to void formation, because of the incomplete impregnation. [62] Komkov et al, showed in one of their studies that the higher the relative viscosity of an epoxide resin, the higher the relative porosity in the composite material when the resin impregnates the reinforcement. [62] Also, as the viscosity of a material increases, then the vapor removal (due to degassing or consolidation) is harder. [60] As said earlier, for this project hand lamination together with vacuum pressing or hot press forming were implemented. This is due to the early research level of the project, the time limitations, the simplicity/quickness of these techniques, and the availability of the equipment which were required for them. Also, these methods would be a first indication of the suppression of air voids inside the material (if the consolidation pressure is appropriate) as well as if the resins are suitable for this kind of project.

For Hot Press Forming or Compression Moulding a *Joos Press 1000 kN* was used, together with aluminum plates as moulds. For the wet lay-up with vacuum pressing, a vacuum pump together with other materials like peel ply, release films, breathers, vacuum bag, etc, on an aluminum plate as a mould was used.

4.5.1. Wet Lamination/Vacuum Pressing

Wet lamination or wet lay-up combined with vacuum pressing is an easy fabrication procedure that relies on the technician's ability for the final quality of the product. It is a simple impregnation of the reinforcement with a handheld roller or brushes in an open-sided mold. Afterward, the pre-impregnated material will be wrapped around with a vacuum bag which will apply vacuum pressure to the material pressing it together, sucking out any air bubbles remaining in the composite, and ensuring that a stiff and strong material will be produced. In this technique the layers of the fibers are stacked into a pre-defined orientation in a mould and then resin (which is mixed with hardener and subjected to degassing) is poured all over the fibers impregnating them. After, the impregnation of each layer the resin is spread out to the whole reinforcement with a handheld roller or a brush, removing all the excessive air which is still present on the material. Then, a vacuum system with a release film, peel ply, breather, vacuum bag, and pump is applied to the mould. The vacuum pump is connected to the setup and a negative pressure of -100 kPa (-1 bar) is reached and the material is left to cure under the defined curing time period.

This procedure for the FFCM/GFRP production on this project follows the exact steps:

1. Prepare the delignified or treated UD flax fibers (accordingly the glass fiber woven fabric).
2. Apply release agent to the open-sided aluminum mould. The release agent is applied three times and is let to dry for 10 minutes.
3. Prepare the polymer mix of the resin with the hardener. Mix it thoroughly for 2 minutes. For more viscous resin systems like Resotech 1200/1204, use the automatic mixer at high rounds per minute (1500-2000 rpm) and under vacuum for more homogenous mixing of the resin with the hardener.
4. Degas the mix, into a degassing chamber with a vacuum.
5. Impregnate the fibers with the polymer and spread the polymer on it carefully, to remove any remaining air.
6. Continue with stacking the following fiber sample on top of the impregnated one and redo the same process for all the remaining ones.
7. Apply release film, peel ply, and breather on the top of the sample.
8. Apply the vacuum bag and connect it with the vacuum pump, via a valve.
9. Apply pressure of -100 kPa (-1 bar) from the pump.
10. Let the system cure for the predefined time period.

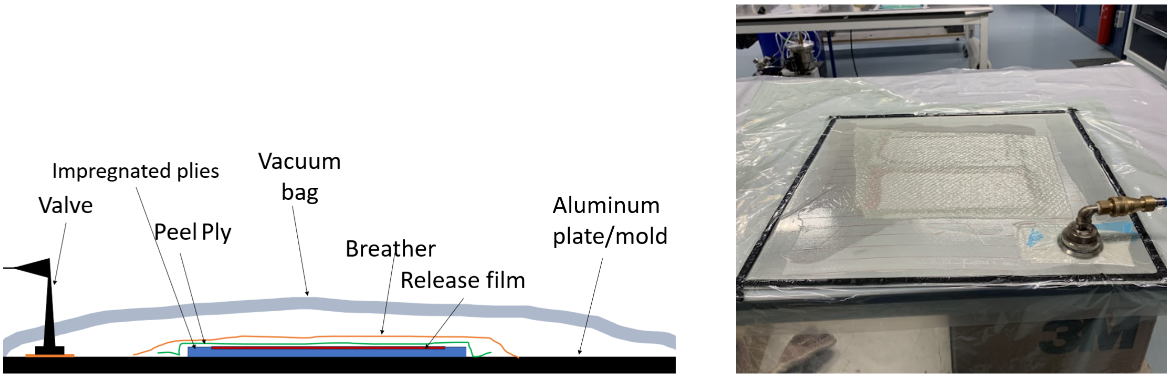

Figure 4.8: Left: Animation and Right: Setup of Wet Lamination/Vacuum Pressing. The vacuum bag, valve, breather, peel ply and aluminum mold can be clearly observed. The samples are cured under the breather material.

4.5.2. Wet Lamination/Hot Press Forming

This process is similar to the previous one, with the major difference being that no vacuum pressing is subjected. Instead, a press is utilized for hot press forming. This is to achieve higher pressures in the pressing of the material than the previous technique, which reached a pressure of -100 kPa and can achieve higher temperatures as well. The high pressure forces the liquid polymer to flow and fill out the voids between the material (i.e. on the porous structure of flax) and therefore try to displace the entrapped air. Also, higher pressure can suppress the air bubbles that are still present in the material as explained earlier, which will be negligible for affecting light transmittance of the material. However, some studies show that pressures above 60 bars in NFCM degrade the fiber significantly and deteriorate the mechanical properties of the material. [63] Therefore, this process should be treated with extreme care and preferably not surpassing high-pressure limits which will destroy the samples.

For the sake of this project, the pressure that will be used is at 1 MPa (10 bars), which is fairly lower than the limit of 60 bars which degrades natural fibers, and fairly higher (X10 times) than the -100 kPa pressure which is achieved with the previous method. With these pressures, there will be enough evidence to judge if the entrapped air is eliminated from the structure of the material. In the study of Pupin et al., the consolidation pressure that is used is at the levels of 345-500kPa (3.5-5 bars) on epoxy resin and fully dissolves the air bubbles in the resin presenting no residual porosity. [60] This means, that the consolidation pressure used at the paper of Pupin is fairly lower than the pressure used in this occasion, however used for an RTM manufacturing procedure. [60] Another study, showed that at the compression moulding on an SMC composite material, the CO_2 bubbles inside of it can be dissolved at a pressure of 0.7 MPa (7 bars), producing parts with very low void content. [64] Finally, Anderson et al. investigated the pressure effect on the void formation in hot press forming produced laminates. [65] The results indicated that by increasing the pressure from approximately 1 to 6 bars, the void content decreased significantly (5 to 1.5%, accordingly). [65] With these literature findings, it is expected that the consolidation pressure of 10 bars is fully sufficient for dissolving air bubbles inside the resin.

This procedure for the FFCM/GFRP production on this project follows the exact steps:

1. Prepare the delignified or treated UD flax fiber flax fibers (accordingly the glass fiber woven fabric).
2. Apply release agent to the two sided aluminum mould. The release agent is applied three times and is let to dry for 10 minutes, in both plates.
3. Prepare the polymer mix of the resin with the hardener. Mix it thoroughly for 2 minutes. For more viscous resin systems like Resotech 1200/1204, use the automatic mixer at high rounds per minute (1500-2000 rpm) and under vacuum for a more homogenous mixing of the resin with the hardener
4. Degas the mix, into a degassing chamber with vacuum.
5. Impregnate the fibers with the polymer and spread the polymer on it carefully, to remove any remaining air, in the lower plate.
6. Continue with stacking the following fiber sample on top of the impregnated one and redo the same process.
7. Place the second plate on top of the impregnated material.
8. Place the mould system into the pressing machine.
9. Program the press into the curing cycle (TTP) of the material, depending on the system.
10. Let the system cure for the predefined time period.

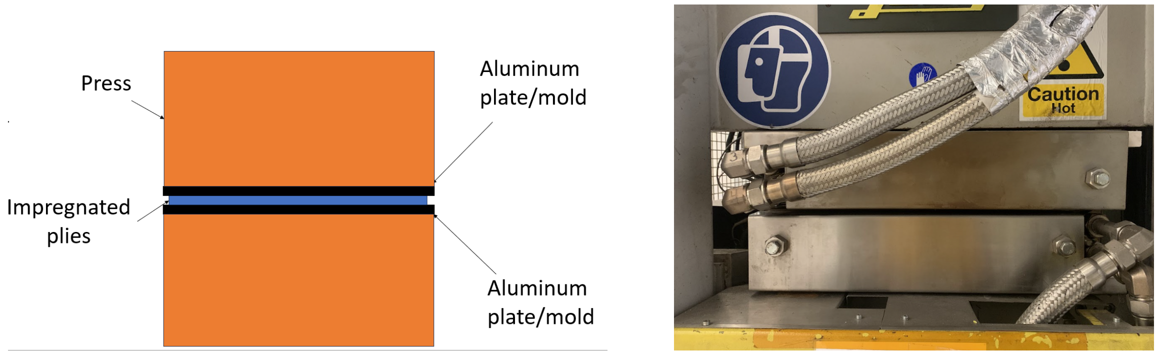

Figure 4.9: Left: Animation and Right: Setup of Wet Lamination/Hot Press Forming. The press, aluminum plates as molds, and the impregnated material are all clearly observed.

4.5.3. Composite Recipes

The design and fabrication of the composite material were based on some recipes which relied on all the previous concepts discussed. These are the materials used for reinforcement (glass fabric or flax fibers), the resin system used as a matrix, the composite fabrication technique, the fiber modification, etc. All these can light up the actions that have to be followed to develop a transparent flax fiber-reinforced composite material. The comparison between these recipes and their results will be discussed in the next Chapter.

Table 4.5: Recipes of composites which were designed for the purpose of this project.

Resin system	**Resoltech 1200/1204**			**Water-Clear/W300**			**Resoltech 1200/1204**			**Water-Clear/W300**		
Reinforcement	**Glass Fiber Woven Fabric**			**Glass Fiber Woven Fabric**			**Delignified Flax Fibers**			**Delignified Flax Fiber**		
Vacuum Pressing	[0/90]	[0/90]$_s$	[0/90]$_{2s}$	[0/90]	[0/90]$_s$	[0/90]$_{2s}$	[0/90]	[0/90]$_s$	[0/90]$_{2s}$	[0/90]	[0/90]$_s$	[0/90]$_{2s}$
	✓	✓	✓	✓	✓	✓	X	X	X	X	X	X
Hot Press Forming	[0/90]	[0/90]$_s$	[0/90]$_{2s}$	[0/90]	[0/90]$_s$	[0/90]$_{2s}$	[0/90]	[0/90]$_s$	[0/90]$_{2s}$	[0/90]	[0/90]$_s$	[0/90]$_{2s}$
	✓	✓	✓	✓	✓	✓	✓	✓	X	✓	✓	X
Resin System	**Resoltech 1200/1204**			**Water-Clear/W300**			**Resoltech 1200/1204**			**Water-Clear/W300**		
Reinforcement	**NaOH/TEMPO/Acetylation Delignified Flax Fibers**			**NaOH/TEMPO/Acetylation Delignified Flax Fiber**			HNO_3**/Probe Sonication Delignified Flax Fibers**			HNO_3**/Probe Sonication Delignfied Flax Fiber**		
Vacuum Pressing	[0/90]	[0/90]$_s$	[0/90]$_{2s}$	[0/90]	[0/90]$_s$	[0/90]$_{2s}$	[0/90]	[0/90]$_s$	[0/90]$_{2s}$	[0/90]	[0/90]$_s$	[0/90]$_{2s}$
	X	X	X	X	X	X	X	X	X	X	X	X
Hot Press Forming	[0/90]	[0/90]$_s$	[0/90]$_{2s}$	[0/90]	[0/90]$_s$	[0/90]$_{2s}$	[0/90]	[0/90]$_s$	[0/90]$_{2s}$	[0/90]	[0/90]$_s$	[0/90]$_{2s}$
	✓	✓	X	✓	✓	X	✓	✓	X	✓	✓	X

5

Results and Discussion

5.1. Fiber Modifications

5.1.1. FTIR Analysis

FTIR analysis was used in this project to identify various molecules and structures which can verify that several fiber modifications, like delignification or acetylation, were successfully implemented. The following graphs depict this exact statement, on the fiber modification which was explained in Chapter 4. Each flax fiber which was modified by delignification, acetylation, nitric acid treatment, or NaOH pre-swelling with TEMPO/acetylation modification was placed on the diamond holder and analyzed.

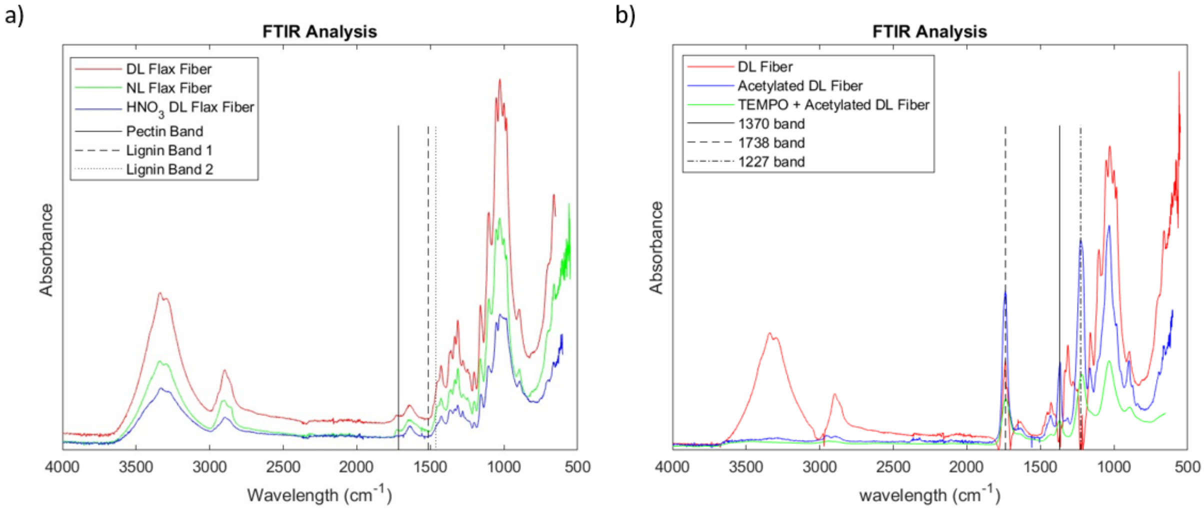

Figure 5.1: FTIR analysis on flax fibers which are modified with several fiber treatments. Important bands, which will assist with the identification of the molecules, are also depicted. a) Natural (NL), Delignified (DL) and Nitric acid with sonication treated (HNO_3) flax fibers, b) Delignified (DL), Acetylated and NaOH/TEMPO/Acetylated flax fibers.

In the above-left graph, the two lignin bands which are noted, belong to the region of 1400-1600, which represents the aromatic groups on the material. Lignin band no 1 is at 1509 cm^{-1} and lignin band no 2 is at 1460 cm^{-1} (aromatic skeletal vibration). [66] These bands can determine if the flax fiber has been fully delignified or not. On these three spectra presented on the first graph which represent a natural (NL) flax fiber (which contains lignin) and two delignified flax fibers (DL, HNO_3DL), there are no characteristic peaks that show the presence of lignin on the material. This might be the case for the natural flax fiber, due to the very low percentage of lignin which is present in the flax fibers (2-5%), in comparison to wood (25-30%). After delignification, the flax fibers lose their characteristic brown color which is due to the phenolic character of lignin, and transform into fully white. Due to the inability to detect lignin markers on the FTIR analysis, lignin content was measured based on the procedure of Appendix A.1, both on natural flax fibers and delignified flax fibers with the process of glacial acetic acid and hydrogen peroxide. The results indicated a weight percentage of 2.96% on natural flax fibers and for the delignified flax fibers a value less than 0.1%, verifying that delignification was successful as it nearly eliminates the light absorptive substance of lignin from natural flax fibers.

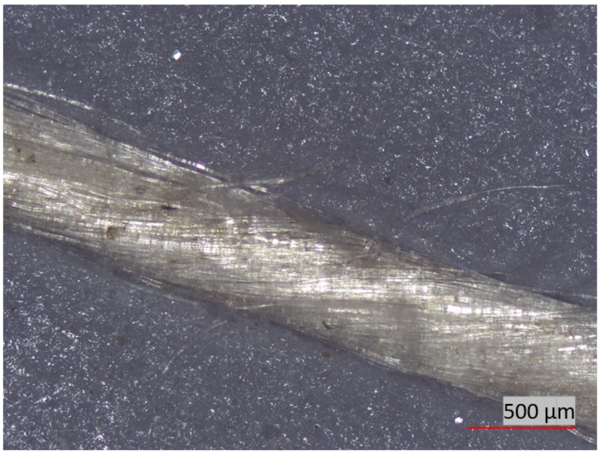

Figure 5.2: Optical Microscopy photo of: Natural (NL) flax fiber. Scale is 500 μm.

Another marker, which is depicted on the graphs is related to the substance of pectin. This marker is at 1717 cm^{-1}, which is related to the phenolic esters of pectin. [67] As explained earlier in Chapter 3, Jiang et al. at his paper stated that the treatment of flax fibers with nitric acid HNO_3 improves the dispersion of flax fibers inside a polymer and reduces fiber agglomeration, due to the fact that nitric acid dissolves pectin, which acts like a matrix for the cellulose elementary fibers, as seen in Figure 2.4. From Figure 5.1, this statement is verified, as no peak is present on the pectin band of 1717 cm^{-1} for the delignified flax fibers which were treated with nitric acid and probe sonication, in comparison to the other types of flax fibers which have a small intensity peak on this wavelength in their spectra. That implies that no pectin is present on the HNO_3DL flax fibers, which assist in an improved dispersion of them on the polymer.

On the area of 3000-3500 cm^{-1}, there is a corresponding peak area for all of the flax fibers on the left graph of Figure 5.1. This area depicts the polar hydroxyl (OH) intramolecular and intermolecular stretching in lignin, cellulose, and hemicellulose. [13] This means that there are several hydroxyl groups present on all the types of flax fibers, making them highly hydrophilic, which is expected but not desired due to the hydrophilic nature of these substances. On the other hand, the right graph depicts two other treated fibers compared to delignified flax fibers. These are delignified flax fibers treated with plain acetylation and delignified flax fibers modified with the pre-swelling/TEMPO/acetylation. From Chapter 2, it is clear that acetylation reacts with the hydroxyl groups that are present on the fiber and replaces them with acetyl group which results in an esterification reaction. This transforms the fiber into a hydrophobic fiber rather than hydrophilic one, because acetyl groups do not attract water molecules. FTIR verifies this expectation from the reduced intensity of the hydroxyl stretching peak area of 3000-3500 cm^{-1}, in contrast to the DL fiber in which this area is present. [13] Also, three extra bands which are being presented on the right graph confirm that the acetylation treatment was successful. The presence of a peak at the band of 1370 cm^{-1} corresponds to the introduction of acetate groups, due to the C-H vibration of methoxy groups, which are indicative of acetyl groups. [13] Furthermore, the two extra peaks on the bands of 1227 cm^{-1} and 1738 cm^{-1} relate to C-O and C=O stretching vibration which also confirm the presence of acetate groups in the fiber. [13] The final result is that acetylation is implemented in both of those fiber treatments, transforming the fiber into a more hydrophobic nature, which is promising for a more complete interphase with a hydrophobic matrix.

5.1.2. SEM and OM images

The surface of the treated and untreated flax fibers are investigated, in order to notice the morphological changes on the structure of them. The following pictures present SEM and OM images of natural, delignified, nitric acid-treated, acetylated, and pre-swelled/TEMPO/acetylated flax fibers.

An interesting picture is Figure 5.2, which shows a magnification of a natural flax fiber. The theory of the structure of flax fibers, which is presented in Chapter 2, can be put into realistic pieces, in this exact picture. It is clear that the technical flax fibers are fiber bundles in the mesoscale, with a diameter in the level of 200-400 μm and they are composed out of numerous small micro-fibers, which are labeled as elementary fibers. These elementary fibers are easily observable in the image above and they are connected together in a ”composite material” form with pectin being the matrix.

Figure 5.3 presents magnified images of four different types of flax fibers in an optical microscope. These are the natural flax fiber, delignified flax fibers, acetylated treated delignified flax fibers, and delignified flax fibers treated with the pre-swelling with an alkali solution (NaOH)/TEMPO/acetylation modification. The first crucial observation which is made in this analysis relates to the carboxylation of the hydroxyl groups which are present on the delignified flax fibers. In the paper from Abe et al., who converted a cotton fiber-reinforced polymer into a transparent material, there are indications that TEMPO-mediated oxidation reacts with replacing the main hydroxyl molecules into carboxyl groups. [15] Before the carboxylation of flax fibers, the paper reports a cellulose swelling procedure with an alkali solution (NaOH). These negative charged carboxyl groups create repulsive loads on the surface of the microfibers and therefore increase the spacing between them, with surface gaps being present due to the repulsiveness. [15] With a bigger empty area between the microfibers, the polymer will be infused and impregnate the flax fibers more thoroughly, leading to a superior interphase which won't be a source of light scattering due to RIM. From Figure 5.3d, there is clear evidence that the swelling pre-treatment is successful, as the fibers have bigger spacing between them in comparison to the others. However, it seems that in this instance, the elementary fibers deform and crumble which can affect their mechanical properties and therefore the final composite materials. This can be assumed to be due to the repulsive forces of carboxylation which spaces the fibers.

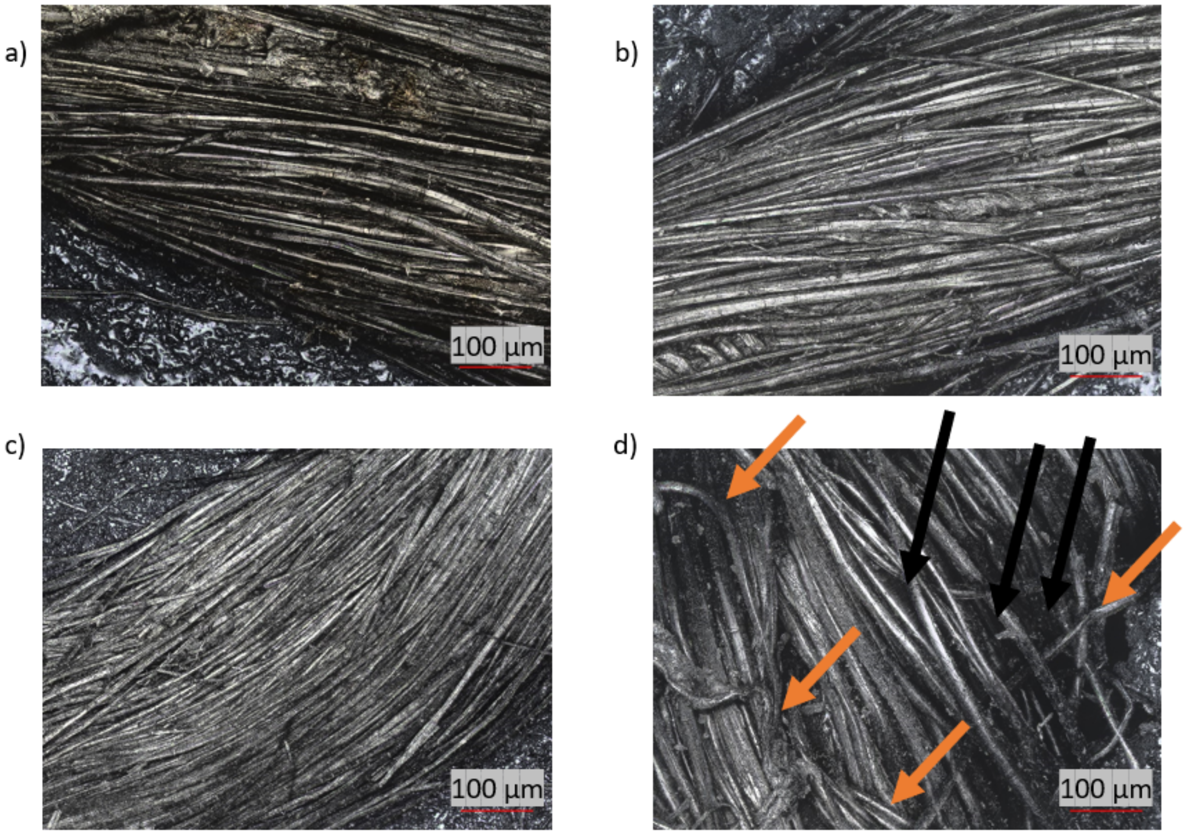

Figure 5.3: Optical Microscopy photos of: a) Natural flax fiber (NL), b) Delignified flax fiber (DL), c) Delignified flax fiber treated with acetylation d) Delignified flax fibers treated with NaOH/TEMPO/acetylation treatment. Scale is 100 μm. Orange arrows: Degraded Fibers, Black Arrows: Spaces Created

Figure 5.4 depicts the aforementioned categories of flax fibers in an even higher magnification, implemented in the SEM equipment. In this image, the natural flax fiber (Figure 5.4a) shows a rough surface that is full of impurities like wax, or other substances, in contrast to the other categories of flax fibers which don't illustrate these impurities. The acid which reacts on the delignification (glacial acetic acid, 4.75 pKa) or acetylation (acetic acid, acetic anhydride, -6.9 pKa) cleans the surface of the flax fibers from wax or other contamination, making it smoother. However, in Figure 5.4c,e, there are signs that the treatment with an aggressive oxidizer such as nitric acid (-1.5 pKa)/ acetic anhydride (-6.9 pKa)/perchloric acid (-15.2 pKa, however in very low quantities) or the treatment with TEMPO which is also an extra step introducing repulsive forces between the fibers degrade the fiber's morphology.

The image above verifies the statement which was made in the paper of Jiang et al. [14] In this paper, the author believes that nitric acid with probe sonication treatment on flax fibers can dissolve pectin and improve the fiber's dispersion in a polymer. Figure 5.4c shows better dispersion and spacing of the elementary flax fibers which can translate into better impregnation and a better interphase between fiber/matrix when the polymer infuses the flax fibers. Also, Figure 5.4e, corresponds with the comments which were a direct result of the mesoscale in Figure 5.3d above. The spacing and creation of air gaps between the fibers are clear in even higher magnifications when the flax fiber is subjected to the pre-swelling treatment with an alkali solution and TEMPO oxidation.

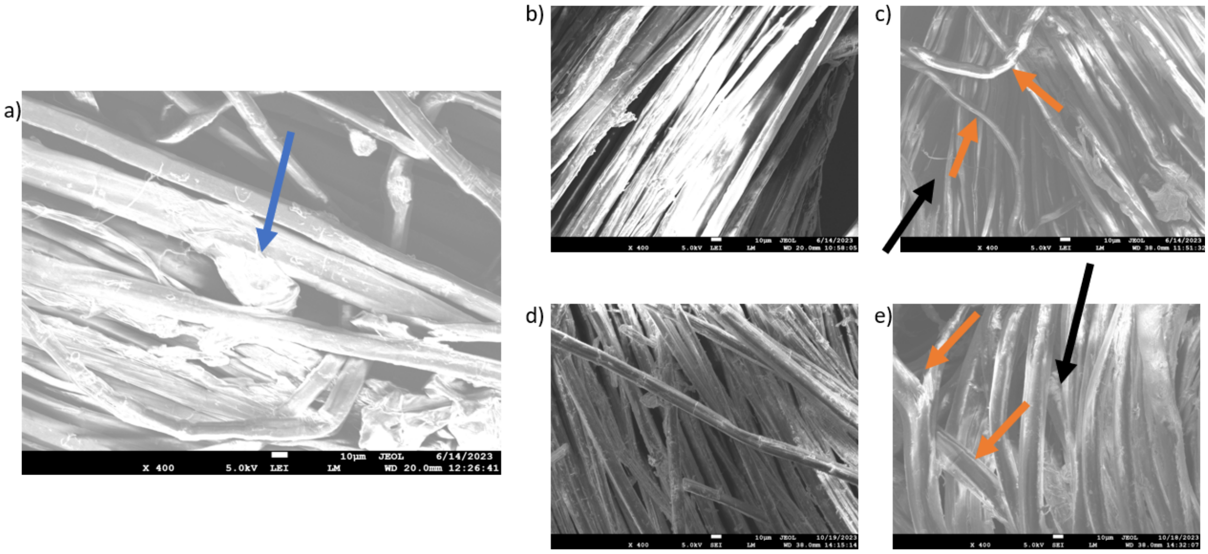

Figure 5.4: Scanning Electron Microscopy photos of: a) Natural flax fiber (NL), b) Delignified flax fiber (DL), c) Delignified flax fiber treated with nitric acid and probe sonication treatment, e) Delignified flax fibers treated with acetylation treatment. e) Delignified flax fibers treated with NaOH/TEMPO/acetylation treatment. Scale is 10 μm. Blue arrow: Impurities, Orange arrows: Deformed Fibers, Black arrows: Spaces created

5.2. Immersion Testing

5.2.1. Benzyl Benzoate with Ethanol

After the flax fiber's modifications, the next step for developing a transparent FFCM is to check for the refractive index of these types of FFs. This will allow, to define the RI of the fiber and afterward to search for a polymer material with identical RI, for infusion. With the matrix and the fiber having a matching RI, the visible light that will hit the material will not refract, reflect, or scatter. As explained earlier, in Chapter 4, two tunable organic compound solutions were created to test for RIM between them and the FF. The RIs of these solutions were already calculated and shown in Tables 4.2 and 4.3.

The first immersion test which was conducted, related to a delignified flax fiber into the organic mix of benzyl benzoate with ethanol. This tunable solution covers a wide range of refractive indices from 1.361 to 1.568, as seen in Table 4.2. The expected result of this procedure is not to have an immediate match between the refractive indices, as a difference in the third digit of this property can lead to light scattering and not an accomplishment of the preferable result. However, this first experiment can narrow down the available range of indices and afterward, another tunable solution with a smaller span can be created to re-check for RIM. Following the immersion of the delgnified flax fiber into these solutions, the main observation which is made is based on the non-accomplishment of the RIM. All the delignified flax fibers were noticeable when immersed in all the solutions. Nevertheless, when the refractive index advances to the level of 1.530 (80% Benzyl Benzoate-20% Ethanol), the fiber becomes slightly less visible. This can relate to partial RIM, with the RI close to 1.530. This fact can be justifiable with the theory presented in Chapters 2-3, which shows that the flax fibers are consisted of high percentages of cellulose, hemicellulose, and low percentages of lignin with RIs presented at Table 3.2. With lignin being the constituent with the highest RI (1.61) and the other two components having RIs close to 1.53 levels, it makes logical sense that eliminating lignin from the flax will lower the levels of the index to this magnitude.

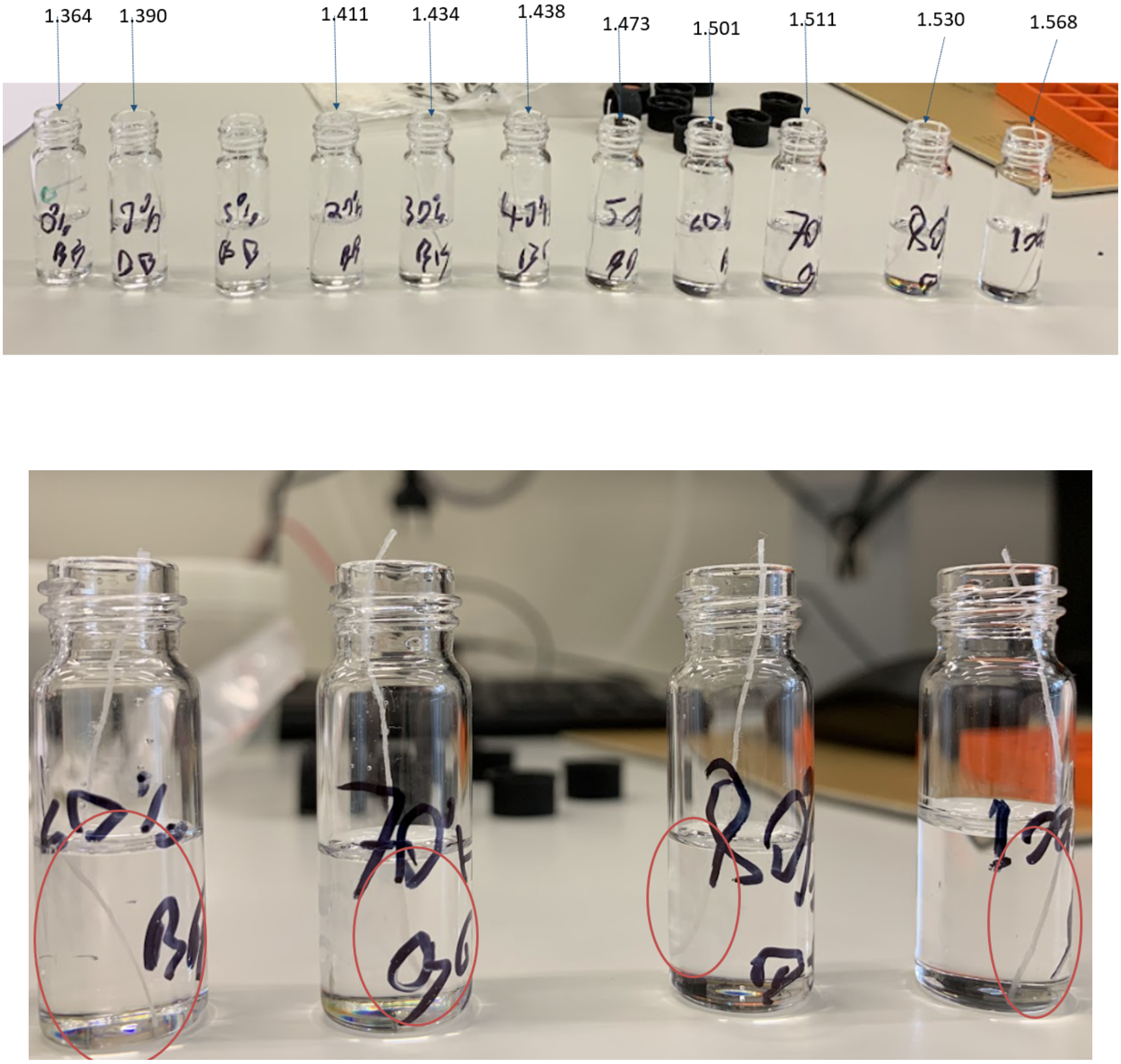

Figure 5.5: Immersion testing with delignified flax fibers into a tunable solution of Benzyl Benzoate and Ethanol. Each solution's volume is 2 mL. The refractive indices of each solution are depicted in the image. Top image, from left to right: 0-100% Benzyl Benozate. Bottom image, from left to right: 60-100% Benzyl Benzoate.

The non-accomplishment of RIM between the delignified flax fiber and the solutions can be attributed to several causes. The most important one is the mismatch between the refractive indices which scatter light. There is an assumption that the delignified flax fiber is lowered down to 1.53 levels, however, the exact RI is not known and a mismatch on the third digit (in this case the mismatches are even in the second digit) with the solution can lead to the fiber being clearly visible due to light scattering and internal reflection.

Another issue could be the hydrophilic character of the delignified flax fiber. As shown in the previous section, FTIR analysis verified that delignified flax fibers contain a lot of hydroxyl groups. [68] Flax fibers are lignocellulosic materials that contain higher percentages of cellulose than wood as well as some extra components, like pectin. Cellulose is hydrophilic, contains a lot of hydroxyl groups and obstructs a smooth interphase between a polymer due to its hydrophilic character, creating gaps in the interphase, which leads to light scattering because of the RI mismatch between the fiber and air. [68] This happens due to the inability of the polar hydrophilic OH groups to bond with the non-polar hydrophobic polymer, because of the hydrogen bonds which in that case hinder the wettability of the interphase of the fiber, creating gaps between the fiber/matrix which are light-scattering and refracting sources. [68] Therefore, RIM is not fully successful, and optical transmittance is reduced.

Table 5.1: RI and observations for the immersion tests of delignified flax fibers with the tunable solution of Benzyl Benozate and Ethanol.

Benzyl Benzoate (vf%)	**Ethanol (vf%)**	**RI**	**Observations**
0	100	1.361	Delignified flax fiber visible
10	90	1.390	Delignified flax fiber visible
20	80	1.411	Delignified flax fiber visible
30	70	1.434	Delignified flax fiber visible
40	60	1.438	Delignified flax fiber visible
50	50	1.473	Delignified flax fiber visible
60	40	1.501	Delignified flax fiber visible
70	30	1.511	Delignified flax fiber visible
80	20	1.530	Delignified flax fiber slightly less visible
85	15	1.540	Delignified flax fiber slightly less visible
100	0	1.568	Delignified flax fiber visible

The high percentage of crystalline cellulose can be also a possible cause of light scattering and therefore reducing the transparency of a material. Native cellulose can have either crystalline structure (like cellulose I which was presented in Chapter 2), or an amorphous structure. [53] It is highly important to understand that in flax fibers, amorphous cellulose is located on the surface of the fiber, while crystalline cellulose is on the core. [69] With delignification, the aggressive oxidizing environment, dissolves the amorphous cellulose and eliminates lignin together with a small amount of hemi-cellulose, which increases the content of crystalline cellulose. The amorphous structure of a material contributes to the high transparency which is desired. [70] This is due to the high atactic structure which presents areas with high spacing and allows light to propagate through it, in comparison to crystalline or semi-crystalline structures. [70] On the other hand, crystalline cellulose structure can affect light transmittance as the spacing between the cellulose crystallites can be relatively smaller than the wavelength of the visible light, and as a result, it does not allow it to propagate through, increasing the light scattering of the material. [70]

Cellulose aggregation is a phenomenon that occurs in NFCM due to the fact that natural fibers tend to form hydrogen bonds with each other because of the polar hydroxyl groups that are present and thus create light-passing obstacles. [68] Cellulose aggregation can lead to light scattering sources in their boundaries, as cited in many cases in the literature. [20], [14], [15]

The small lumen of flax fibers can be problematic for the achievement of RIM. A big difference between flax fibers with wood's structure is that wood contains a honeycomb structure with big lumens which can reach 10-70μm in contrast to elementary flax fibers which's the whole fiber's diameter can reach the same levels, as seen in Figure 2.4. [10] That implies that the lumen of flax fibers is extremely smaller than 10-70μm and therefore the impregnation of it with a polymer is more challenging because the flow of the polymer inside the lumen will be problematic. A small lumen can hinder the infusion of these solutions in the interior structure of flax because of remaining entrapped air inside the structure of flax fibers, leading to light scattering.

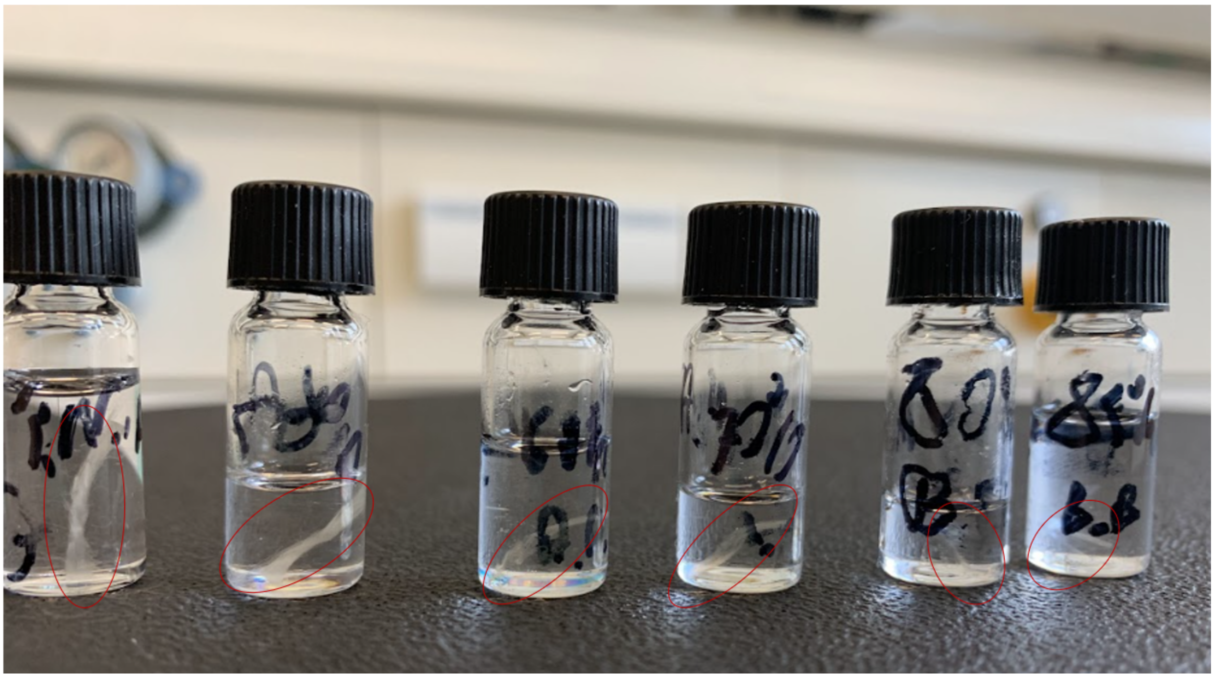

Figure 5.6: Immersion testing with delignified flax fibers which have been subjected to nitric acid treatment with probe sonication, into a tunable solution of Benzyl Benozate and Ethanol. These solutions are not of constant volume. 40-85% Benzyl Benzoate.

To tackle some of these issues, the aforementioned fiber modifications are implemented. This implies, that new immersion tests were conducted with treated delignified flax fibers immersed in the same organic solutions. The immersion tests of delignified flax fibers treated with nitric acid and probe sonication are presented in Figure 5.6. These tests showed slightly better results than the same checks with plain DL flax fibers. The eye test shows that the borders of these treated FFs are again slightly visible in the solution, however less visible in comparison to the previous occasion. Especially, when the solution is composed of 80-85% of B.B. and 15-20% ethanol (R.I. = 1.530-1.540), the results show (Figure 5.6) that the fiber is not fully invisible, but it is in fact partially visible. This can be attributed to the better dispersion and impregnation of the fiber into the hydrophobic organic solution. The hindering of fiber aggregation allows the (partially) matching solution to penetrate the fibers with more ease, reducing the number of inadequate interphases and achieving RIM between them. After the treatment with nitric acid, the fibers turn softer and fluffier and fibrillation occurs, which can be an effect of pectin removal from the nitric acid which works as a matrix between the cellulose fibers. In other words, the pectin removal corresponds to the freedom of the elementary fibers from the fiber bundles, which allows a superior impregnation of the fibers due to better dispersion and spacing of them.

A delignified flax fiber which is treated with NaOH/TEMPO pre-swelling treatment and followed by acetylation is immersed into the same solutions of Benzyl Benzoate and Ethanol. Again, the most promising outcome was extracted from the mixtures of 80-85% of B.B. and 15-20% ethanol (R.I. = 1.530-1.540). This implies, that the fiber modifications (except from delignification, due to elimination of lignin) are not affecting the refractive index of the flax fiber (at least in high levels $\approx$0.01-0.02), as in all cases the partial match of the fiber with the solutions was made at 1.53-1.54 levels. As before, the fiber treatment seems to decrease the visibility of the DL fiber inside the solution. In this case, it can be attributed, to the fact that the alkaline treatment swells the fiber's structure, TEMPO-oxidation provides the available fiber spacing and acetylation eliminates any remaining hydroxyl groups which can contribute to the imperfect interphase. In this way, the fiber/matrix interphase is more complete than before, without excessive interphase gaps and the impregnation of the fiber into the solution is also greater, due to the swelling of the it. Also, the cellulose structure seems to widen the lattice planes which can let the light pass through it with more ease and less diffuse reflection/scattering phenomena.

These eye observations of the impregnated fiber with Benzyl Benzoate and Ethanol solution, suggest that the required RI of the delignified flax fiber should be around the level of 1.53-1.54. This means, that a new testing process which will alter the refractive index of the solutions based on the second or even the third digit of the RI value around 1.53, should be implemented. This is why in the following subsection, two organic solutions that have closer RIs are used. This will decrease the wide range of RIs of the previous mixture. The fiber modifications seem to assist in the effort of eliminating the borders of the flax fiber inside a solution, each in its own characteristic way.

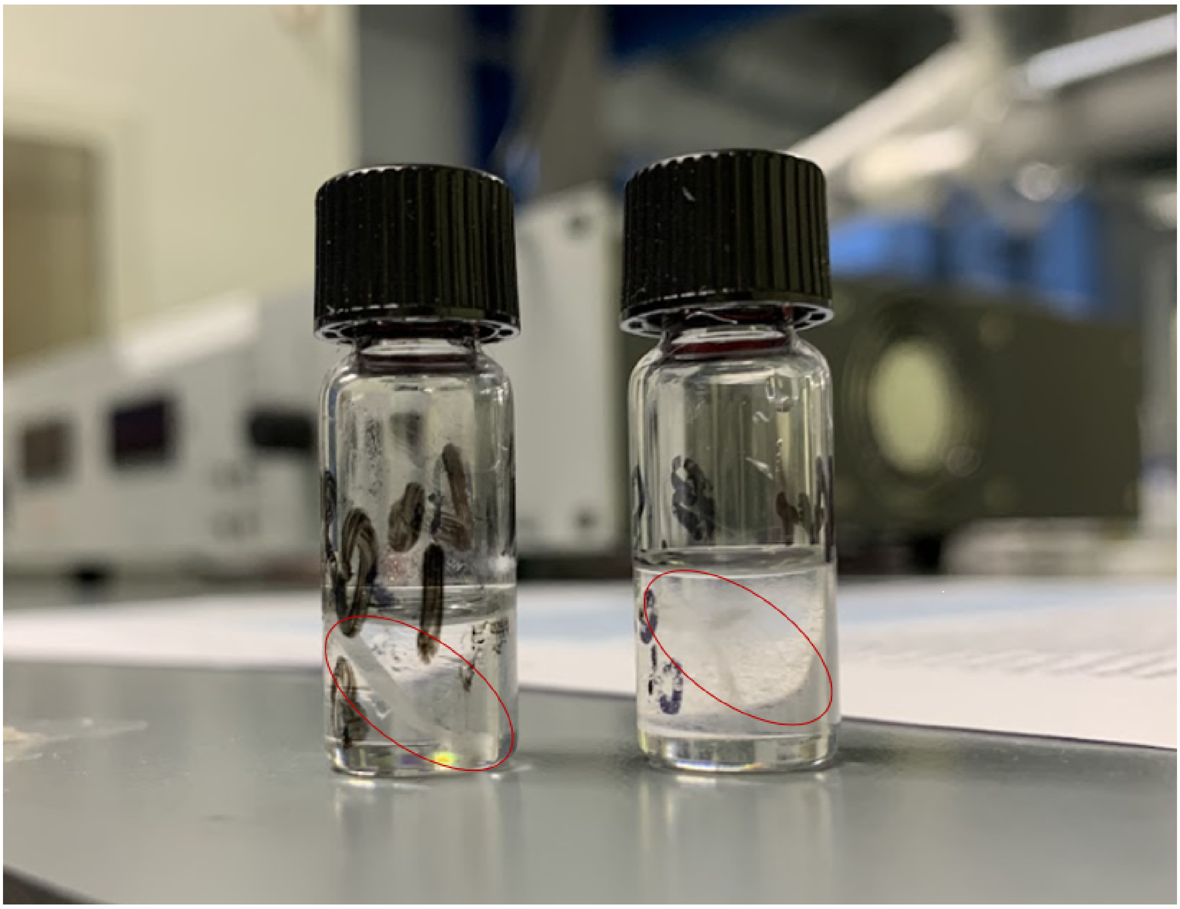

Figure 5.7: Immersion testing with delignified flax fibers which have been subjected to TEMPO-oxidation and acetylation, into a tunable solution of Benzyl Benozate and Ethanol of 2 mL volume. Left: 80% Benzyl Benzoate-20% Ethanol: RI = 1.530, Right: 85% Benzyl Benzoate-15% Ethanol: RI = 1.540.

5.2.2. Ethyl Cinnamate with Ethyl Salicylate

This procedure is the next step in the immersion testing for the delignified flax fibers, in order to estimate their RI and achieve a RIM. As explained earlier, the RIs of the mixtures that were created with Ethyl Cinnamate and Ethyl Salicylate are approximating better at the levels of 1.53-1.54. This is due to the very close indices of these compounds. Table 4.3 shows the calculation of RIs of the full mixture selection which was implemented with an Abbe's refractometer, starting from 1.521 and reaching to 1.558 with varying the concentration of the compounds, as seen on Table 4.3. In this case, the variation was based on the second and third digits of the property in contrast to the previous testing method which presented a variation on a bigger range. Based on the previous results, tuning the property on this range can give a clearer depiction of the RIM between the constituents.

The results of the eye test are depicted in Figure 5.8 and it shows that plain delignified flax fibers do not match perfectly with the organic solutions. The causes which can be responsible for this phenomenon are the same, as presented earlier. The target of this test was to eliminate the first major cause, which is the RI mismatch between the fiber and the solution, by shrinking the range of the available RI and possibly matching them. Unfortunately, this did not occur (at least in full capability), meaning that either the delignified flax fiber has a different index or all the additional causes presented earlier (entrapped air, high crystalline cellulose content, etc), hinder RIM.

The solutions that have an RI close to 1.530-1.540 seem to have a better match with the flax fiber, whereas, in the other solutions, the DL fiber is fully distinguishable. That verifies the initial assumption that the RI of DL flax fiber could be around the range of 1.530-1.540. On the other hand, no perfect RIM is accomplished, meaning that the borders of the fibers are still distinct on all of the occasions. To this degree, the other causes seem to be more probable for the hindering of this phenomenon.

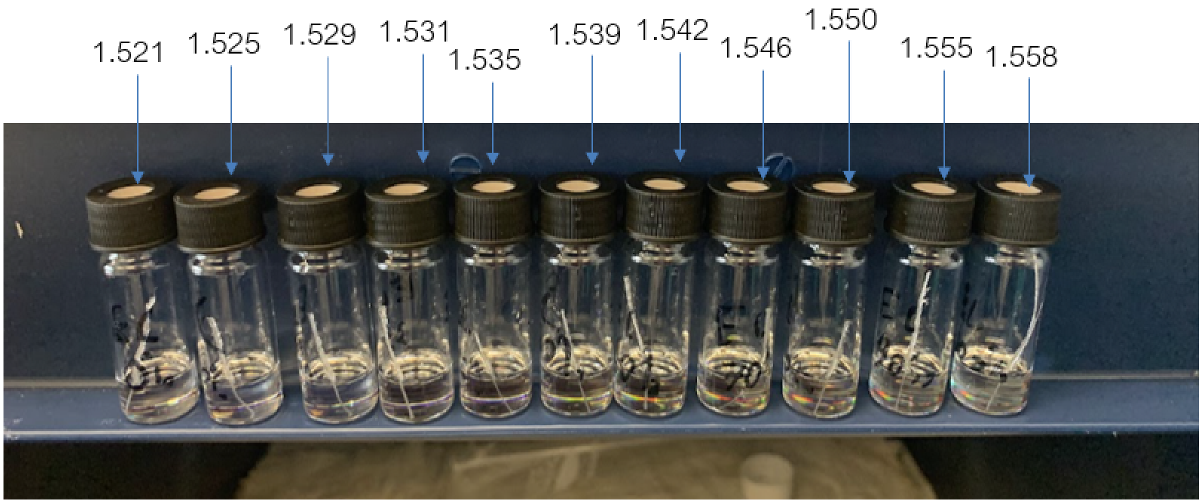

Figure 5.8: Immersion testing with delignified flax fibers into a tunable solution of Ethyl Cinnamate and Ethyl Salicylate. The solution's volume was 1 mL. The refractive indices of each solution are depicted in the image. From left to right: 0-100% Ethyl Cinnamate.

Table 5.2: RI and observations for the immersion tests of delignified flax fibers with the tunable solution of Ethyl Cinnamate and Ethyl Salicylate.

Ethyl Cinnamate (vf%)	Ethyl Salicylate (vf%)	RI	Observations
0	100	1.521	Delignified flax fiber visible
10	90	1.525	Delignified flax fiber visible
20	80	1.529	Delignified flax fiber slightly less visible
30	70	1.531	Delignified flax fiber slightly less visible
40	60	1.535	Delignified flax fiber slightly less visible
50	50	1.539	Delignified flax fiber slighlty less visible
60	40	1.542	Delignified flax fiber visible
70	30	1.546	Delignified flax fiber visible
80	20	1.550	Delignified flax fiber visible
85	15	1.555	Delignified flax fiber visible
100	0	1.558	Delignified flax fiber visible

Again, the newly treated flax fibers with either nitric acid/probe sonication or NaOH/TEMPO/Acetylation treatment were re-immersed into the EC/ES mixture, to observe if the modifications on the surface of the fiber can assist in the elimination of the interphase borders of the fiber/matrix. Figure 5.9 presents the DL flax fibers which have been subjected to the nitric acid/probe sonication treatment, and the eye test shows that the treated fiber is surely less visible in the same solution than the untreated DL flax fiber. Particularly, in the range of 30-50% the modified treated DL flax fiber seems to be tougher to be detected in the solution. Better infusion of the polymer in the interior structure of the fiber for the reasons which were presented earlier (better dispersion, obstructing of fiber aggregation) and closer approximation of RIM due to the narrowing of the range of the solution indices result in a more complete matching between the fiber and the solution, than in BB/Ethanol's case.

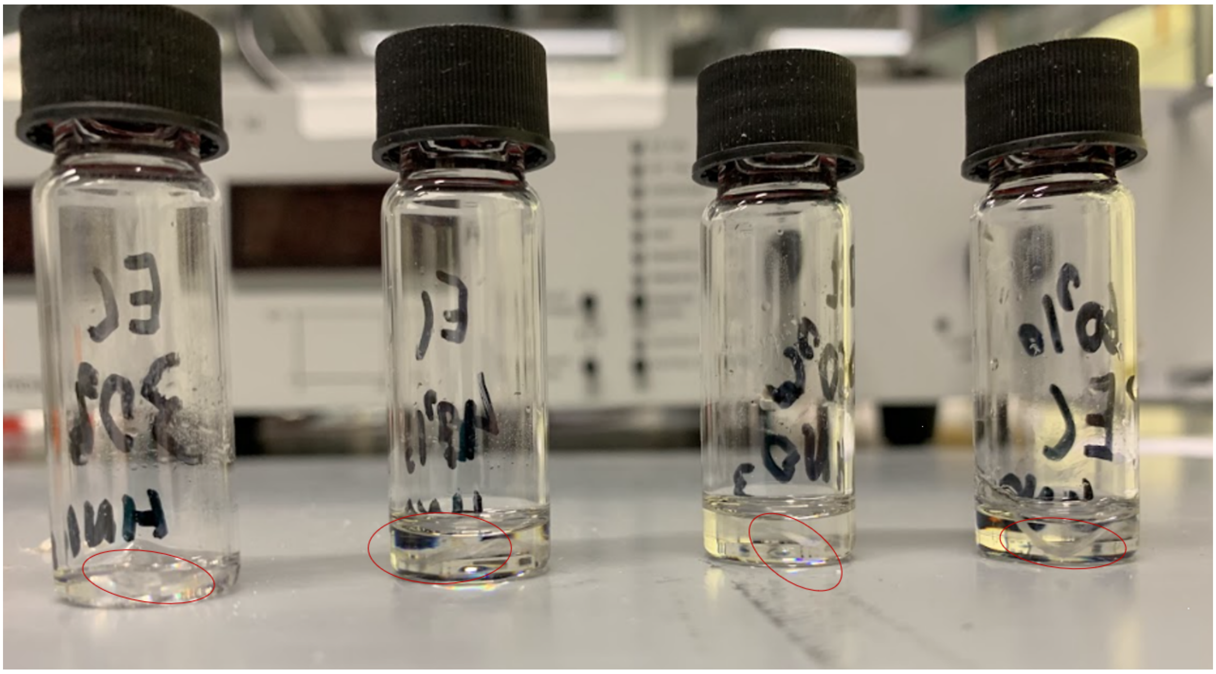

Figure 5.9: Immersion testing with delignified flax fibers which have been subjected to nitric acid treatment with probe sonication, into a tunable solution of Ethyl Cinnamate and Ethyl Salicylate. The solution's volume is 0.5 mL. From left to right: 30-60% Ethyl Cinnamate.

5.2.3. Polymers

The final immersion testing was implemented with polymer materials which can act as a potential matrix in the flax fibers and constitute a composite material. The polymer systems which were used had a very important parameter in common. Both of them, presented a RI very close to 1.530-1.540, as seen in Table 4.4. The immersion tests were implemented for both polymer systems combined with treated and untreated delignified flax fibers.

Figure 5.10 presents the outcome of immersion tests of treated and untreated DL flax fibers in the two polymers which were used in this project. The polymers were left to cure for the pre-specified period of time (48 hours for ”Water-Clear”/W300 epoxy resin at RT, 24 hours for Resoltech 1200/1204 at RT, and 16 hours at 60^0C). The results show that all the fibers are fully distinguishable in both resin systems. The ”Water Clear” epoxy resin seems to be fully transparent as a polymer in contrast to the Resoltech 1200/1204 which seems to be more opaque.

The flax fibers are fully distinct in all the occasions presented in Figure 5.10. Especially in the immersion of the three categories of fibers on the ”Water Clear” epoxy casting resin (RI = 1.538), the fibers are even more easily observable than in Resoltech epoxy's case (RI = 1.560), due to the polymer system being more transparent despite having a closer RI to the assumed RI of DL flax fibers. The refractive indices of the polymers are shown in Table 4.4. Moreover, it seems that the NaOH/TEMPO-oxidation/acetylation-treated delignified flax fiber presents better compatibility than the other fibers because it is less visible in the interior structure of the polymer. That can be attributed again to the better wettability and impregnation of the fiber due to the bigger spacing of the fibers in the fiber bundles and also the better interphase compatibility between the fiber and the matrix. These reasons make this occasion more suitable for immersion and therefore it presents satisfying results in this check-up.

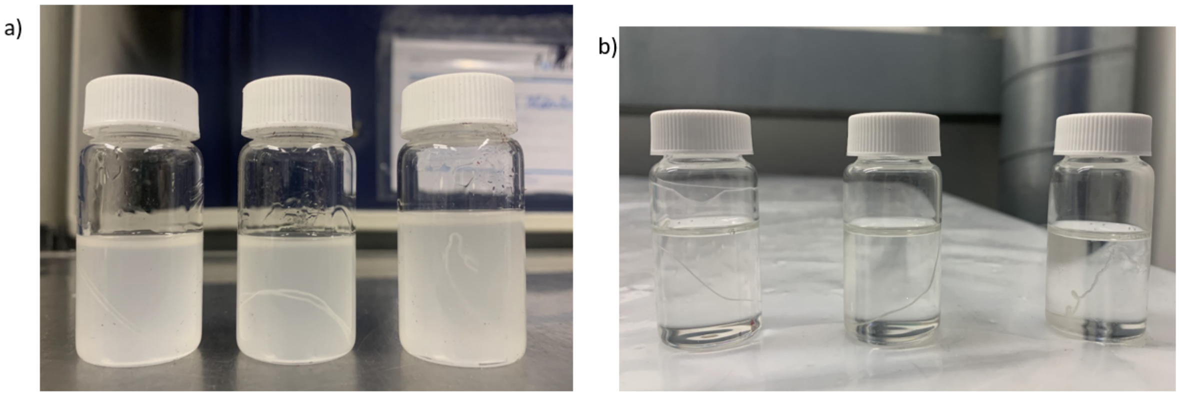

Figure 5.10: Immersion testing with delignified flax fibers which have been subjected to various modifications, into a) Resoltech 1200/1204 polymer system, RI = 1.560 b) ”Water Clear”/W300 epoxy resin, RI = 1.538. From left to right: Delignified Flax Fiber, Nitric Acid Treated Delignified Flax Fiber, TEMPO/Acetylation Treated Delignified Flax Fiber. In each sub-figure (a,b) a total weight of 50 grams of liquid resin and 17.5 grams of hardener was used for the total immersion testing of the three types of fibers in 5 mL vials.

Despite the fact, that the flax fibers were visible and distinct inside the polymers, which could indicate that the composite material would not be transparent, it would be intriguing to investigate if pressure from the manufacturing techniques can contribute to higher optical transparency on these fiber/polymer combinations, with increasing the immersion of the polymer in the interior structure of the fiber, or dissolving any remaining air bubbles due to inadequate degassing of the polymer or remaining moisture in the hydrophilic fiber. The same exact observation was made on the immersion tests on organic solutions which were conducted and shown earlier in the report. These tests covered a wide range of RI (based even on the third digit) and did not achieve a full RIM. This is why the assumption which is followed based on these results is that optical transparency is hindered mainly due to other issues like interphase problems, interior scattering, or air bubbles present in the material. This would show if pressure can be a decisive point in the accomplishment of high light transmittance in an FFCM even if RIM is not fully achieved, solving some of these different issues. Therefore, the fabrication of the composites with these constituents (polymer/fiber) is investigated in more detail, even if the RIM results are not satisfying.

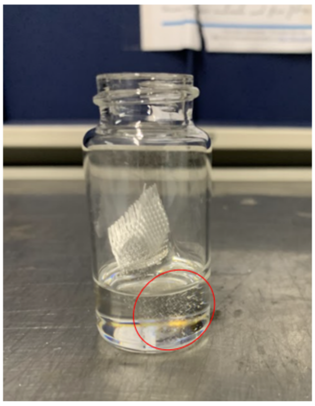

Figure 5.11: RIM between glass fibers and liquid epoxy casting resin ”Water Clear” (without hardener W300). RI of the glass fibers = 1.547, RI of the ”Water Clear” resin = 1.549.

Being aware, that the RI of the glass fibers (1.547) is extremely close to the RI of the ”Water Clear” epoxy casting resin (without the hardener) an extra immersion test was conducted to seek for RIM. Figure 5.11 shows the immersion of glass fibers into the liquid uncured resin ”Water Clear” (without hardener, RI = 1.549 from Table 4.4). It is clear by the eye test that on this occasion a nearly full RIM is achieved. The borders of the glass fiber woven fabric are nearly eliminated, and the fabric disappears inside the liquid.

5.3. Composite Materials

5.3.1. Glass Fiber Reinforced Polymers

The first samples which were created, had glass fiber woven fabric as a reinforcement. These would be the reference materials for this project giving first indications about the manufacturing technique as well as for achieving transparency. It should be less challenging for the glass fibers to achieve transparency as a reinforcement in a composite material because of the absence of some of the important issues which are raised for natural fibers, such as their unhomogenity or their hydrophilic character which creates interphase gaps. Also, the RI of the glass fibers is fully known. The glass fibers presented a refractive index of 1.547 based on the datasheet provided. This suggests that the glass fibers have a bigger refractive index than the assumed one of the delignified flax fibers. However, the interphase of the glass fibers with the polymers which are used to impregnate them is expected to be more complete with fewer interphase gaps, due to compatibility conditions and homogeneity of the glass fibers compared to the highly inhomogeneous flax fibers, as presented in Figures 5.3, 5.4. This implies fewer interphase gaps and better bonding between the fibers and the polymer which will create fewer light scattering spots and will allow visible light to pass through without major refraction ($n_{polymer} - n_{air} >> n_{polymer} - n_{fiber}$). Table 4.5, depicts the various glass fiber composite materials which were created during this project. For GFRPs, both vacuum pressing and hot press forming techniques were conducted after a wet lay-up. Both resins were used as a matrix, and three types of lay-ups were fabricated ($[0/90]$, $[0/90]_s$, $[0/90]_{2s}$). Figure C.1 located in the Appendix, shows some basic steps of the GFRP production with wet lay-up/vacuum pressing.

Table 5.3: RI of the polymer matrices, glass fibers as well as the difference between them.

	”Water Clear”/W300	**R1200/1204**	**Glass Fiber Woven Fabric**
Refractive index, n	1.538	1.560	1.547
$\Delta RI_{glassfiber-polymer}$	0.009	0.013	-

The glass fiber-reinforced composite materials which were produced are demonstrated in Figure 5.12. The materials are placed over a TU Delft paper of DASML, for demonstration purposes. In this way, the transparency of the material can be described by observing the letters beneath the specimens. The first observation of these specimens relies on how much the thickness of the material can affect its optical quality. For these twelve different specimens, the thickness was calculated and presented in Table 5.4. As thickness increases it is obvious by the naked eye that light transmittance decreases significantly in all cases. This can be explained, by two main causes. Firstly, it is a fact that the refractive index of both polymer systems is not identical to the refractive index of the glass fibers. The difference is in the second to third digit as the glass fiber has an RI of 1.547 in comparison to the RI of the cured polymers (Resoltech 1200/1204 = 1.560, WC/W300 = 1.538). This mismatch scatters light slightly and does not eliminate the borders of the glass fibers making them invisible inside the polymer, and with the increase of the light path, the refraction and backward scattering phenomena would be more intense. The second major cause, involves the increase of the number of interphases between the glass fibers and the polymer, as the thickness increases. This implies more light scattering sources and more RI mismatches (due to interphasial or matrix defects) on the interior of the material. In more specific detail, the chromatic aberration of the material seems to be more intense as the thickness increases. Light scattering due to RI mismatch causes dispersion of the particles of light, which separates the white light into different particles which either are transmitted, reflected, or absorbed and thus causes chromatic aberration, as explained in Chapter 3. [71] Another problem that was encountered, was the ”squeeze out” phenomenon. This relates to sucking or squeezing out the resin from the reinforcement due to the high pressure, strong applied vacuum, or less amount of resin, and results in poor impregnated areas of the reinforcement, with dry regions of high surface roughness of it. This will lead to more exposure of glass fibers in the air and therefore stronger light scattering due to higher RI mismatch. These dry areas occurred more on the ”vacuum pressed” samples than the ”hot pressed” samples, which outcomes in lower light transmission on them, possibly due to excessive vacuum pressure. A paradigm can be the 8-layer GFRP $[0/90]_{2s}$ composite material which is composed of glass fiber woven fabric and ”Water Clear” epoxy casting resin. This is the bottom right material in Figure 5.12b. It is clear, that the material is not transparent at all, and has high light scattering intensity. In this material, there are multiple dry areas of glass fibers which were not impregnated correctly and the ”squeeze out” phenomenon occurred. Surface roughness is an additional light reflection issue which was not investigated in depth during this project, as the literature states that RIM and light absorption are more significant issues in NFCMs.

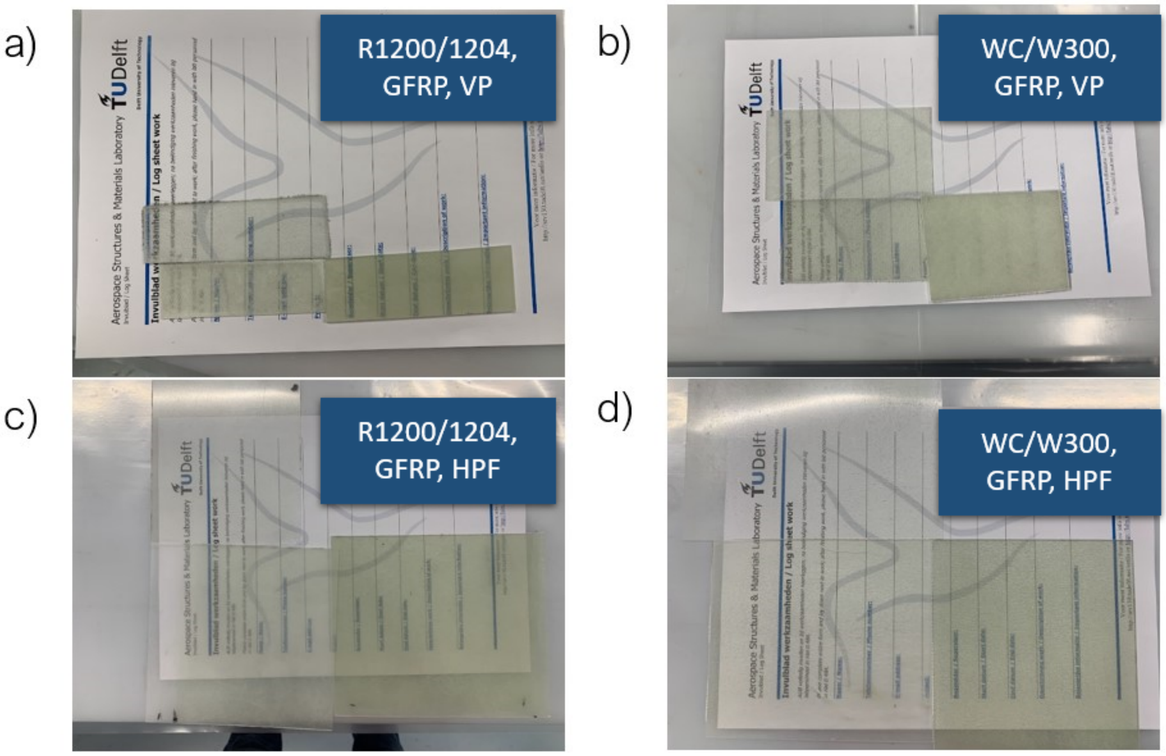

Figure 5.12: Glass Fiber Reinforced Composite Materials which were produced based on the recipes on Table 4.5. In every sub-figure: Top-Left: $[0/90]$, Bottom-Left: $[0/90]_s$, Bottom-Right: $[0/90]_{2s}$ a) Resoltech 1200/1204 as a resin with wet lamination/vacuum pressing technique, b) Water Clear/W300 epoxy casting resin system as a resin with wet lamination/vacuum pressing technique, c) Resoltech 1200/1204 as a resin with wet lamination/hot press forming technique, d) Water Clear/W300 epoxy casting resin system as a resin with wet lamination/hot press forming technique.

The laminates that were produced by hot press forming seemed to have higher optical quality for both of the composite combinations. This can be due to better impregnation of the glass fibers as the pressure which is achieved in this case is 10X times higher than in vacuum pressing. This means that the void content after curing should be lower because the air bubbles inside the material (due to the wet-lamination even after the degassing of the material) should be dissolved inside the material due to the consolidation pressure. [61] As explained earlier, the pressure of 10 bars which is used on this occasion (hot press forming) seems to be high enough based on the literature for dissolving a big percentage of air bubbles inside a material, in comparison to the vacuum pressure which was subjected (-1 bar). [60], [64] Figure 5.13 verifies that the air bubbles in the interior of the material are definitely reduced in size and number however, they are not fully eradicated. The big voids present on the left sub-image (Vacuum Pressing case) scatter light significantly, contributing to the fact that some of the glass fibers are visible. On the other hand, the hot press-formed sample shows a smaller void size, which does not affect the fiber's visibility due to intrinsic light scattering. Moreover, as explained earlier the thickness of the material affects the light transmittance, which can be verified by the samples. Table 5.4 shows that the vacuum pressing technique produces samples with higher thickness than the according samples from the hot press forming technique (some of them have even double the thickness), possibly due to the greater densification that occurs because of the higher pressures of hot press forming technique. This can correspond to higher transparency for the specimens generated with hot press forming for all the reasons explained earlier.

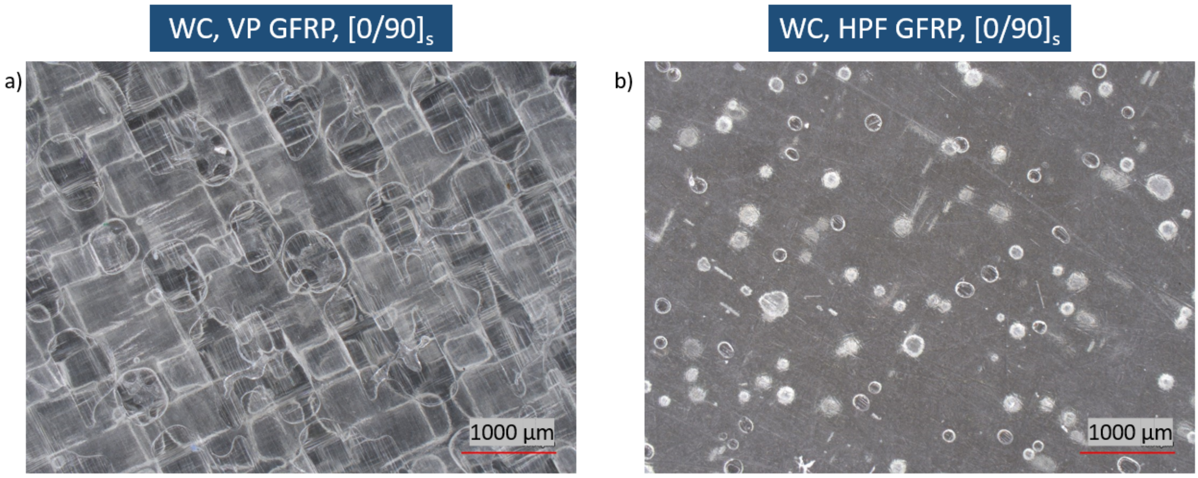

Figure 5.13: Optical Microscopy photos of the top surface of the glass fiber reinforced composite materials. a) $[0/90]$, ”Water-Clear”/W300 epoxy system, Vacuum Pressing, b) $[0/90]$, ”Water-Clear”/W300 epoxy system, Hot Press Forming. The scale is depicted on each sub-figure.

The optical microscopy photos of the cross-section of the Glass Fiber Reinforced Materials which were produced with wet/lamination and hot press forming techniques, are depicted in Figure 5.14. The fibers can be well observed on both occasions of the warp and weft directions. The dots describe one occasion of the fiber woven’s direction, while the longitudinal fibers can be also noticed. The dispersion of the 4-ply composite material seems homogenous with the fibers being distributed all around the available space on the interior structure of the material, not forming aggregations which can scatter light due to fiber boundaries. Another observation is the minimal amount of the interphasial defects’ size and number, with a low number of micro-voids being present in either the interphase or the matrix (as microcracks). However, some bigger size voids are noticeable on the samples which can be responsible for the light scattering that is present on the 4-ply materials and can make the color visible due to inner reflection (backward scattering) of some wavelengths (light dispersion due to RI mismatch). The low interphasial defect number be attributed to the hydrophobic nature of the glass fiber which ensures better compatibility, and therefore more complete interphase with the polymer. A strong reason for the fine optical quality and transparency of the GFRP materials, is the previous statement, due to the decreased light scattering from the air gaps.

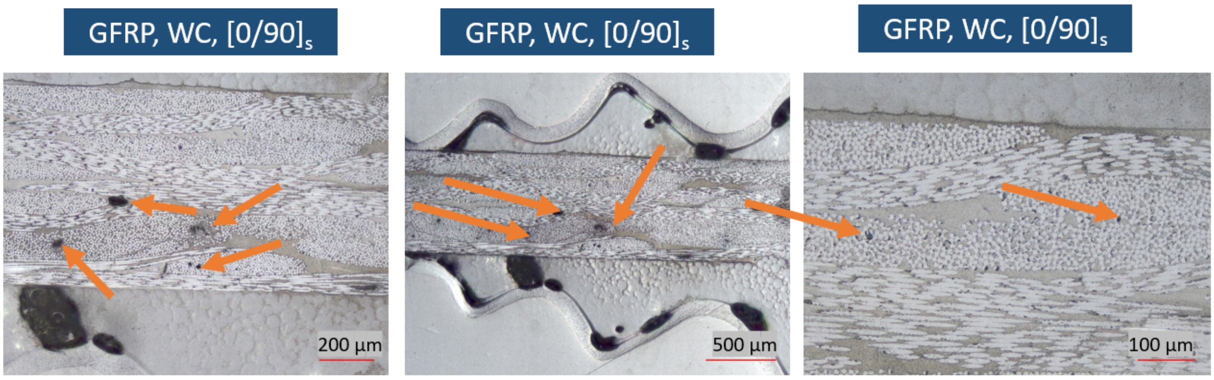

Figure 5.14: Optical Microscopy photos of the cross-section surface of the GFRP materials. Black arrows: Fiber aggregation, Orange arrows: Voids. The scale is depicted on each sub-figure.

5.3.2. Flax Fiber Reinforced Polymers

However, the outmost target of the whole research is to create a transparent (or even translucent) composite material that is reinforced by flax fibers. Based on the actions implemented in the previous sections, the fibers have already been modified by the appropriate fiber treatments and the last step of producing a composite is to combine the reinforcement with the matrix. Table 4.5 depicts the composite materials that were designed to construct a functional FFCM. Three different flax fiber types were utilized, all explained earlier, together with the two polymers that were used as a matrix. For the fabrication of these materials, it was decided that only wet lamination/hot press forming, was worth to be followed as a composite manufacturing technique, mainly because it presented better optical results for GFRPs (on optical transparency) and because of the time limitations of the project. Furthermore, the 8-layer $[0/90]_{2s}$ material, was decided not to be developed as well, again for time limitations reasons.

Figure 5.15 shows an overall comparison between all the flax fiber-reinforced composite materials created and a transparent wood composite subjected to acetylation treatment. In each sub-figure two different types of materials are depicted, with 2 plies ($[0/90]$) and 4 plies ($[0/90]_s$), accordingly. All the materials produced are highly translucent but not fully transparent, as the text beneath them is clearly observable but slightly blurry on nearly all occasions, due to forward scattering and refraction. Additionally, a slight chromatization is visible on the majority of the materials, as they present a slight orange-to-yellow color. This can be connected with the absorption of light in low wavelengths (400 nm), which allows the complementary color from the color wheel to be seen to the bare eye as explained in Chapter 3. Appendix D shows all the flax fiber reinforced composite materials depicted in the image below, in higher resolution.

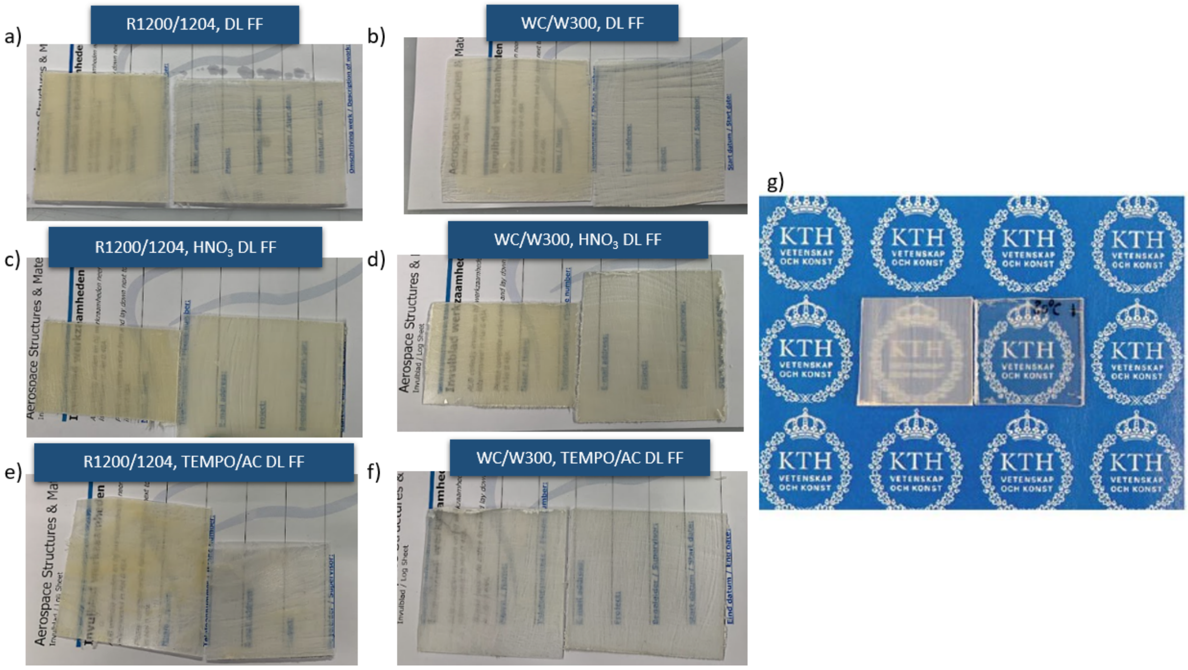

Figure 5.15: a-f) An overall depiction of all the developed transparent FFCMs in this project. In every subfigure a)-f) Left: $[0/90]_s$, Right: $[0/90]$, g) Depiction of non-acetylated (left) and acetylated (right) transparent wood with PMMA. [13]

The only noticeable variation between the materials is seen in Figure 5.15f, in which the chromatization of the material diminishes. That can be attributed to the finer interphase that acetylation treatment creates which decreases the debonding gaps, responsible for scattering and absorption of light (at low wavelengths as it will be discussed in the section on Light Transmission), as well as the better dispersion of fibers due to TEMPO-oxidation (carboxylation) which ensures a superior polymer infusion and due to the cellulose swelling. These observations make this trio of modifications a crucial treatment that can assist in increasing the optical quality of the material. However, this does not occur on both occasions for both polymer matrices, showing that the RIM between the fiber and the matrix also plays a huge role in improving optical transparency. Due to the absence of color in the occasion of Figure 5.15f, it seems that the RI mismatch between the epoxy polymer system of ”Water-Clear”/W300 and the treated DL flax fiber, is lower than the opposite system with R1200/1204 as a matrix, which presents chromatized regions due to intense light scattering and light dispersion. The modified flax fibers are again slightly visible, however at a lower level than the previous cases (Delignified FFCM, HNO3/PB Delignified FFCM), possibly due to the reduction of the interphasial defects. The fact that the fibers are still visible means that a full RIM has not occurred yet. Light scattering in Figure 5.15e can also occur because some fibers of the UD-coupon crumbled and degraded excessively due to the highly oxidizing environment or the repulsion forces created (TEMPO-oxidation) of the fiber treatments (Figure 5.3 and 5.4). Some of these fibers even snapped and were fractured possibly because of the pressure during curing or the high oxidizing environment of the treatment, as they were visibly degraded inside the material. This could re-introduce fiber aggregation phenomena as these fibers could leave their initial position and move freely in the interior of the material prior to curing, and they could end up sticking into other fibers, resulting in higher diffuse reflection or light scattering because of fiber boundaries. On the other hand, HNO_3/PB treated samples showed again the same slight discoloration, not having important divergencies with the plain delignified flax fiber reinforced composites, showing that this treatment is not as effective as the previous trio modifications which present superior optical quality.

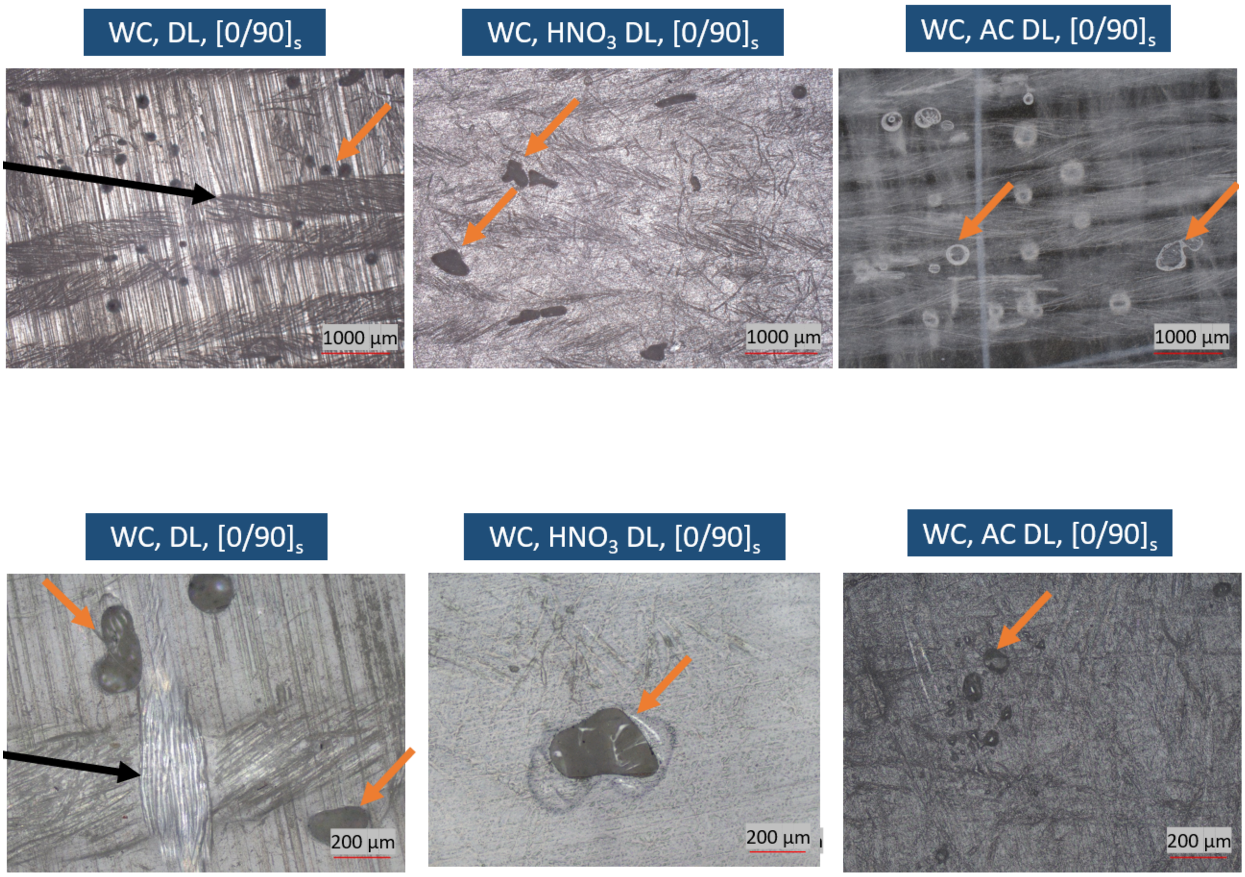
WC, DL, $[0/90]_s$ WC, HNO_3 DL, $[0/90]_s$ WC, AC DL, $[0/90]_s$

WC, DL, $[0/90]_s$ WC, HNO_3 DL, $[0/90]_s$ WC, AC DL, $[0/90]_s$

Figure 5.16: Optical Microscopy photos of the top surface of the transparent flax fiber composite materials. WC: ”Water Clear”/W300 epoxy resin system, DL: Delignified flax fiber coupons. HNO_3 DL: Delignified flax fiber coupons treated with nitric acid/probe sonication, AC DL: Delignified flax fiber coupons treated with NaOH/TEMPO/Acetylation, Black arrows: Poor impregnated flax fibers, Orange arrows: Voids. The scale is depicted on each sub-figure.

Correlating these materials to the non-acetylated transparent wood composite of 1.5 mm thickness, the optical comparison seems to be very close. However, acetylated transparent wood is surely more clear and see-through compared to all the FFCMs. Based on the optical results, delignification seems to be the most crucial fiber treatment for increasing light transmittance in a flax fiber-reinforced composite material, due to the elimination of the light-absorptive substance of lignin from its structure and lowering its RI, while the trio modifications of NaOH/TEMPO-oxidation/Acetylation is an extra helping hand on tackling some of the aforementioned issues and contributing to higher optical transparency on the material.

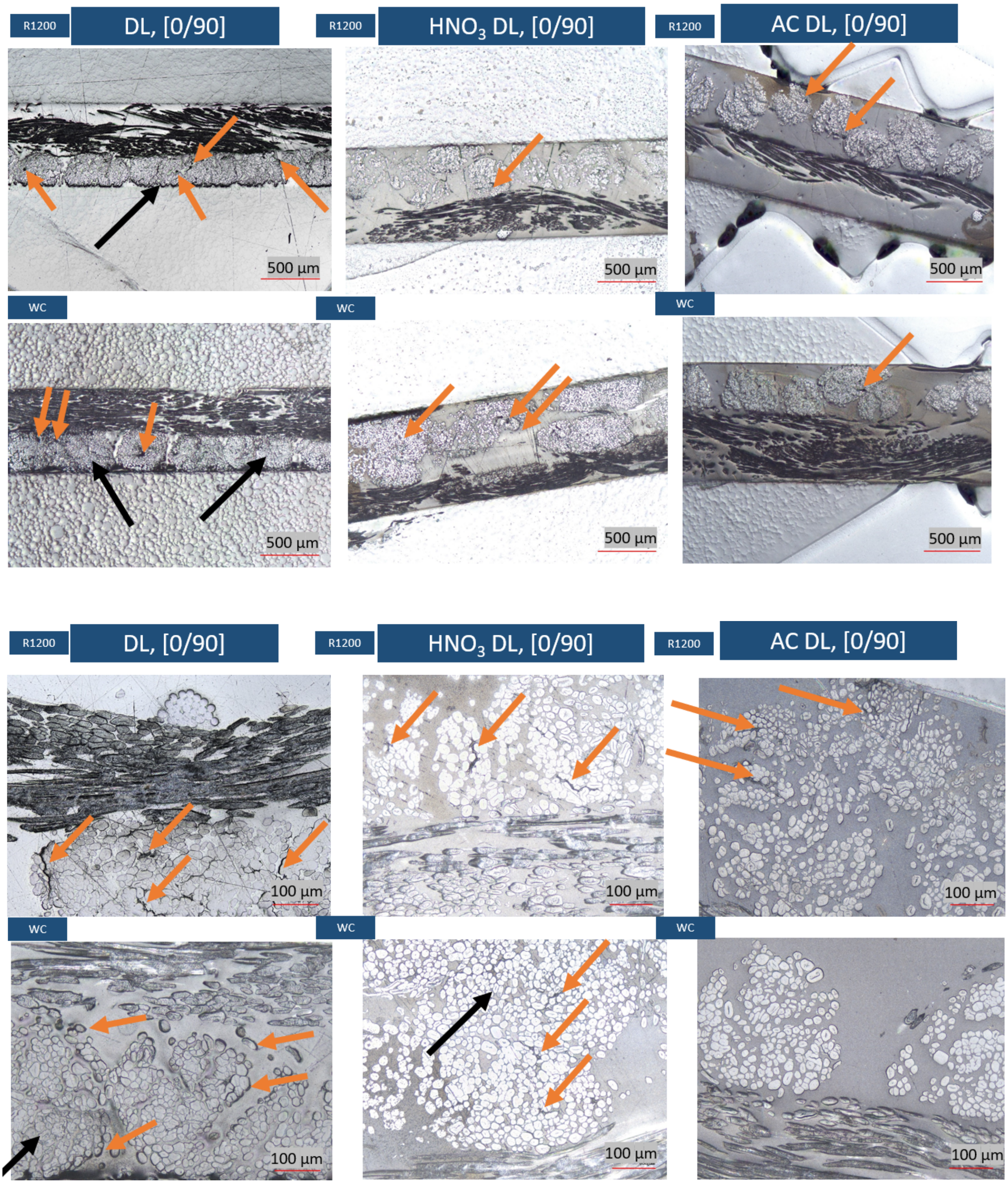

Figure 5.17: Optical Microscopy photos of the cross-section of the transparent flax fiber composite materials in 500 and 100 μm scales. DL: Delignified flax fiber coupons. HNO_3 DL: Delignified flax fiber coupons treated with nitric acid/probe sonication, AC DL: Delignified flax fiber coupons treated with NaOH/TEMPO/Acetylation, Black arrows: Fiber aggregations, Orange arrows: Voids. The scale is depicted on each sub-figure.

Diving in-depth into the interior structure of the composite materials, optical microscopy photos of the top surface of the materials were extracted to investigate if air voids or poorly impregnated fibers were present on the surface. Figure 5.16 shows that the void number in the 4-ply materials with ”Water-Clear”/W300 as a matrix, is reduced in the case of the treated samples, in comparison to the other untreated occasion, which presented a higher number of air surface gaps (100-200μm size). The reduction of the number of these gaps is critical for increasing light transmittance in material as they can scatter light significantly due to scattering or refraction/dispersion due to RI mismatch, and drive the fibers to be visible. There are also big voids present on the interphase of some fibers (as seen in the 200 μm scale image of DL composite material), which verify the expected poor interphase of fiber/matrix. Additionally, the plain delignified samples showed poorly impregnated flax fibers on the surface in contrast to the treated materials, which did not depict that problem. This can be attributed to either the poor compatibility between the hydrophilic natural fiber (full of hydroxyl groups as FTIR verified) and the hydrophobic matrix or due to fiber aggregations that did not allow the polymer to infuse deeply into the structure of the fiber. On the other hand, the treated samples with either nitric acid or TEMPO-oxidation did not showcase the issue of poor fiber impregnation, mainly due to the better fiber dispersion they assumed to have due to the treatments.

Following, Figure 5.17 illustrates the optical magnification of the cross-section of the composites which were reinforced by UD orientation of the three different types of flax fibers. In this Figure, the two different orientations of the fibers can be clearly observed. For instance, the dots that can be depicted on either the bottom or top side of the material describe one orientation (for example 90^0 UD fibers), while the black longitudinal lines that are located exactly above them on the top side of the material describe the perpendicular fiber orientation (on this occasion 0^0). Also, the small dots are the cellulose elementary flax fibers composing the cluster of the technical fiber. Comparing the three types of fibers, it seems that a big difference is the spacing of the elementary fibers on the DL composite materials which seem to be compacted due to the structure and applied pressure and can also be interpreted as an obstacle to a quality polymer infusion, visually observed from the black arrows on this image pointing to some of the multiple cellulose fiber aggregations that are present on these occasions, which can be created due to the hydrogen bonds that the hydroxyl groups (which are present in the flax fibers) can form or because of the high applied pressure which densified the material and accumulated the fibers together. [68] The fiber boundaries can be intrinsic light scattering sources and can hinder a more complete fiber impregnation. [20]. In Figure 5.17, the 500 μm image of the 2-layered non-treated (DL) ”Water-Clear”/W300 and R1200/1204 composites, verifies that the spacing on this composite is extremely compact presenting less space for the polymer matrix to infiltrate. The orange arrows show some of the debonding gaps that are present and become light-scattering sources. These were possibly created due to the presence of hydroxyl groups on the hydrophilic non-modified delignified flax fibers or due to the poor impregnation quality which introduced air inside the material or solvents/reaction by-products that tried to escape during curing and might have created micro-cracks in the interior structure of the material. On the contrary, the fibers appear to have better dispersion in both treated samples, while the interphasial defects reduce by a higher margin when the trio modifications are implemented, verifying the better compatibility between the fiber and the matrix. Also, the amount of defects in FFCMs appears to be higher than in GFRPs and they present a higher number of regions with an accumulation of fibers, meaning the dispersion of glass fibers is finer.

5.4. Light Transmittance

5.4.1. Glass Fiber Reinforced Polymers

Total light transmittance was calculated based on the Uv/Vis spectroscopy machine which was presented in Chapter 4. The transmittance graphs for each specimen are depicted in Figure 5.18, with the continuous lines describing the hot press formed samples and the dashed lines correlating to the vacuum pressed samples. The results verify the optical observations that were made previously, about the wet lamination/hot press forming technique, which produced superior specimens regarding their optical transparency. To be more specific, 2-layer $[0/90]$ composite material which was composed of ”Water Clear”/W300 and created by hot press forming, showed a higher total light transmittance than 80%, in comparison to the according material which was created with vacuum pressing which showed 20% lower magnitude of total light transmittance. The same can be said for the laminates which were Resoltech 1200/1204 matrix-based. This can be attributed to the higher pressure that was achieved with hot press forming (10 bars) than vacuum pressing (1 bar). This high pressure consolidated and reduced the air bubbles that were present inside the material during the infusion of the polymer in the pre-impregnated material, in contrast to vacuum pressing which showed an increased number and size of air voids, because of the lack of dissolution of air by the low pressure. Optically, this can be confirmed by the eye test in Figure 5.12 and 5.13. However, on the occasion of Resoltech 1200/1204, the 2-layer laminates didn't have such a big difference showing 77% and 75% for the two different techniques accordingly, in contrast to the $[0/90]_s$ laminates which presented a wider gap in the levels of light transmittance (approximately 13%). Higher thickness implies higher air percentage in the composite material, which with lower pressure than the consolidation pressure can lead to the formation of voids. These voids refract the visible light particles and even backscatter/reflect some particular wavelengths of light as presented in Figures 3.4. All the 8-layered laminates presented even lower optical light transmittance, in the levels of 50-60%. There was an instance of 25% total light transmittance for the 8-layer "Water-Clear"/W300 epoxy-based GFRP $[0/90]_{2s}$, which as explained in the previous paragraphs presented numerous dry areas due to excessive "squeeze out" phenomenon, seen in Figure 5.12b.

Also, particular interest is raised in how the chromatization of the materials can be interpreted. Based on what wavelength the light transmittance is decreased, implies an absorption of a particular light radiation due to the dispersion of light, as explained in Chapter 3. The observed color can be estimated from the color wheel, presented in Figure 3.3. In Figure 5.18 the absorption of light occurs at nearly 400-450 nm (light transmittance shows a steep shoulder at this wavelength), which can transform the material into yellow to light orange. Additionally, in some samples, there is a broader shoulder near 600 nm on the majority of the samples, which produces a blue color but at low intensity. The combination of yellow and blue can result in a green color which is visible and confirmed in Figure 5.12. The intensity of the color depends on the proportion of the light which is absorbed. The 2-layer $[0/90]$ hot press formed GFRP which has "Water-Clear" as a matrix, presents a minimum transmittance of 70% near 400 nm (which is maximum at this wavelength) and even lower absorption intensity on the broader shoulder of 600 nm, and this is why the composite material happens to be the least colorful out of them all (i.e. in contrast to the 8-layer "Water-Clear" composite material which presents a transmittance of lower than 30-40% at 400 nm and higher absorption rates at 600 nm because of the more intense light scattering phenomena, which makes it green). GFRP of vacuum pressing technique presents even stronger absorption shoulders on 400 nm (steep) and 600 nm (broad) with lower light transmittance values, making the intensity of green radiation stronger.

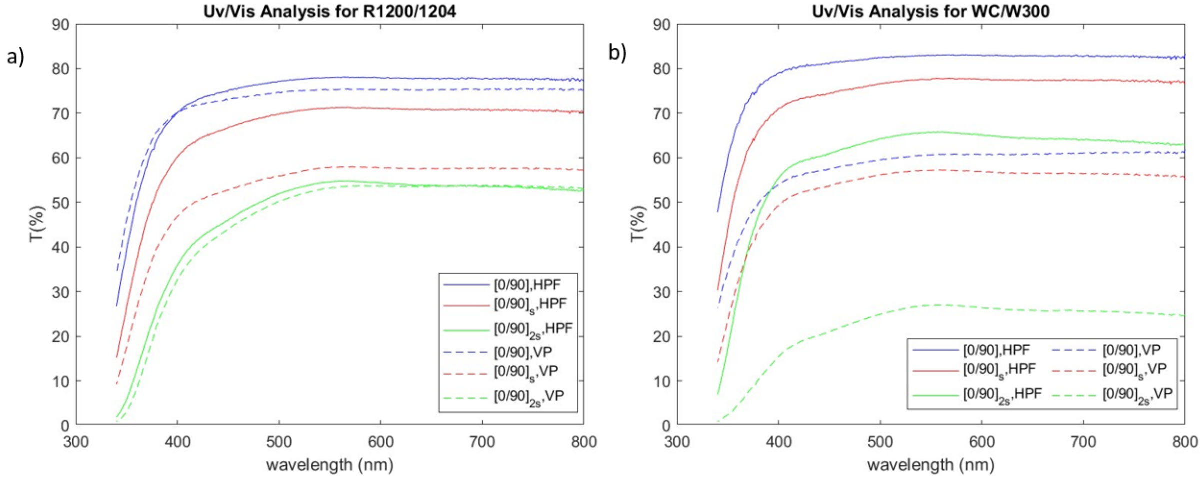

Figure 5.18: Total Light Transmittance of the GFRPs which were presented in Figure 5.12. a) GFRPs that have Resoltech 1200/1204 polymer system as a matrix, b) GFRPs that have "Water Clear"/W300 polymer system as a matrix. Continous line: Hot Press Formed samples, Dashed lines: Vacuum Pressed samples

Comparing the two polymers used as matrices for the GFRPs, it seems that they have minor differences in the laminates of the same plies. The hot-pressed composite materials with "Water Clear"/W300 resin system provide a +5-10% maximum optical transmittance when compared to the hot-pressed Resoltech 1200/1204 glass fiber composite materials, possibly to lower RI contrast between the constituents. On the other hand, vacuum-pressed composites showed the opposite trend, with Resoltech 1200/1204 composites being superior. This is possibly justified due to the bad impregnation quality and ”squeeze out” phenomenon of these materials, due to the lower viscosity of the ”Water Clear”/W300 polymer system. The difference in the RIs on both of these resins with glass fibers is on the second digit to the third digit, as seen in Table 5.3. The literature stands, that as lower the possible difference between the RIs, the higher the optical transmittance would be. [5] This is partially true, as seen from the results in this case, as the WC/W300 polymer system approaches better the RI of the glass fibers but not in all cases the one which shows the higher transparency. Impregnation of the fibers or void content can become crucial parameters as well for optical transparency. For example, the viscosity of the ”Water Clear”/W300 resin system, is significantly lower than the according viscosity of R1200/1204 which ensures better impregnation of the fibers with possibly lower void content. [62] This will create fewer light scattering sources which can lower the optical transmittance. However, due to this lower viscosity, the ”squeeze out” phenomenon in vacuum pressed samples can occur which can leave dry areas, that also scatter light. Therefore, a balance in this issue should be taken into consideration.

Table 5.4: Thicknesses and maximum light transmittance of all the GFRP materials which were produced.

	Thickness (t) of sample in mm						Maximum light transmittance (T) of sample in %					
Resin system	**Resoltech 1200 + Hardener 1204**			**Water-Clear + Hardener W300**			**Resoltech 1200 + Hardener 1204**			**Water-Clear + Hardener W300**		
Reinforcement	**Glass Fiber Woven Fabric**			**Glass Fiber Woven Fabric**			**Glass Fiber Woven Fabric**			**Glass Fiber Woven Fabric**		
Vacuum Pressing	[0/90]	$[0/90]_s$	$[0/90]_{2s}$	[0/90]	$[0/90]_s$	$[0/90]_{2s}$	[0/90]	$[0/90]_s$	$[0/90]_{2s}$	[0/90]	$[0/90]_s$	$[0/90]_{2s}$
	0.63	1.11	2.45	0.64	1.04	2.12	75.17	57.41	52.99	61.08	55.69	24.53
Hot Press Forming	[0/90]	$[0/90]_s$	$[0/90]_{2s}$	[0/90]	$[0/90]_s$	$[0/90]_{2s}$	[0/90]	$[0/90]_s$	$[0/90]_{2s}$	[0/90]	$[0/90]_s$	$[0/90]_{2s}$
	0.52	0.61	1.40	0.46	0.64	1.34	77.31	70.17	52.17	82.20	76.78	62.86

The results of the GFRPs, produced in this scope of research can be correlated to the literature (benchmark comparison). Kim et al., produced a one-layer 1 mm thick GFRP material with various resin systems as a matrix, shown at Figure 1.2. [5] The material was produced by wet-lamination without applying any pressure during curing. The RIs of the polymers used presented a difference in the third to the second digit with the glass fibers, with the lowest being 0.004 (lower than the difference between the polymers and the RI of the glass woven fabric used in this project, 0.009 and 0.013). The best result concerning optical transmittance was 72%, nearly 10% less than the best result depicted in Table 5.4. This implies that pressure can be a decisive factor in the preparation of a transparent composite material, flowing the polymer more sufficiently on the surface of the fibers, reducing the defects which can be significant for transparency, even in a higher number of interphases (1-layered material of Kim to 2-layered material here). Also, the thickness of the materials has a significant difference between the composites of Table 5.4 and the composite of Kim (1 mm). This is also crucial because the light has to propagate in a smaller path decreasing the chances of intense refraction. Caydamili et al., also developed a 2 mm thick transparent GFRP, manufactured by RTM having 5, 10, and 29 layers. [72] The maximum light transmittance for a 5-layer GFRP composite material was 87%, 5% higher than the maximum light transmittance for a 2-layer GFRP and 10% higher for a 4-layer material, however both cases in lower fiber volume fractions than the GFRPs presented in this report, due to the increased thickness (2 mm for all the samples). These results show that the values of the transparent GFRPs of Table 5.4, seem to be in agreement with the results from the literature.

5.4.2. Flax Fiber Reinforced Polymers

Again light transmittance was calculated using the Uv/Vis spectrophotometer and produced the graphs in Figure 5.19. Five different locations on each composite material were randomly chosen, and placed on the sample holder. This was implemented to investigate how well the flax fibers dispersed into the materials and in what way this affects light transmittance. For example, there might be some resin-rich areas on the sample, allowing light to pass through without having to scatter due to the fiber/matrix interaction, which will show increased transmittance values. On the other hand, in some regions of the material, flax fibers are densely distributed and aggregations can occur, scattering visible light with higher intensity. From these five measurements, an average and standard deviation are calculated. The standard deviation can indicate how homogeneously are the fibers dispersed. The lower the standard deviation, the more homogeneous the structure the composite material presents. Figure 5.19 depicts the average transmittance curves extracted out of the measurements of all the randomly picked locations which presented a geometry of 27X18 mm elliptical shape (based on the sample holder), while Table 5.5 shows the average maximum light transmittance values for each measurement as well as the standard deviation for the measurement. The overall measurement of each location in each sample is demonstrated on the Appendix D

Delignified Flax Fibers

The 2-layered $[0/90]$ flax fiber reinforced composite material which contained plain delignified flax fibers as a reinforcement in two different directions and Resoltech 1200/1204 as a matrix, presented an average maximum light transmission of 70.31% and a standard deviation of 1.68%, while the 4-layered $[0/90]_s$ composite material with the same constituents, presented an average maximum light transmittance of 56.99% nearly 15% less, while the standard deviation was at 1.77%. On the other hand, when the polymer matrix was switched from Resoltech 1200/1204 to the epoxy resin system of ”Water Clear”/W300 with identical reinforcement, the second group of graphs showed a slight decrease in the maximum transmittance for the 2-layered composite at 68.43% and a standard deviation of 1.41%, while the 4-layered composite peaked at 49.90%, which showed a 7% decrease from the previous occasion (R1200/1204). The standard deviation of the $[0/90]_s$ ”Water Clear”/W300 matrix-based FFCM stayed at a low level of 0.96%. The low-value standard deviations for all the FFCMs, show that there are minor differences in the change of measurement’s location on light transmittance, meaning that the flax fibers were homogeneously dispersed in the interior of the materials possibly due to the high accumulation between them, which is not desired (Figure 5.17).

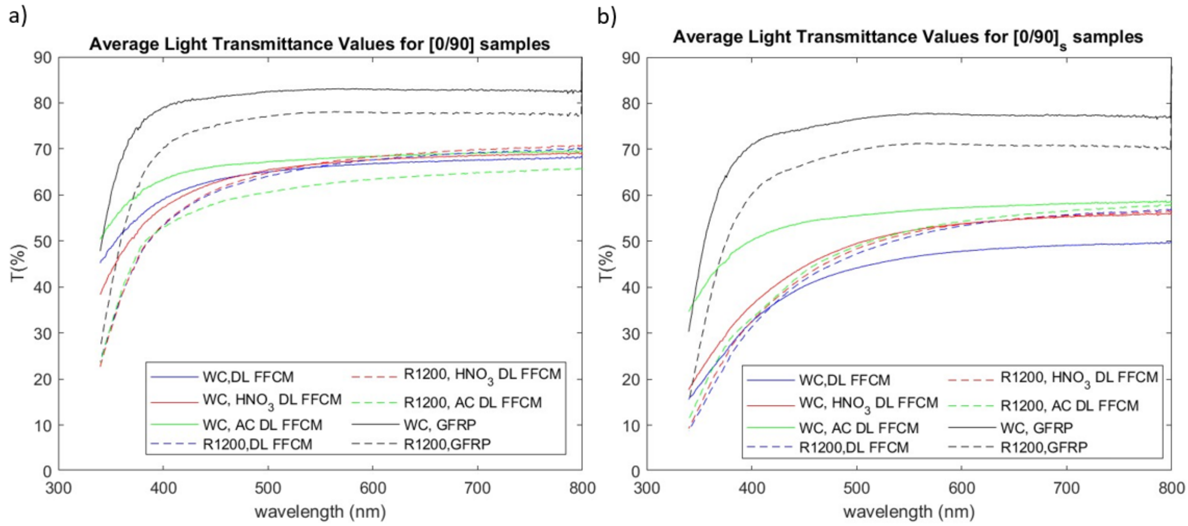

Figure 5.19: An overall comparison graph of the average total light transmittance curves of all the FFCM created during this project. a) $[0/90]$, b) $[0/90]_s$. Straight lines: WC/W300, Dashed lines: R1200/1204, Blue color: Delignified flax fibers, Red Color: Nitric acid/probe sonication treated delginified flax fibers, Green Color: NaOH/TEMPO-oxidation/Acetylation treated delignified flax fibers.

Also, there is a small difference which lies in the fiber volume fraction which is nearly 3% less for the ”Water-Clear”/W300 $[0/90]$ (42.47%) composite in comparison to the according material with the opposite resin system (39.91%). The fiber volume fraction was calculated with the ImageJ analysis software and the procedure is explained in Appendix B.5. The 4-layered R1200/1204 FFCM presented also a 5 % higher fiber volume fraction. This affects the optical transmittance as more fiber/matrix interphases which can decrease transmittance are present on the material or fiber aggregations due to the higher vf% percentage and the tendency of the fibers to form these clusters. This small difference between those two samples introduced uncertainty when comparing them and could have the opposite direction if the fiber volume fraction was the same (higher transmittance for the WC/W300 material). Normalization on the light transmittance values was not pursued during this project because the transmittance values are not only analogous to the fiber volume fraction but to the RI mismatch between the fiber and the matrix which can have higher contrast between two constituents and therefore give lower values even if the fiber vf% is quite lower. From the previous samples, it is clear that the $[0/90]$ composite materials of 0.8-0.9 mm thickness, present a fraction of total transmitted light which is close to 70%, close to the levels of transparent wood composite's levels which were presented on numerous occasions from the literature in Chapter 3 (Figures 3.10, 3.12, 3.13), in higher vf of the natural reinforcement (approximately 40%), compared to them. These levels were 80-90% for materials with a thickness close to 1 mm (lower volume fraction 5-20%).

Here the transmittance decreases significantly at the range of 400-500 nm (blue color in Figure 5.19), which can relate to a yellow to orange color, based on the color wheel of Figure 3.3. In contrast to the GFRPs, the broad absorption shoulder is not present in these graphs, in any case, making the absorption color which leads to blue, not an issue. This outcome results only in the light yellow to orange color, which can be verified from Figure 5.15, in which the four different samples present a light yellow to orange color, with the intensity of it again depending on the percentage of transmittance on those wavelengths (↓ transmittance = ↑ absorbance = higher intensity). The $[0/90]_s$ materials demonstrated a lower transmittance than 30%. However, the WC/W300 presented a 55-60% light transmittance in some locations at these low wavelength thresholds in the 2-layered materials presenting nice optical quality (superior transparency less intensity of chromatization), in contrast to the $[0/90]_s$ which showed lower transmittance values of approximately 30% and a steeper absorption shoulder, thus higher intensity of the light yellow color. Also, the 2-layered R1200/1204 composite material gave a minimum value close to 45-50% in comparison to the according material with 4-plies which showed a more diverse minimum light transmittance of 25-30%, again with a steeper absorption shoulder than the 2-ply samples. This implies higher color intensity on the R1200/1204 samples, possibly due to higher RI contrast on the composites which is verified from Figure 5.15.

Table 5.5: Thicknesses, fiber volume fraction, and average maximum light transmittance together with the standard deviation for all the FFCM materials which were produced with treated or untreated delignified flax fibers as reinforcement.

	Maximum light transmittance of each sample (T) in %			
Resin system	**Resoltech 1200/1204**	**Resoltech 1200/1204**	**Water-Clear/W300**	**Water-Clear/W300**
Reinforcement	**DL Flax Fiber UD Coupon**	**DL Flax Fiber UD Coupon**	**DL Flax Fiber UD Coupon**	**DL Flax Fiber UD Coupon**
Hot Press Forming	[0/90]	$[0/90]_s$	[0/90]	$[0/90]_s$
Thickness (mm)	0.93	1.03	0.82	0.99
Fiber Volume Fraction (%)	39.91	38.46	42.47	44.57
Average	**70.31**	**56.99**	**68.43**	**49.90**
Standard Deviation	**1.68**	**1.77**	**1.41**	**0.96**
Resin system	**Resoltech 1200/1204**	**Resoltech 1200/1204**	**Water-Clear/W300**	**Water-Clear/W300**
Reinforcement	HNO_3**/Probe sonication** **DL Flax Fiber UD Coupon**	HNO_3**/Probe sonication** **DL Flax Fiber UD Coupon**	HNO_3**/Probe sonication** **DL Flax Fiber UD Coupon**	HNO_3**/Probe sonication** **DL Flax Fiber UD Coupon**
Hot Press Forming	[0/90]	$[0/90]_s$	[0/90]	$[0/90]_s$
Thickness (mm)	0.83	1.10	0.86	1.17
Fiber Volume Fraction (%)	37.08	43.42	34.40	39.26
Average	**70.84**	**56.65**	**69.29**	**56.10**
Standard Deviation	**2.93**	**1.07**	**1.49**	**3.60**
Resin system	**Resoltech 1200/1204**	**Resoltech 1200/1204**	**Water-Clear/W300**	**Water-Clear/W300**
Reinforcement	**TEMPO/Acetylation** **DL Flax Fiber UD Coupon**	**TEMPO/Acetylation** **DL Flax Fiber UD Coupon**	**TEMPO/Acetylation** **DL Flax Fiber UD Coupon**	**TEMPO/Acetylation** **DL Flax Fiber UD Coupon**
Hot Press Forming	[0/90]	$[0/90]_s$	[0/90]	$[0/90]_s$
Thickness (mm)	0.74	0.84	1.01	1.18
Fiber Volume Fraction (%)	36.89	42.44	40.42	32.52
Average	**65.98**	**58.08**	**69.78**	**57.93**
Standard Deviation	**3.23**	**4.12**	**0.20**	**1.92**

Nitric Acid/ Probe Sonication Treated Delignified Flax Fibers
The results also indicate a total optical light transmittance of nearly 70% for both $[0/90]$ laminates which were treated with HNO_3/probe sonication, a value which did not differentiate from the previous composite materials that were untreated, as seen from Table 5.5. However, the critical dissimilarity was on the fiber volume fraction of the "Water-Clear"/W300 $[0/90]$ sample which presented a slight decrease of 8% (42.47% vs 34.40%) on the 2-ply samples. The difference between the two total transmittance levels of the treated and untreated FFCMs was less than +1%, while for the 4-ply material was nearly +7% (approximately 5% lower fiber volume fraction), signifying the success of the treatment on this set of samples. However, the standard deviation showed slightly increased values, with an increase of +2.5% of the $[0/90]_s$ and no increase on the 2-ply material.

These results show that the fibers' spacing of these nitric acid-treated samples is as homogenous as the previous untreated ones and transmittance can stay equally close or higher. This can be attributed to the stoppage of the formation of aggregates in elementary cellulose fibers and better dispersion/homogeneity of them (particularly on the $[0/90]_s$ samples) which will reverse the phenomenon of light reflection and scattering on the boundaries of them. For the two Resoltech 1200/1204 matrix-based $[0/90]$ and $[0/90]_s$ composite materials, the difference in optical transmittance between the treated and untreated FFCMs was approximately +0.5%, while for the 4-ply materials it was -0.3%. The fiber volume fraction remained at the same levels for the 2-layered material (39.91% vs 37.08%) while the 4-layered material presented a 7% increase on fiber vf% while holding optical transmittance on exactly the same value. Again this verifies the assumption that nitric acid treatment becomes efficient considering higher optical transmittance when the fiber number is multiplied in the interior of the material (higher fiber volume fraction, more plies, etc), because of the more homogeneous dispersion of the microfibers which can form agglomerations on high numbers.

The previous comments imply that the treatment was not fully effective in terms of increasing light transmittance and defies the assumption that a wider spacing of the elementary flax fibers can affect optical transparency in all cases. Only on one occasion, the HNO_3/probe sonication treated FFCM show a slight increase in maximum light transmittance than the untreated FFCM ("Water-Clear"/W300, $[0/90]_s$). The results of low standard deviation values, confirm the optical observations of good homogeneity. However, the standard deviation values were not lower than the according values of the untreated FFCMs. Erasing the cause of fiber spacing in the interior of the material, and after observing the numerous defects in Figure 5.17, again the main cause of not accomplishing even better light transmittance becomes the defects/gaps which are present in the material due to the inadequate wetting and interphasial bonding of the fiber/matrix.

Again comparing the two polymers, the differences between them in terms of maximum light transmittance are minimal (1.5% for $[0/90]$ materials and 0.5% for $[0/90]_s$). However, the light absorption shoulder which is present near the 400 nm threshold (red lines at Figure 5.19), shows that the WC/W300 polymer matrix composites transmit a higher intensity of light at that wavelength (50-55% in 2-ply materials, 25-35% in 4-ply materials) in contrast to R1200/1204 materials which show a 5-10% decreased value on this wavelength (45-50% in 2-ply materials, 25-30% in 4-ply materials) decrease. This implies that the absorption is slightly stronger for these materials, making the color intensity also more intense, as seen in Figure 5.17. These results make it more clear that in terms of RIM, the delignified flax fibers seem to have a closer RI with the WC/W300 polymer system (1.538) than the R1200/1204 (1.560), as the chromatic aberration can be caused by light dispersion due to RI mismatch of the fibers with the matrix. The higher the mismatch the stronger the bending of some wavelengths of light which can be scattered around and absorbed or reflected.

NaOH/TEMPO/Acetylation Treated Delignified Flax Fibers
The final results of the composite materials which were treated with NaOH/TEMPO-oxidation/Acetylation modification indicate the same levels as the previous maximum light transmittance values of treated and untreated FFCM. This implies that the maximum light transmittance on the visible spectrum does not differentiate based on the fiber modification that is implemented. The $[0/90]$ modified composite materials with "Water-Clear"/W300 present an average maximum light transmittance of 69.78% which has a minor difference of $\pm$0.5% with the previous occasions, while the $[0/90]_s$ show a small difference with the according to HNO_3/probe sonication treated composite material of near +2% and +8% with the untreated delingified FFCM. The same trend is noticed on the Resoltech 1200/1204 composite materials, with a -5% difference in maximum total light transmittance on the $[0/90]$ samples and +2% for the $[0/90]_s$ composite

material. Possibly this small increase of values in a higher number of plies can be justified with the more complete interphase between the fiber/matrix. However, the differences in the values are lower than expected. This can be attributed to the influence of the RIM on the polymer with the flax fibers, which is not fulfilled. This concept seems to be the only similarity in all cases, giving the same transmittance values in all cases in the $[0/90]$ samples. The standard deviation values lie on low and comparable values with the HNO_3/probe sonication treated and untreated FFCM. Especially the ”Water Clear”/W300 composite materials show the lowest values out of all the previous samples created with 0.20% and 1.92% (1.49% and 3.60% accordingly for HNO_3/PB samples, 1.41% and 0.46% for the untreated samples), while the Resoltech 1200/1204 samples present a minor increase from the previous samples, possibly due to the fiber breakage/fracture which was observed at those samples, which can affect fiber dispersion and create more aggregations.

The results suggest that the NaOH/TEMPO-oxidation/Acetylation treatment is also not fully effective in increasing the maximum optical transmittance. However, the chromatization of the material is fully absent in the case of the ”Water-Clear”/W300 composite materials, meaning that this treatment might assist in minimizing absorbance on lower light wavelengths. For these samples the peak presents at 400-450 nm (green color) in Figures 5.19, however, the absorbance remains at low levels (55-60% for the $[0/90]$, 40-45% for the $[0/90]_s$) even when it occurs. This ensures that the color’s intensity will be at low levels, which is fully confirmed by its absence of color in Figure 5.15f. On the other hand, this is not fully the case for the Resoltech 1200/1204 samples as they show a similar transmittance shoulder at low wavelengths (comparable to the HNO_3/PB treated and untreated samples, even starting from lower maximum light transmittance) increasing the color’s intensity. These can be seen in Figure 5.15e, on which the material presents some regions of light yellow to orange color (especially on the $[0/90]_s$ on which scattering phenomena are more intense). The switch of the fiber’s character from hydrophilic to hydrophobic, and therefore the better interphase was assumed to be the main action of increasing optical transparency in the WC/W300 samples. However, this is confirmed only in low wavelengths (where the other materials presented higher absorption rates) and this can indicate that the interphasial voids might play a significant role in light transmittance on these wavelengths. By reducing the number of these light scattering issues, light is absorbed/scattered lightly on those wavelengths compared to the other samples, reducing the color’s intensity.

Comparison Analysis

Furthermore, comparing the results of the transparent FFCMs with those of the transparent GFRPs from the previous section, it is apparent that there are considerable but not huge differences between the highest optical transmittance in the visible light spectrum of those two when comparing the $[0/90]$ materials (7-12% on R1200/1204 and 13-14% on ”Water Clear”/W300), even though the thickness of the FFCM is nearly 1.5X times higher than the GFRPs. However, when adding more plies, like in the case of $[0/90]_s$ the transmittance plummets, showing a greater difference of 12-14% for the Resoltech 1200/1204 and 20-26% for the ”Water Clear/W300”, while the difference of thickness between the GFRPs and FFCMs remains in high levels (R1200/1204: 0.61/1.03, 1.10, 0.84 and ”Water Clear”/W300: 0.64/0.99, 1.17, 1.18). That can be due to the increase of light path or the probability of a defect being present in the material which scatters light and the inhomogeneous character of the flax fibers (glass fibers are more homogeneously dispersed in the interior of the material as observed from OM photos), which can result in poor impregnation of the fiber or fiber aggregation which scatters light as well. However, there is also another crucial factor here. Glass fibers are not hydrophilic, meaning that they do not contain -OH groups which can deteriorate the interphasial quality, creating gaps due to air volatiles or inadequate wetting in contrast to DL flax fibers (Figure 5.14 shows few interphasial voids in comparison to the increased number of them in Figure 5.17). A more complete interphase between the constituents of the FRC correlates to fewer gaps and less intense RI mismatch of the gaps with the constituents. This means that the increase of plies and thickness affects more the FFCMs than the GFRPs, which is verified by the comparison of the graphs in Figure 5.20 and 5.22. This comparison can ensure that these natural fiber composite materials can be considered as functional materials which exemplify a sufficient level of optical transparency (high translucency), being compared to high transmittance levels of GFRPs like the 2-layered low thickness samples which presented high transparency near 80% (Figure 5.12c and d) while reducing the CO_2 emissions and energy required for production (Figure 2.1), increasing the environmental character of these materials due to natural fibers.

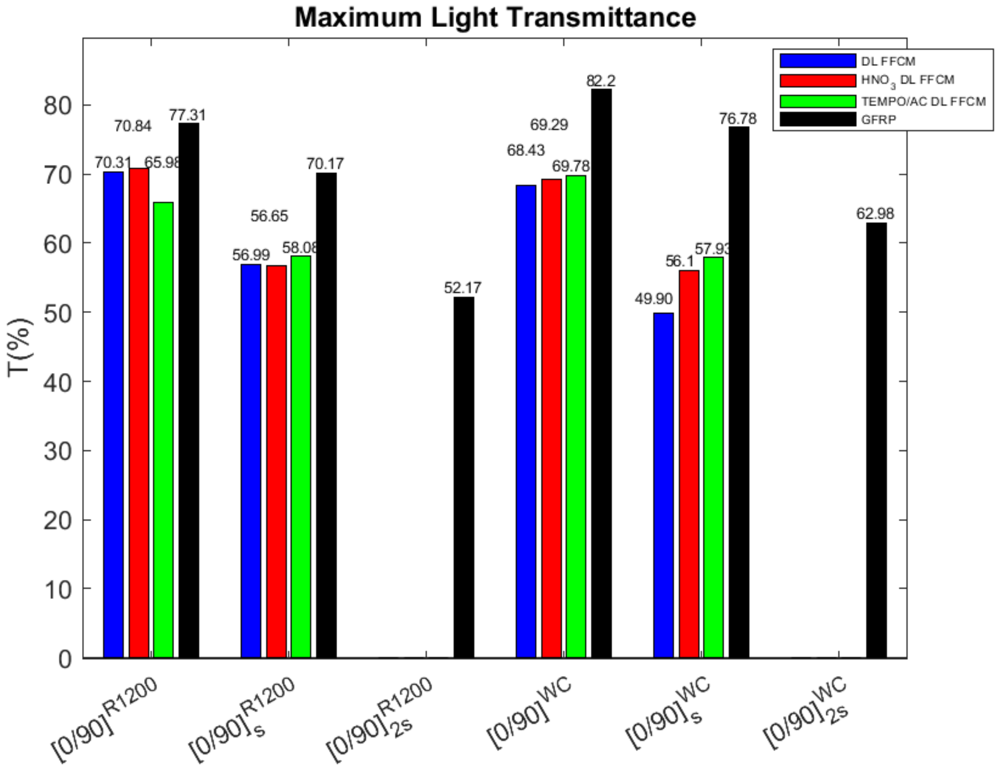

Figure 5.20: An overall comparison graph of the maximum light transmittance value for all the composite samples created during this project.

A comparison of the results of the developed functional FFCM which were fabricated in the scope of this project with other functional NFCM which were discovered in the literature, is depicted in the next Figure. For this comparison, only the 2-layered flax fiber composite materials were used, due to the relatively close thickness (0.8-1 mm) and higher transparency they presented which is analogous to the transparent wood and cotton-reinforced composite materials from the literature. These transparent wood materials of 1.2 mm thickness and 5-40% cellulose volume fraction (as seen in Figure 3.10) developed by Li et al., are depicted with yellow and magenta. [10] Another transparent wood formation that was introduced into the comparison analysis was the non-acetylated (green color) and acetylated (brown color) materials of the research of Li et al., depicted in Figure 5.21, with a thickness of 1.5 mm and a cellulose volume fraction of 30% in each of them. [13] The last material plugged into the comparison analysis was the cotton fiber-reinforced transparent material (light blue color) which was treated with the trio of modifications that the last set of FFCMs were modified with. [15] The graph demonstrates that low-volume fraction transparent wood of 5% mm gives 15-20% higher values of total light transmittance than the maximum value of FFCM in low-volume fractions. However, when the cellulose vf is increased to the levels of the developed FFCMs (40%) transparent wood of 1.2 mm gives a significantly lower transmittance (58%) than the developed transparent FFCM with the same vf. The same is observed on the non-acetylated transparent wood formulation of Li with 1.5 mm thickness and 30% volume fraction, with 64% total light transmittance concerning the 65-70% value of the transparent FFCM developed on this project with 5-10% higher volume fraction of the reinforcement, while acetylation boosts the optical transparency of transparent wood into 20% higher levels of light transmittance in comparison to the transparent FFCMs. Finally, the cotton fiber reinforced polymer composite which was treated with the trio of modifications showed again 15% higher light transmittance than the FFCM vs the maximum value and nearly 20% higher being compared to the according FFCM that was modified with the same trio of modifications. The higher transmittance values of the low volume fraction NFCMs can be attributed to the better interphase and infusion of the matching polymer system to the porous wood's structure (bigger lumens and the pores created from the removal of lignin), the significantly lower volume fraction of these NFCMs which reduces the number of light scattering interphases and refractive index mismatches in the interior of the material. However, when the reinforcement volume fraction is increased to 30-40% levels on transparent wood, the

FFCM shows 5-12% higher total light transmittance, presenting enhanced results compared to transparent wood.

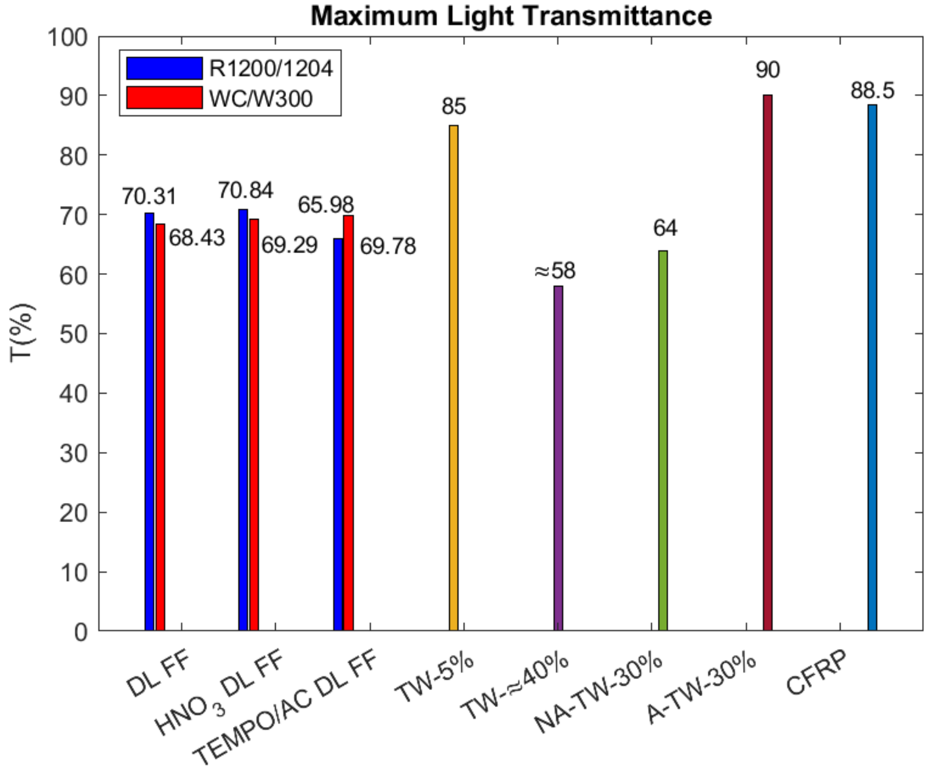

Figure 5.21: An overall comparison graph of the maximum light transmittance value for the $[0/90]$ samples created during this project (36-42% vf) with other transparent natural fiber composites from the literature. TW-5%: Transparent Wood, 1.2 mm, 5% vf [10], TW-≈40%: Transparent Wood, 1.2 mm, 40% vf [10], NA-TW-30%: Non-acetylated transparent wood, 1.5 mm, 30% vf [13], A-TW-30%: Acetylated transparent wood, 1.5 mm, 30% vf [13], CFRP: Transparent Cotton Reinforced Polymer treated with NaOH/TEMPO/Acetylation treatment [15].

Furthermore, comparing the absorption shoulders that are responsible for low wavelength absorption and chromatization of the materials, in Figure 5.19 and Figures 3.12, 3.13 extracted from literature, can result in similar shoulders and rates between the non-acetylated transparent wood and WC/W300 composite materials reinforced with treated delignified flax fibers. The best result outcomes from the NaOH/TEMPO/Acetylated treated flax fiber composite materials (green line), which seem to approximate the light transmittance values in low wavelength (around 400 nm in 2-ply materials which is 55-60%) in the non-acetylated transparent wood infiltrated with PMMA (approximately 60%). The acetylated transparent wood from Figure 3.13 or the transparent wood infiltrated with PVP from Figure 3.12, illustrate more gentle shoulders and higher total light transmittance, resulting in higher transparency on the materials as seen from Figure 5.15.

Figure 5.22 shows an overall graph about how the thickness of the sample affects total light transmittance. It is transparent that as long as each sample's thickness is increased, the transmittance shows a downtrend. GFRPs achieve lower thickness possibly due to the smaller diameter of the glass fibers (229 μm) than a random measurement of a flax fiber's diameter (364 μm) from an OM image. However, this value of the flax fiber's diameter can be even higher due to the inhomogeneity of these twisted fibers. The thickness of the sample can be decisive in the propagation of light in the interior of the material, as the path of light can be higher which can affect the obstacles of light transmission as light absorbance or more intense scattering due to defects. This is derived mathematically by the Beer-Lambert law, which states that the absorbance of a medium is directly proportional to the thickness of the specimen the light passes through, as well as the concentration of various particles in the material and the molar absorptivity (how strong a material absorbs and attenuates light): [73]

$$A = \epsilon c l \tag{5.1}$$

with A being the absorption of the material, ϵ is the molar absorptivity of the material, c is the concentration of the particles in the material (mol/cm^3) and l is the thickness of the sample in cm. If it is assumed that in a composite material with the same constituents (delignified flax fibers and polymer matrices), the molar absorptivity is identical (an intrinsic material property) then absorption is proportional to the concentration of the material (higher void or even fiber volume fraction) and the light path (thickness of the material). This is verified by the descent of the values with the increase of thickness. It is also clear that as the plies and thickness of the materials are increased, the light-hindering issues which are more severe in FFCM (light absorption, interphasial defects due to hydrophilic character of flax fibers, inhomogeneity of fibers, cellulose aggregations, RI mismatch, higher thickness, etc) affect harshly the light transmittance values due to the increase of the number of fibers in the interior structure of the material. This is reflected in the above figure as the maximum light transmittance decreases only 5-7% with increasing the plies from 2 to 4 in GFRPs, while in FFCM the drop near 10-15% levels.

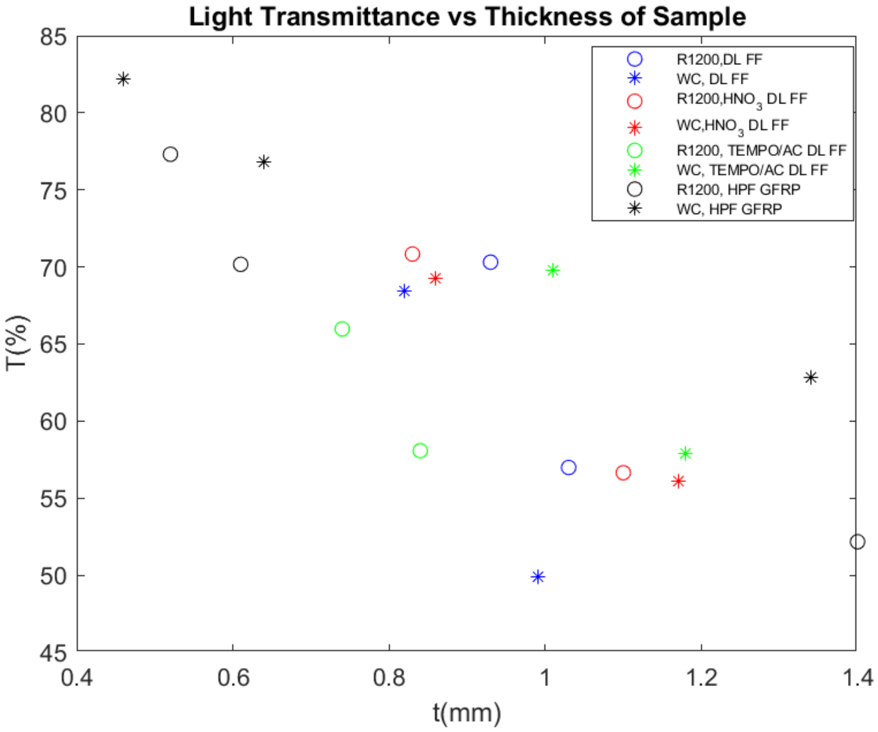

Figure 5.22: A graph of the maximum total light transmittance for a variety of samples created during this project, in relation to its thickness.

5.5. Mechanical Properties

Flexural testing was implemented on the GFRP and FFCM materials for investigation of their properties when subjected to bending, such as flexural stiffness and flexural strength. The specimens which were used for testing are depicted in Figure B.5 and as explained previously they were designed to be cut into a length of 65 mm ± 3 mm and a width of 17 mm ± 3 mm. Because of the variation of fiber volume fraction from sample to sample, all the flexural properties were normalized to 40% fiber volume fraction. For the GFRPs only the 2-ply and 4-ply materials were tested, because they would represent reference materials for comparing the flexural values of the transparent FFCMs (in these materials no 8-ply materials were fabricated, Table 4.5). Table 5.6 presents the flexural properties which were calculated from the 3-point bending tests implemented in this project. In this Table, the average value of the three testes specimens as well as the normalized properties at 40% fiber vf and the standard deviation for these values, are depicted. The density of the material is also calculated which is an important aspect of the specific properties demonstrated in Figure 5.23. All the normalized values extracted from the 3-point bending tests for each specimen tested are depicted in Appendix D. The specific properties were calculated with the ratio of each flexural property divided by the density of the material/specimen. In this image, the flexural properties of the acetylated transparent wood developed by Li et al. which was subjected to 3-point bending testing are also depicted, for comparison purposes. [13]

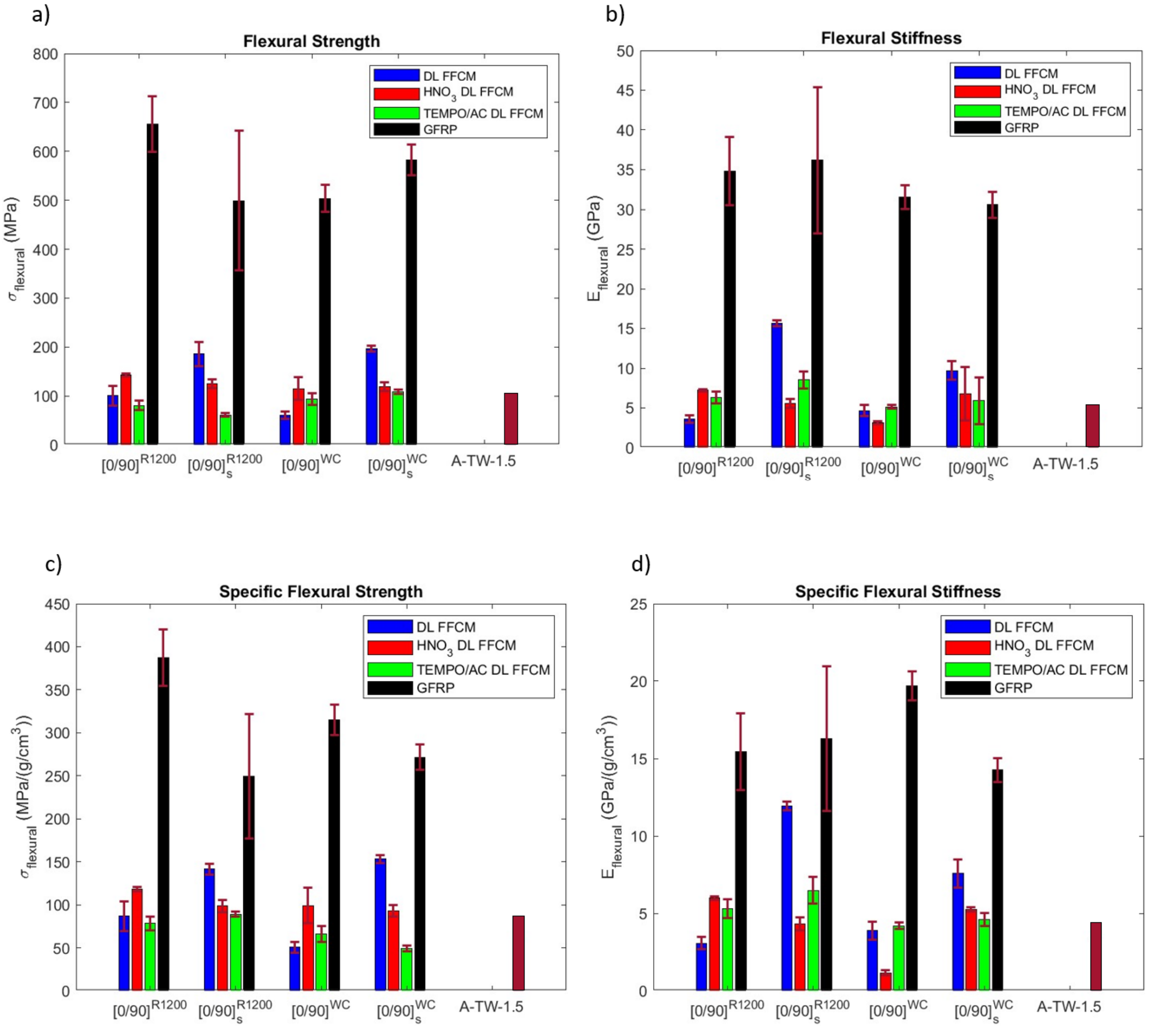

Figure 5.23: A graph of the normalized flexural properties for all the composite samples created during this project plus the 30% vf acetylated transparent wood of 1.5 mm thickness (A-TW-1.5) normalized at 40% fiber volume fraction. a) Flexural Strength b) Flexural Stiffness c) Specific Flexural Strength d) Specific Flexural Stiffness

All the results concerning the average normalized flexural strength or stiffness of the 4-ply FFCM specimens appear to decrease significantly from the plain delignified flax fiber composites compared to the treated samples, in both polymer's cases. The high average flexural strength which was calculated in the 4-ply materials (R1200/1204 vs WC/W300, 185.63 MPa vs 196.25 MPa), decreased significantly (32% for R1200/1204, 40% for WC/W300) when they were treated with nitric acid/probe sonication treatment, while the values deteriorate even in a higher margin (65% for R1200/1204, 45% for WC/W300) when treated by the trio modification of NaOH/TEMPO/Acetylation treatment. The average flexural stiffness (R1200/1204 vs WC/W300, 15.69 GPa vs 9.71 GPa) decreases in high proportions as well, for both treatments case in the 4-ply materials. On the other hand, the 2-ply materials show a different trend. It seems that the nitric

Table 5.6: Average and normalized (at 40%vf) flexural strength and stiffness for the composite samples produced during this project.

	Flexural Properties			
Resin system	**Resoltech 1200/1204**	**Resoltech 1200/1204**	**Water-Clear/W300**	**Water-Clear/W300**
Reinforcement	**Glass Fiber Woven Fabric**	**Glass Fiber Woven Fabric**	**Glass Fiber Woven Fabric**	**Glass Fiber Woven Fabric**
Hot Press Forming	[0/90]	[0/90]$_s$	[0/90]	[0/90]$_s$
Thickness (mm)	0.52	0.61	0.46	0.64
Fiber Volume Fraction (%)	39.42	52.43	30.56	63.65
Average Flexural Strength (MPa)	655.94	644.06	384.94	925.75
Normalized Flexural Strength (MPa)	**665.59**	**499.36**	**503.84**	**581.77**
Standard Deviation (MPa)	**112.68**	**285.04**	**56.63**	**62.81**
Average Flexural Stiffness (GPa)	34.32	34.32	24.09	48.65
Normalized Flexural Stiffness (GPa)	**34.82**	**26.18**	**31.53**	**30.57**
Standard Deviation (GPa)	**8.52**	**18.40**	**2.97**	**3.34**
Density (g/cm^3)	1.718	1.970	1.600	2.143
Specific Flexural Strength ($MPa.cm^3/g$)	**387.47**	**249.41**	**314.88**	**271.49**
Specific Flexural Stiffness ($GPa.cm^3/g$)	**15.43**	**16.29**	**19.70**	**14.26**
Resin system	**Resoltech 1200/1204**	**Resoltech 1200/1204**	**Water-Clear/W300**	**Water-Clear/W300**
Reinforcement	**DL Flax Fiber UD Coupon**	**DL Flax Fiber UD Coupon**	**DL Flax Fiber UD Coupon**	**DL Flax Fiber UD Coupon**
Hot Press Forming	[0/90]	[0/90]$_s$	[0/90]	[0/90]$_s$
Thickness (mm)	0.93	1.03	0.82	0.99
Fiber Volume Fraction (%)	39.91	38.46	42.47	44.57
Average Flexural Strength (MPa)	100.60	178.60	64.28	218.67
Normalized Flexural Strength (MPa)	**100.83**	**185.63**	**60.55**	**196.25**
Standard Deviation (MPa)	**40.19**	**48.52**	**15.77**	**11.53**
Average Flexural Stiffness (GPa)	3.57	15.08	4.94	10.82
Normalized Flexural Stiffness (GPa)	**3.58**	**15.69**	**4.66**	**9.71**
Standard Deviation (GPa)	**0.91**	**0.76**	**1.39**	**2.35**
Density (g/cm^3)	1.161	1.313	1.197	1.281
Specific Flexural Strength ($MPa.cm^3/g$)	**86.82**	**141.37**	**50.58**	**153.21**
Specific Flexural Stiffness ($GPa.cm^3/g$)	**3.08**	**11.95**	**3.88**	**7.58**
Resin system	**Resoltech 1200/1204**	**Resoltech 1200/1204**	**Water-Clear/W300**	**Water-Clear/W300**
Reinforcement	HNO_3**/Probe sonication DL Flax Fiber UD Coupon**	HNO_3**/Probe sonication DL Flax Fiber UD Coupon**	HNO_3**/Probe sonication DL Flax Fiber UD Coupon**	HNO_3**/Probe sonication DL Flax Fiber UD Coupon**
Hot Press Forming	[0/90]	[0/90]$_s$	[0/90]	[0/90]$_s$
Thickness (mm)	0.83	1.10	0.86	1.17
Fiber Volume Fraction (%)	37.08	43.42	34.40	39.26
Average Flexural Strength (MPa)	132.24	136.14	98.98	116.88
Normalized Flexural Strength (MPa)	**142.66**	**125.44**	**115.10**	**119.08**
Standard Deviation (MPa)	**6.01**	**18.19**	**47.59**	**17.80**
Average Flexural Stiffness (GPa)	6.69	6.01	2.65	6.61
Normalized Flexural Stiffness (GPa)	**7.22**	**5.54**	**3.09**	**6.74**
Standard Deviation (GPa)	**0.31**	**1.08**	**0.38**	**0.38**
Density (g/cm^3)	1.205	1.274	1.161	1.282
Specific Flexural Strength ($MPa.cm^3/g$)	**118.36**	**98.47**	**99.10**	**92.86**
Specific Flexural Stiffness ($GPa.cm^3/g$)	**5.99**	**4.34**	**1.16**	**5.25**
Resin system	**Resoltech 1200/1204**	**Resoltech 1200/1204**	**Water-Clear/W300**	**Water-Clear/W300**
Reinforcement	**TEMPO/Acetylation DL Flax Fiber UD Coupon**	**TEMPO/Acetylation DL Flax Fiber UD Coupon**	**TEMPO/Acetylation DL Flax Fiber UD Coupon**	**TEMPO/Acetylation DL Flax Fiber UD Coupon**
Hot Press Forming	[0/90]	[0/90]$_s$	[0/90]	[0/90]$_s$
Thickness (mm)	0.74	0.84	1.01	1.18
Fiber Volume Fraction (%)	36.89	42.44	40.42	32.52
Average Flexural Strength (MPa)	74.12	64.84	94.41	88.07
Normalized Flexural Strength (MPa)	**80.37**	**61.11**	**93.46**	**108.08**
Standard Deviation (MPa)	**19.44**	**6.96**	**22.77**	**8.26**
Average Flexural Stiffness (GPa)	5.83	9.02	5.18	4.80
Normalized Flexural Stiffness (GPa)	**6.32**	**8.51**	**5.13**	**5.91**
Standard Deviation (GPa)	**1.49**	**2.10**	**0.54**	**1.00**
Density (g/cm^3)	1.192	1.215	1.222	1.240
Specific Flexural Strength ($MPa.cm^3/g$)	**78.42**	**88.98**	**65.77**	**49.26**
Specific Flexural Stiffness ($GPa.cm^3/g$)	**5.30**	**6.48**	**4.20**	**4.60**

acid/probe sonication treatment assists in the improvement of the flexural properties presenting higher flexural strength in both polymers' occasions (R1200/1204 vs WC/W300, 142.66 MPa vs 115.10 MPa) and higher flexural stiffness in the R1200/1204 composite sample (higher than a double value compared to the untreated sample's stiffness), while the WC/W300 value seems to reduce slightly (1.5 GPa-33%). Nearly all the flexural properties of the modified flax fibers with NaOH/TEMPO/Acetylation utilized as reinforcement in R1200/1204 and WC/W300, seem to decline. The only exemption could be the 2-ply material with WC/W300 as a matrix, which shows a slight increase in both the flexural strength (untreated vs treated, 60.55 MPa vs 93.46 MPa, at 35%) and flexural stiffness (untreated vs treated, 4.66 MPa vs 5.13 MPa, at 9%).

Despite the decline in flexural properties in the majority of the samples, the standard deviation, appeared to decrease, particularly regarding the R1200/1204 values. The flexural strength values particularly appear to converge in the three specimens tested in each case, in both treated samples with R1200/1204 (untreated vs treated 2-plies/4-plies, 40.19/48.52 MPa vs 7.22/5.54 MPa, 19.44/6.96 MPa) showing better homogeneity in the materials, attributed in the treatments with nitric acid and TEMPO-oxidation which give better dispersion and fewer fiber aggregations. The standard deviation for the average flexural stiffness on the according specimens seems to stay on the same level or slightly increase depending on the treatment. For the WC/W300 matrix-based specimens, the story is different. For the 2-ply materials, the standard deviation of the flexural strength increases for both treatments (untreated vs treated 2-plies, 15.77 MPa vs 47.59, 22.77 MPa), while for the 4-ply cross materials it either slightly increases or decreases depending on the treatment. Regarding flexural stiffness the standard deviation values decrease. These values for standard deviation show that in the 4-ply materials, the treatments are not as effective as in the previous case for increasing homogeneity and dispersion of fibers, and that can be attributed to the high pressures and lower viscosity for these materials, which can tighten the space between the fibers resulting in fiber aggregations or degraded fibers.

Comparing the flexural values of the FFCMs developed in the scope of this research with values extracted from the literature (Table 5.7), the trend shows that flexural strength and stiffness are inferior to these values. Only the woven fabric-reinforced materials seem to be comparable to the flax fiber-reinforced composite materials created, with minor differences in contrast to the higher-level UD FFCMs. This can be attributed to the contribution of the longitudinal direction of flax fibers in these UD materials which present superior flexural properties (stronger and stiffer direction) in this direction compared to the mechanically inferior transverse direction, which contributes in both the woven fabric materials from the literature and the cross-ply materials developed in this project.

The flexural testing showed that the values of the GFRP woven composite materials are not on the same levels as the ones from the FFCMs. In all cases, the GFRPs had approximately four to six times higher values. Also, for 4-ply materials, the plain DL FFCM presents higher flexural properties, while for the 2-ply materials, the nitric acid-treated samples seem to present higher values on these properties. This highlights the importance of balancing the extra fiber treatments to not deteriorate the mechanical properties of the materials. One possible reason for the reduction of the magnitude of these properties can be the aggressive treatments with oxidizers that can deform the fiber structure, thus not allowing the reinforcement to provide the finest behavior. As explained earlier, nitric acid (-1.5 pKa), perchloric acid (-15.2 pKa), and acetic anhydride (-6.9 pKa) are all strong oxidizers, which if applied and used for long periods can deteriorate the structure of fiber (possibly degrading cellulose). Also, the TEMPO-mediated oxidation carboxylates the surface of the flax fibers which can deform the fiber's surface from repulsive forces due to the negatively charged molecules. All these observations are verified from OM and SEM images. Another cause can be the interphasial or matrix defects which can also affect the properties of the materials. Additionally, the absence of hydrogen bonds due to acetylation might be essential to the increase of the optical quality of the material, however, it will decrease the strength that cellulose fibers provide to the composite material because it can block the hydrogen bonds that consist of the glucose units of cellulose into microfibrils, in the case of NaOH/TEMPO/Acetylation. Beldzki et al., investigated how the acetylation degree of the flax fibers can influence the tensile and flexural properties of composite materials. [22] Figure 2.9 shows that if the acetylation degree overcomes 18% then the flexural properties of the composite materials are dropped from the untreated values. [22] Possibly if the acetylation degree reaches an even higher level the properties would deteriorate more. Alix et al., also researched how different chemical treatments affect the properties of flax fibers. [30] Figure 2.10 shows that the treated flax fibers with acetylation presented a significantly lower tensile strength than the untreated fibers. [30]

The same can be assumed to apply to the flexural strength as well. However, when comparing the values of transparent FFCMs with acetylated transparent wood of 1.5 mm thickness (normalized from 30% fiber volume fraction to 40% vf), the majority of the flexural values presented in these graphs were higher. This shows that these FFCMs can be comparable with other functional NFCMs. These values were a normalized flexural strength of 105.2 MPa (78.9 MPa at 30% vf) and a normalized flexural stiffness of 5.33 GPa (4 GPA at 30% vf).

Table 5.7: Average and normalized (at 40%vf) flexural strength and stiffness for FFCM extracted from the literature. [34], [35], [36]

	Flexural Properties				
Study	Kong	Kong	Goutianos	Goutianos	Bcomp
Ply Orientation	UD	Woven	UD	Woven	UD
Fiber Volume Fraction (%)	35	35	28	29	54
Average Flexural Strength (MPa)	188	108.70	190	140	377
Normalized Flexural Strength (MPa)	**214**	**124**	**271**	**193**	**279**
Average Flexural Stiffness (GPa)	9.7	6.7	16	10	32.6
Normalized Flexural Stiffness (GPa)	**11.08**	**7.6**	**23.37**	**13.79**	**22.8**

When comparing the specific flexural properties (flexural properties divided by the density of the material), the differences between the GFRPs and the FFCMs on the values of flexural strength and stiffness, are decreased. This is due to the lower density of the FFCMs (approximately 1.1-1.3 g/cm^3) than the GFRPs (1.7-2.1 g/cm^3) and very close to the density of the acetylated wood (1.2 g/cm^3). Especially, the specific flexural strength and stiffness values of the DL FFCMs are relatively close to the according value of the GFRPs. Nearly all the flexural properties of the treated and untreated DL FFCMs are higher than the properties of the acetylated transparent wood, as seen in Figure 5.23.

Part III

Summarization

6
Conclusion

In conclusion, this report covers the development of a new natural-fiber-based, less energy-intensive, and functional composite material. The research objective focused on fabricating a flax fiber-reinforced composite material with a direct goal of having the highest possible optical transparency. To evaluate if the objective of the thesis is accomplished, the answers to the four research questions that were asked in the introduction Chapter should be judged.

The first question regarding the research of this topic introduced in Chapter 1, was the biggest obstacle and challenge for developing a fully transparent flax fiber-reinforced composite material. The inability to detect this RI was pivotal to decrease the light scattering issues as low as possible. Immersion testing with organic compounds, a simple and cheap procedure for detecting the RI of a fiber was implemented, with either Ethanol/Benzyl Benzoate or Ethyl Cinnamate/Ethyl Salicylate, both with different RI ranges between 1.361 to 1.568 (with steps on the second decimal) for the first solution and 1.521 to 1.558 (with steps on the third decimal). The results didn't show a full RIM, however, they showed a partial RIM near 1.53-1.54 values, limiting the matching range to this significantly smaller span. Poor fiber/matrix interphase, presence of air, intrinsic light scattering in cellulose structure, and light scattering due to cellulose aggregations are some of the reasons identified for the inability to detect the property. A more detailed investigation of the RI of the delignified flax fiber is required.

The facts show that delignification is the most crucial fiber treatment as it eliminates light absorption transforming the fiber's color from a brown opaque to a white (more translucent) color and gives high light transmittance values (55-70% maximum optical transmittance) when infused with a polymer matrix that has a close RI. The delignification which is followed in this report, was based on a solution of hydrogen peroxide (H_2O_2) and glacial acetic acid. As an extra important step in increasing the optical transparency, NaOH/TEMPO/Acetylation treatments tackled additional crucial issues (chromatic aberration or decrease of voids). This trio of treatments ensures a swelling process of cellulose structure, better dispersion of elementary flax fibers, and greater interphase between the fiber/matrix with fewer debonding gaps, presenting the highest magnitude in light transmittance values and giving the best-looking samples.

Moreover, as stated by the literature a match between the fibers and a polymer regarding the refractive index is the second most important action for a transparent NFCM, which is confirmed by the research in this report. Two polymers were selected to be tested as suitable candidates for a polymeric matrix in developing a transparent flax fiber-reinforced material. The primary philosophy for the selection was the RIM between the fiber/matrix. However, without knowing the exact RI of the delignified flax fiber, a trial and error test was implemented with polymers being close to the range of the partial RIM range, resulting from the immersion testing. These polymers were the epoxy materials, Resoltech 1200/1204 (1.560) and "Water-Clear"/W300 (1.538) polymeric systems. Ultimately, from these two materials WC/W300 presented the best optical results (especially when combined with the NaOH/TEMPO/Acetylated DL flax fibers), with low absorption rates (meaning low chromatic intensity) on low wavelengths of visible light. The flexural properties of the materials were similar and comparable to other transparent NFCMs.

The last research question concerned the two different production techniques implemented, combining wet lamination with either vacuum pressing or hot press forming. The latter showed better optical results and lower void size (a serious light scattering issue), consolidating some of the volatiles inside the polymer, but not fully eliminating them. More research on higher pressures or different techniques is required, for superior optical properties.

With relatively close transmittance values of the transparent FFCM (55-70%) to transparent wood or cotton, comparable specific flexural properties, and showcasing functionality, the applications of transparent wood can be generalized to the FFCMs. First and foremost, the ease of observing the interior structure of these transparent materials, causes damage evolution (microcrack propagation) to be effortlessly spotted in the material, without any destructive method to be conducted. Therefore, the repair or the total fracture prognosis of the material can be quicker, more efficient, and with fewer obstacles. The thermal insulation of flax fibers (thermal conductivity of 0.17 $W/m.k$ in the transverse direction) and the epoxy matrices (0.17-0.21 $W/m.k$) can be considered on the same levels as wood's insulation properties(0.15 $W/m.k$), superior to glass's insulation properties (1 $W/m.k$) making it attractive for smart building panels, as seen in Figure 3.20. [54], [74], [75] Additionally, the density of the transparent FFCM (1.1 -1.3 g/cm^3) is relatively lower than the density of GFRP (1.7-2.1 g/cm^3) or glass (2.4-2.8 g/cm^3), favoring the design of lightweight structures. Another suitable application for these materials can be low-thickness coatings in solar cell applications, which can ensure light capturing due to increased light scattering (will increase light path improving the probability of the cell catching the photon) and light transmittance in some of these FFCMs, and therefore generate energy. [11]

This master thesis report aims to give insight and resourceful knowledge in the main fields described previously and answer the questions that a novel researcher can raise. It is safe to say that the answers to some of these questions resulted in important points that drastically improve the current research on transparent flax fiber-reinforced composite materials by the information provided. Some of them can be the re-implementation of immersion testing on a smaller span of refractive indices using organic compounds close to 1.53-1.54 levels or the improvement of fiber/matrix adhesion with NaOH/TEMPO-oxidation/Acetylation fiber treatment on the interphase of the composite material which provides fewer debonding gaps and reduces light scattering/chromatic aberration significantly. More research on this topic can be pivotal to increasing the light transmittance levels to even higher degrees, based on points concluded from this report. To this extent, this report paves the way for future research on the production of a flax fiber-reinforced composite material that will exhibit functional properties like optical transparency.

7

Future Research Recommendations

7.1. Production Technique

A topic worth to be investigated is the change in the production technique of composite materials. Wet lamination is a simple and quick technique that does not require complex equipment or complicated production procedures. However, this research project showed that wet lamination introduces entrapped air in the interior structure of the material. The belief was that with a high pressure following the hot press forming technique these air bubbles would be dissolved in the liquid resin. This did not occur in full capability even in 10 bars of pressure, the bubbles reduced in size but they were present in the material leading to scattering sources and deteriorating the mechanical performance of the material. An investigation of higher pressures (however lower than 60 bars, which degrades the structure of the natural fibers) would be pivotal for producing a transparent NFCM with this technique. [63]

Another interesting technique for producing the desirable outcome could be resin transfer molding (RTM). Caydamili et al. developed a transparent GFRP with numerous plies, following a modified and unmodified RTM procedure for production. [72] The modified RTM (L-RTM) consisted of two glass plates which ensured the smooth surface roughness of the material and an injection hose that injected the degassed resin into the reinforcement and let it cure at 1 bar pressure. The results showed transparent GFRPs with 85-87% maximum light transmittance for a 5-10 ply GFRP, with no significant defects present in the interior structure to influence light scattering. [72] On the other hand, the typical RTM procedure uses a mold to inject the resin inside it, and 5 bar of applied pressure. The results indicated high transmittance again for the RTM samples. With this production technique, the air voids could be minimized and light scattering due to them would not be a serious problem for optical transparency.

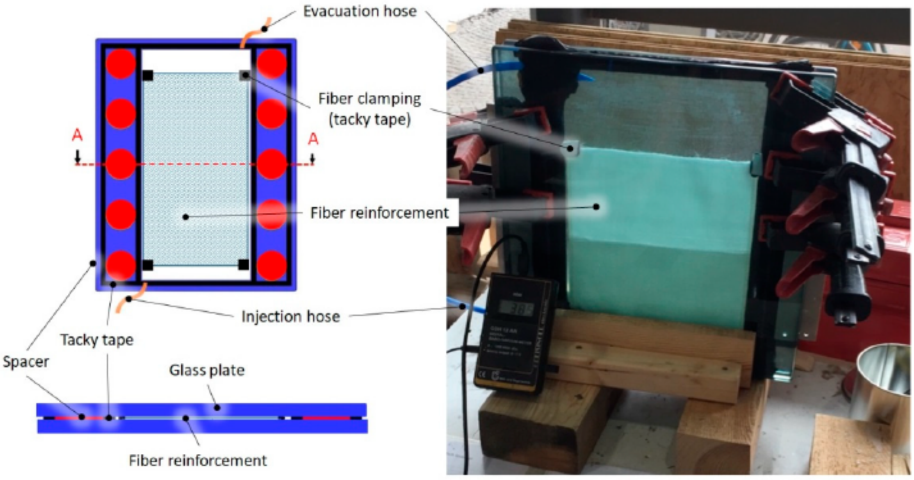

Figure 7.1: L-RTM setup for producing the transparent GFRPs. [72]

7.2. Delignified Flax Fiber's RI Detection

A second significant aspect which created several problems during this research was the inability to detect the exact refractive index of the delignified flax fiber. This occurred due to several reasons. One of them could be the failure to detect the RI in the ranges created on this project with the immersion tests with organic compounds. A second reason is the inability to remove entrapped air inside the lumen of the fiber which could result in light scattering due to strong RI contrast between air, the fiber, and the polymer. Also, the bad wettability and permeability of the compound in the interior of the delignified flax fiber due to the lack of pressure could be another cause for the non-detection of the desired RI.

Different organic compounds with narrow RI ranges near 1.53-1.54 values can be re-created and tested for higher accuracy on the RI detection. Moreover, an investigation with other RI detection techniques presented in Chapter 3 could be of big assistance. Becke's line or Heyn's method could be easier because they use an optical microscope to detect if there is a mismatch between a liquid and a fiber. By a trial and error technique, the RI of the fiber could be measured with more accuracy.

7.3. Matching Polymer Matrix Selection

The next step from the previous recommendation is to select a matching polymer with a better match with the RI of the fiber. In this project, two epoxy polymer systems were selected for infusion with an RI of 1.538 (WC/W300) and 1.560 (R1200/1204). However, with not having the full picture of the RI of DL FF, this was a trial-and-error process of achieving transparency. Even if the RI of DL FF is not fully estimated, other polymer matrices which are utilized on many occasions in transparent wood like PMMA (1.49), PVP (1.53), ABPE (1.536), and different kinds of epoxies can be introduced as polymer matrices in a functional FFCM to achieve optical transparency. [10], [11], [13], [15]

7.4. Fiber Modifications

Numerous fiber modifications were implemented to assist in the search for optical transparency in a flax fiber-reinforced composite material. Some of these treatments were a helping hand in clarifying some issues identified in these materials, however, it seemed that they affect negatively the flexural properties of the material. A thorough investigation of these treatments and how they affect the fiber's structure, deteriorating the mechanical performance has to be implemented. For example, the acetylation treatment is fully effective on flexural properties when it reaches an acetylation degree of 18% seen in Figure 2.9, which was not explored in the scope of this research. [22] Nitric acid treatment also deteriorated the mechanical performance of the FFCMs, so a more efficient protocol regarding the duration of the treatment should be established. Furthermore, a plain acetylation treatment can also be conducted to avoid the carboxylation repulsive forces which can degrade the fiber's cellulose fibers, and observe if it is as effective as a single treatment as it is in combination with other treatments.

Also, other treatments can be explored as well. Benzoylation treatment transforms the fiber's nature into less hydrophilic as well, so it might be worth investigating more thoroughly. [27] Other delignification treatments (i.e. with Sodium Chlorite and an acetate buffer solution) can be implemented to investigate if they are more effective than the treatment followed in this project with hydrogen peroxide and glacial acetic acid. [10]

References

[1] Ori. Daniel Isaac M. Ishai. *Engineering Mechanics of Composite Materials (2nd Edition) - 1.1 Definition and Characteristics.* Oxford University Press, 2006.

[2] Arup Dey et al. “A Review on Filament Materials for Fused Filament Fabrication”. In: *Journal of Manufacturing and Materials Processing* 5 (June 2021), p. 69. DOI: `10.3390/jmmp5030069`.

[3] Sabu Thomas. *Polymer Composites, Macro- and Microcomposites : Macro- and Microcomposites*. Vol. 1. John Wiley & Sons, 2012.

[4] Anil N Netravali. *Advanced Green Composites*. John Wiley & Sons, 2018.

[5] Dong-Kyu Kim et al. “Transparent glass-fiber-reinforced epoxy composites and their optical characteristics”. In: *Composites Science and Technology* 232 (2023), p. 109848. DOI: `https://doi.org/10.1016/j.compscitech.2022.109848`.

[6] University of Twente. *Functional Materials*. 2023. URL: `https://www.utwente.nl/en/max-planck-center/research/Functional/`.

[7] Li Y. et al. “Optically Transparent Wood: Recent Progress, Opportunities, and Challenges”. In: *Advanced Optical Materials* (2018). DOI: `https://doi.org/10.1002/adom.201800059`.

[8] Li Y. et al. “Transparent wood for functional and structural applications”. In: *Phil. Trans. R. Soc. A376: 20170182* (2018). DOI: `http://dx.doi.org/10.1098/rsta.2017.0182`.

[9] Libo Yan et al. “Flax fibre and its composites – A review”. In: *Composites Part B: Engineering* 56 (2014), pp. 296–317. DOI: `https://doi.org/10.1016/j.compositesb.2013.08.014`.

[10] Yuanyuan Li et al. “Optically Transparent Wood from a Nanoporous Cellulosic Template: Combining Functional and Structural Performance”. In: *Biomacromolecules* (2016). DOI: `10.1021/acs.biomac.6b00145`.

[11] Mingwei Zhu et al. “Transparent and haze wood composites for highly efficient broadband light management in solar cells”. In: *Nano Energy* (2016). DOI: `https://doi.org/10.1016/j.nanoen.2016.05.020`.

[12] Zhu Mingwei et al. “Highly Anisotropic, Highly Transparent Wood Composites”. In: *Advanced Materials* 28.26 (2016), pp. 5181–5187. DOI: `https://doi.org/10.1002/adma.201600427`.

[13] Yuanyuan Li et al. “Towards centimeter thick transparent wood through interface manipulation”. In: *J. Mater. Chem. A* 6 (3 2018), pp. 1094–1101. DOI: `10.1039/C7TA09973H`.

[14] Yizhou Jiang et al. “Printable highly transparent natural fiber composites”. In: *Materials Letters* (2020). DOI: `https://doi.org/10.1016/j.matlet.2020.128290`.

[15] Abe K. et al. “Fabrication of optically transparent cotton fiber composite”. In: *J Mater Sci 53* (2018). DOI: `https://doi.org/10.1007/s10853-018-2309-1`.

[16] Barth M. et al. *Carbon footprint and sustainability of different natural fibres for biocomposites and insulation material : study providing data for the automotive and insulation industry*. Nova-Institut GmbH, 2015.

[17] W. Woigk et al. “Interface properties and their effect on the mechanical performance of flax fibre thermoplastic composites”. In: *Composites Part A: Applied Science and Manufacturing* (2019), pp. 8–17. DOI: `https://doi.org/10.1016/j.compositesa.2019.04.015`.

[18] Mi Li et al. “Recent advancements of plant-based natural fiber–reinforced composites and their applications”. In: *Composites Part B: Engineering* 200 (2020), p. 108254. DOI: `https://doi.org/10.`

1016/j.compositesb.2020.108254. URL: https://www.sciencedirect.com/science/article/pii/S1359836820333047.

[19] Ansys. *Granta EduPack software*. 2022. URL: https://www.ansys.com/products/materials/granta-edupack.

[20] Sonja Osbild. *Optically transparent natural fibre reinforced composites*. MSc Thesis - ETH Zurich, 2018.

[21] O'Sullivan A.C. "Cellulose: the structure slowly unravels". In: *Cellulose* (1997), pp. 173–207. DOI: https://doi.org/10.1023/A:1018431705579.

[22] Bledzki Andrzej et al. "The effects of acetylation on properties of flax fibre and its polypropylene composites". In: *eXPRESS Polymer Letters* Vol. 2 (2008), pp. 413–422. DOI: 10.3144/expresspolymlett.2008.50.

[23] Brian Thomas et al. *Encyclopedia of Applied Plant Sciences*. Vol. 2nd. Elsevier, 2003, pp. 206–208.

[24] Shanshan Huo et al. "Chemical and Mechanical Properties Studies of Chinese Linen Flax and Its Composites". In: *Polymers and Polymer Composites* 21 (June 2013), pp. 275–286. DOI: 10.1177/096739111302100502.

[25] Bos H.L. et al. "Tensile and compressive properties of flax fibres for natural fibre reinforced composites". In: *Journal of Materials Science 37* (2002), pp. 1683–1692. DOI: https://doi.org/10.1023/A:1014925621252.

[26] G.C. Davies et al. "Effect of Environmental Relative Humidity and Damage on the Tensile Properties of Flax and Nettle Fibers". In: *Textile Research Journal* 68 (1998), pp. 623–629. DOI: 10.1177/004051759806800901.

[27] Parameswaranpillai J Thyavihalli Girijappa YG Mavinkere Rangappa S et al. "Natural Fibers as Sustainable and Renewable Resource for Development of Eco-Friendly Composites: A Comprehensive Review." In: *Front. Mater. 6:226* (2019). DOI: 10.3389/fmats.2019.00226.

[28] Li H. et al. "Recent Progress in Flax Fiber-Based Functional Composites". In: *Adv. Fiber Mater. 4* (2022). DOI: https://doi.org/10.1007/s42765-021-00115-6.

[29] Fabienne Samyn et al. "Preparation and flame retardancy of flax fabric/ polybenzoxazine laminates". In: *Fire and Materials 45* (2021). DOI: https://doi.org/10.1002/fam.2839.

[30] S. Alix et al. "Effect of chemical treatments on water sorption and mechanical properties of flax fibres". In: *Bioresource Technology* 100 (2009), pp. 4742–4749. DOI: https://doi.org/10.1016/j.biortech.2009.04.067.

[31] T.G. Yashas Gowda et al. "Polymer matrix-natural fiber composites: An overview". In: *Cogent Engineering* 5:1 (2018), pp. 623–629. DOI: 10.1080/23311916.2018.1446667.

[32] K Van de Velde et al. "Thermoplastic polymers: overview of several properties and their consequences in flax fibre reinforced composites". In: *Polymer Testing* 20 (2001), pp. 885–893. DOI: https://doi.org/10.1016/S0142-9418(01)00017-4.

[33] Lut Pil et al. "Why are designers fascinated by flax and hemp fibre composites?" In: *Composites Part A: Applied Science and Manufacturing* 83 (2016). Special Issue on Biocomposites, pp. 193–205. DOI: https://doi.org/10.1016/j.compositesa.2015.11.004.

[34] Changduk Kong et al. "Study on structural design and analysis of flax natural fiber composite tank manufactured by vacuum assisted resin transfer molding". In: *Materials Letters* 130 (2014), pp. 21–25. DOI: https://doi.org/10.1016/j.matlet.2014.05.042.

[35] Goutianos S. et al. "Development of Flax Fibre based Textile Reinforcements for Composite Applications". In: *Appl Compos Mater* 13 (2006), pp. 199–215. DOI: https://doi.org/10.1007/s10443-006-9010-2.

[36] Bcomp. *Datasheet of ampliTex Art. no 5025 UD fabric 280 gsm*. 2016.

[37] Notox. *Technologies*. 2023. URL: https://en.notoxsurf.com/pages/technologies.

[38] Babolat. *Pure Aero Tennis Racquet*. 2022. URL: `https://www.babolat.com/us/pure-aero-unstrung/3324922000908.html`.

[39] NPSP B.V. *Nabasco 8010 Material*. 2023. URL: `https://www.npsp.nl/en/material/nabasco-8010`.

[40] Bcomp. *Automotive and Interior Panels*. 2022. URL: `https://www.bcomp.ch/solutions/automotive-interior-panels/`.

[41] Jeannine Volchko/Lumitex. *Visible Light Spectrum: From a Lighting Manufacturer's Perspective*. 2018. URL: `https://www.lumitex.com/blog/visible-light-spectrum`.

[42] Jai Singh et al. *Optical Properties of Materials and Their Applications*. Vol. 2nd. John Wiley & Sons, 2020, pp. 1–31.

[43] J. W. S. Hearle et al. *Physical Properties of Textile Fibres*. Vol. 4th. Woodhead publishing, 2008, pp. 690–707.

[44] Dajun Fan et al. "Review of Refractive Index-Matching Techniques of Polymethyl Methacrylate in Flow Field Visualization Experiments". In: *International Journal of Energy Research* (2023). DOI: `https://doi.org/10.1155/2023/3413380`.

[45] W. Russ Algar et al. "Demonstration of the Spectrophotometric Complementary Color Wheel Using LEDs and Indicator Dyes". In: *Journal of Chemical Education* 93.1 (2016), pp. 162–165. DOI: `10.1021/acs.jchemed.5b00665`.

[46] William Reusch. *Visible and Ultraviolet Spectroscopy*. 2013. URL: `https://www2.chemistry.msu.edu/faculty/reusch/virttxtjml/spectrpy/uv-vis/spectrum.htm`.

[47] Navid Zobeiry et al. "Fabrication of transparent advanced composites". In: *Composites Science and Technology* 197 (2020), p. 108281. DOI: `https://doi.org/10.1016/j.compscitech.2020.108281`.

[48] J Rheims et al. "Refractive-index measurements in the near-IR using an Abbe refractometer". In: *Measurement Science and Technology* 8.6 (1997), p. 601. DOI: `10.1088/0957-0233/8/6/003`.

[49] American Society for Testing et al. "Standard Test Method for Measuring the Transmissivity of Transparent Parts". In: *ASTM D1003* 15.03 (2018). DOI: `10.1520/F1316-18`.

[50] Frey M. et al. "Fabrication and Design of Wood-Based High-Performance Composites". In: *J. Vis. Exp.* (2019). DOI: `10.3791/60327`.

[51] Thabisile Brightwell Jele et al. "Engineered transparent wood composites: a review." In: *Cellulose* (2023). DOI: `https://doi.org/10.1007/s10570-023-05239-z`.

[52] Shennan Wang et al. "Wood xerogel for fabrication of high-performance transparent wood". In: *Nat. Commun* 14 (2023), p. 2827. DOI: `https://doi.org/10.1038/s41467-023-38481-x`.

[53] "Improving the properties of UD flax fibre reinforced composites by applying an alkaline fibre treatment". In: *Composites Part A: Applied Science and Manufacturing* 37.9 (2006), pp. 1368–1376. DOI: `https://doi.org/10.1016/j.compositesa.2005.08.016`.

[54] Tian Li et al. "Wood Composite as an Energy Efficient Building Material: Guided Sunlight Transmittance and Effective Thermal Insulation". In: *Advanced Energy Materials* 6.22 (2016), p. 1601122. DOI: `https://doi.org/10.1002/aenm.201601122`.

[55] Resoltech Advanced Technology Resins. *Datasheet of Resoltech 1200 Hardeners 1204 - 1206 - 1208 Structural epoxy laminating system*. 2023. URL: `https://www.resoltech.com/en/markets/1200-detail.html`.

[56] RG Faserverbundwerkstoffe GmbH. *Safety Data Sheet of Epoxy Casting Resin 'Water Clear'*. 2023. URL: `https://www.ezentrumbilder.de/rg/pdf/si_en_107106.pdf`.

[57] RG Faserverbundwerkstoffe GmbH. *Safety Data Sheet of Hardener W300*. 2023. URL: `https://www.ezentrumbilder.de/rg/pdf/si_en_100149.pdf`.

[58] PerkinElmer. *LAMBDA UV/Vis and UV/Vis/NIR Spectrophotometers 850/950/1050*. 2007. URL: `https://resources.perkinelmer.com/corporate/cmsresources/images/44-74450bro_lambda8509501050.pdf`.

[59] American Society for Testing et al. “Standard Test Method for Flexural Properties of Polymer Matrix Composite Materials”. In: *D7264/D7264M-15* 15.03 (2015). DOI: `10.1520/D7264_D7264M-07`.

[60] Cédric Pupin et al. “Formation and suppression of volatile-induced porosities in an RTM epoxy resin”. In: *Composites Part A: Applied Science and Manufacturing* 94 (2017), pp. 146–157. DOI: `https://doi.org/10.1016/j.compositesa.2016.12.006`.

[61] Pupin C. et al. “Predicting Porosity Formation in Phenolic Resins for RTM Manufacturing: the Porosity Map”. In: *Composites: Part A* (2017). DOI: `http://dx.doi.org/10.1016/j.compositesa.2017.05.023`.

[62] Komkov M.A. et al. “The influence of epoxide resin viscosity on impregnation of fiber reinforcement”. In: *Polym. Sci. Ser* (2015). DOI: `https://doi.org/10.1134/S1995421215040073`.

[63] Luisa Medina et al. “Process related mechanical properties of press molded natural fiber reinforced polymers”. In: *Composites Science and Technology* 69.9 (2009). Special Issue on the 12th European Conference on Composite Materials (ECCM12), organized by the European Society for Composite Materials (ESCM), pp. 1404–1411. DOI: `https://doi.org/10.1016/j.compscitech.2008.09.017`.

[64] T.S. Lundström et al. “Dissolution of Voids during Compression Molding of SMC”. In: *Journal of Reinforced Plastics and Composites* 29.12 (2010), pp. 1826–1837. DOI: `10.1177/0731684409336369`.

[65] J.P. Anderson et al. “Formation of voids in composite laminates: Coupled effect of moisture content and processing pressure”. In: *Polymer Composites* 36.2 (2015), pp. 376–384. DOI: `https://doi.org/10.1002/pc.22952`.

[66] Marion Frey et al. “Delignified and Densified Cellulose Bulk Materials with Excellent Tensile Properties for Sustainable Engineering”. In: *ACS Applied Materials & Interfaces* 10.5 (2018). PMID: 29373784, pp. 5030–5037. DOI: `10.1021/acsami.7b18646`.

[67] Spinei M et al. “The Influence of Extraction Conditions on the Yield and Physico-Chemical Parameters of Pectin from Grape Pomace.” In: *Polymers (Basel)* 14 (Mar. 2022). DOI: `10.3390/polym14071378`.

[68] Mohammed Mohammed et al. “Surface treatment to improve water repellence and compatibility of natural fiber with polymer matrix: Recent advancement”. In: *Polymer Testing* 115 (2022), p. 107707. DOI: `https://doi.org/10.1016/j.polymertesting.2022.107707`.

[69] Carlos Vila et al. “Use of thermogravimetric analysis to monitor the effects of natural laccase mediators on flax pulp”. In: *Bioresource Technology* 102.11 (2011), pp. 6554–6561. DOI: `https://doi.org/10.1016/j.biortech.2011.03.068`.

[70] Yunyin Lin et al. “Transparent semi-crystalline polymeric materials and their nanocomposites: A review”. In: *Polymer Engineering & Science* 60.10 (2020), pp. 2351–2376. DOI: `https://doi.org/10.1002/pen.25489`.

[71] Image Engineering. *Chromatic Aberration*. URL: `https://www.image-engineering.de/library/image-quality/factors/1074-chromatic-aberration`.

[72] Yavuz Caydamli et al. “Transparent Fiber-Reinforced Composites Based on a Thermoset Resin Using Liquid Composite Molding (LCM) Techniques”. In: *Materials* 14.20 (2021). DOI: `10.3390/ma14206087`.

[73] Jim Clark. *The Beer-Lambert Law*. URL: `https://chem.libretexts.org/Bookshelves/Physical_and_Theoretical_Chemistry_Textbook_Maps/Supplemental_Modules_(Physical_and_Theoretical_Chemistry)/Spectroscopy/Electronic_Spectroscopy/Electronic_Spectroscopy_Basics/The_Beer-Lambert_Law`.

[74] Masoud Bodaghi et al. “On the relationship of morphology evolution and thermal conductivity of flax reinforced polypropylene laminates”. In: *Frontiers in Materials* 10 (2023). DOI: `10.3389/fmats.2023.1150180`.

[75] Lei Guo et al. “Study on the thermal properties and insulation resistance of epoxy resin modified by hexagonal boron nitride”. In: *e-Polymers* 21.1 (2021), pp. 681–690. DOI: `doi:10.1515/epoly-2021-0069`.

[76] TAPPI T 222. “Acid-insoluble lignin in wood and pulp”. In: (2006). URL: `https://www.tappi.org/content/sarg/t222.pdf`.

[77] Sigma Aldrich. *What is FTIR Spectroscopy*. 2023. URL: `https://www.sigmaaldrich.com/NL/en/technical-documents/technical-article/analytical-chemistry/photometry-and-reflectometry/ftir-spectroscopy`.

[78] Justin Tom. *UV-Vis Spectroscopy: Principle, Strengths and Limitations and Applications*. 2021. URL: `https://www.technologynetworks.com/analysis/articles/uv-vis-spectroscopy-principle-strengths-and-limitations-and-applications-349865`.

[79] Element. *Optical Microscopy versus Scanning Electron Microscopy in Medical Device Testing*. 2023. URL: `https://www.element.com/nucleus/2018/optical-microscopy-versus-scanning-electron-microscopy-in-medical-device-testing`.

[80] Susan Swapp. *Scanning Electron Microscopy*. 2023. URL: `https://serc.carleton.edu/research_education/geochemsheets/techniques/SEM.html`.

[81] George Youssef. “Chapter 11 - Characterization of polymers”. In: *Applied Mechanics of Polymers*. Ed. by George Youssef. Elsevier, 2022, pp. 273–299. DOI: `https://doi.org/10.1016/B978-0-12-821078-9.00016-8`.

A

Fiber Modifications

A.1. Delignification Treatment

For the delignification fiber modification, one methodology was used, as explained earlier in Chapter 4. This methodology is fully certified by the literature for wood, and it was decided that it can be sufficient for flax fibers as well. Below, the soaking of the fiber coupons in the hydrogen peroxide and glacial acetic acid solution overnight (which changes a bit color from brown to light brown) and the final result of the fully white and lignin-free flax fiber coupons, are depicted. All the equipment and chemicals were provided by the Aerospace and TNW faculty.

Figure A.1: Delignification procedure based on H_2O_2 and glacial acetic acid. From left to right: Natural flax fiber coupons before delignification, Flax fibers during delignification procedure, Delignified Flax fibers after delignification procedure.

For the lignin measurement, a procedure which is followed for measurement of it in wood veneers is followed. This procedure has the exact steps: [76]

- Prepare 100 ml of 72% sulphuric acid using concentrated acid and DI water.
- Add 15 ml of the acid to a glass beaker. Add 1 g of delignified or native flax fibers.
- Stir the fibers inside the solution until they are dissolved.
- Let the material in the solution for 2h at room temperature. Stir it occasionally.
- Add 400 ml of DI water into a 1 L flask and add the previously treated fibers with the solution. Then dilute the solution until the beaker is up to 575 ml (3% sulphuric acid).
- Boil the solution for 4 h and add hot water to ensure that the volume is constant.
- Let the solution rest overnight, allowing the lignin insoluble to precipitate in the bottom of the flask.
- Filter through a cellulose filter in a vacuum filter setup.
- Wash the filter to eliminate any acid residuals from the lignin.
- Dry the filter in a non-vacuum oven at 105^0C to a constant weight, then cool off and weigh the remaining lignin.

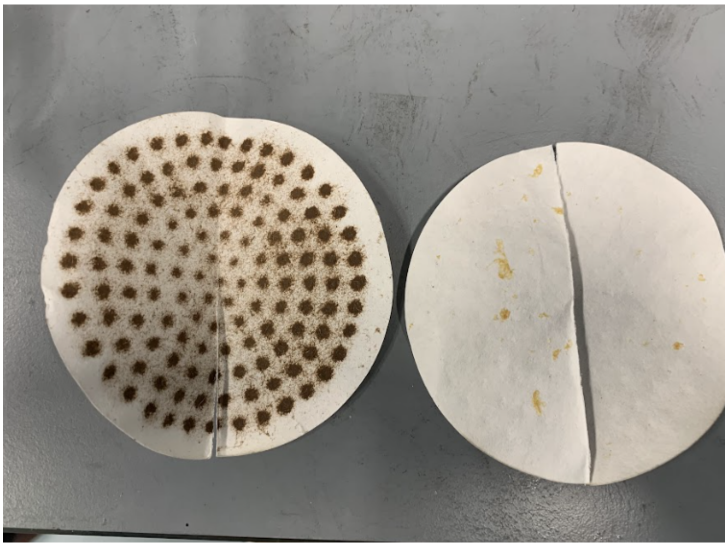

Figure A.2: Cellulose filters with the residual lignin from the fibers. Left: Native Flax Fibers, Right: Delignified Flax Fibers

A.2. Nitric Acid/Probe Sonication treatment

For the nitric acid/probe sonication fiber modification, one methodology was used, as explained earlier in Chapter 4. This methodology used HNO_3 as a reactive oxidant on the previously delignified flax fiber coupons and afterward probe sonication setup for 30 minutes at 450 W. The fibers were demonstrated as more fluffy than before as seen in the Figure below. All the equipment and chemicals were provided by the TNW faculty.

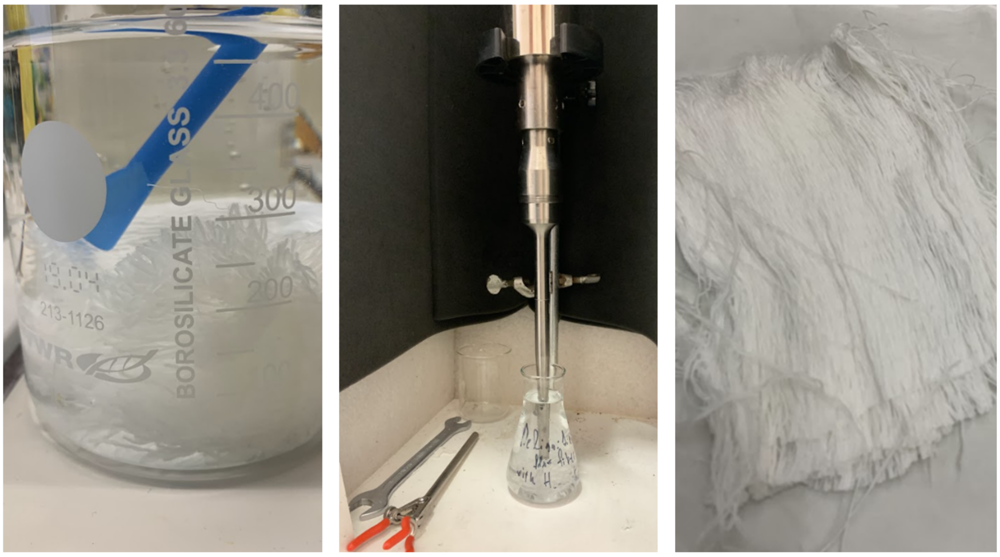

Figure A.3: Left: Delignified flax fiber coupons immersed in HNO_3 Middle: Probe sonication setup for the delignified flax fiber coupons which are immersed in water. Right: The treated flax fiber coupons.

A.3. Acetylation Treatment

For the acetylation fiber modification, two different methodologies were used, as explained earlier in Chapter 4. These two methodologies were differentiated based on the amount of chemical substances that were used for the fiber treatment. The first one involved a technique with a bigger amount of chemicals used (100 ml of toluene, 50 ml of acetic anhydride, and 5 ml of perchloric acid). In comparison, the second technique required the usage of lower amounts of oxidizing agents (50 ml of toluene, 10 ml of acetic anhydride, 10 ml of acetic acid, and a minimal amount of perchloric acid). The results presented that the first occasion showed extremely harsh conditions for the flax fibers as they were fully oxidized and degraded after the treatment showing ash and tar-like signs. This is due to the high amount of the highly oxidizing catalyst which was used (perchloric acid, -15.2 pKa), which accelerated the reaction, excessively. On the other hand, the second methodology showed non-degraded flax fibers and based on the FTIR analysis previously, acetylation was successfully implemented. This implies that the second technique involved the correct amount of chemical agents for the acetylation procedure. All the equipment and chemicals were provided by the TNW faculty.

Figure A.4: Left: Degraded flax fibers due to the high amount of oxidizing catalyst (perchloric acid), Right: Not-degraded flax fibers with a lower amount of oxidizing catalyst.

B

Equipment/Measurement Methods

B.1. FTIR Spectroscopy

Fourier Transform Infrared Spectroscopy is a type of spectroscopy that uses infrared radiation as a tool for identifying various molecules or compounds. The concept relies on the fact that when infrared radiation hits a sample, a proportion of the initial intensity of it, is absorbed from the sample. [77] After this action, the transmitted infrared radiation hits a detector and generates spectra. These spectra give information about specific molecules and structures that are present in the material. [77] In many materials the covalent bonds which are present in it, absorb infrared radiation and produce some actions, such as vibrational movements like stretching or bending of the molecules. [77] For each bond and functional group, the spectra or peak of transmittance/absorbance is pre-specified. The graph recorded, involves the wavelength of the infrared radiation on the x-axis and the transmittance/absorbance on the y-axis. By identifying each peak on this graph an image of what functional groups are present on the material can be depicted. FTIR spectroscopy is used in many sectors such as organic chemistry, materials science, and the pharmaceutical industry. [77]

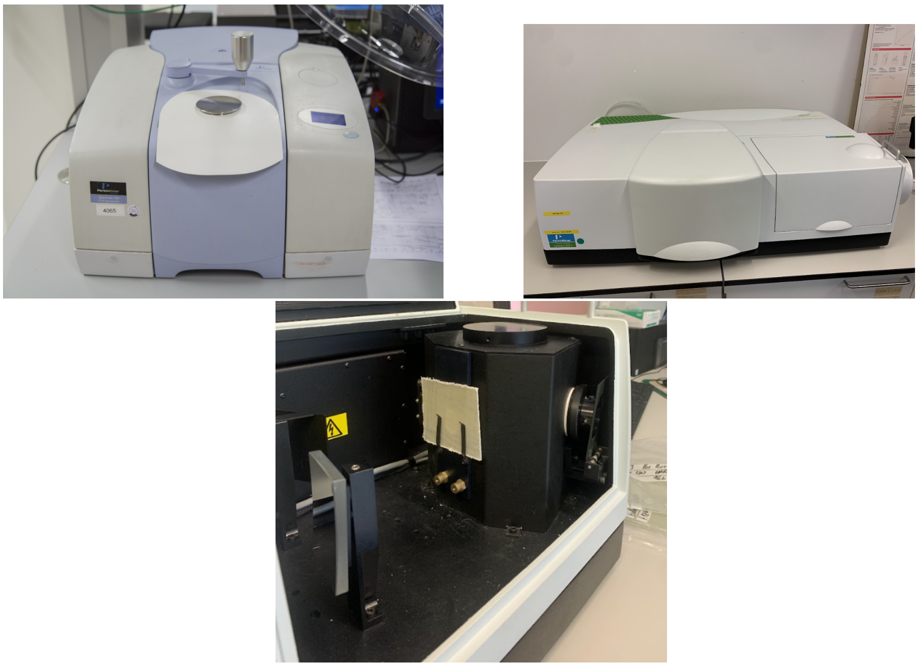

Figure B.1: Top Left: PerkinElmer Spectrum 100 FTIR setup., Top Right: PerkinElmer model 1050S Uv/vis spectrophotometer setup. Bottom: FFCM sample placed on the front port of the integrating sphere of PerkinElmer 1050S Spectrophotometer..

B.2. Uv/Vis Spectroscopy

Ultraviolet/Visible (Uv/vis) Spectroscopy is an experimental non-destructive technique that has the same fundamental concept as FTIR, however using radiation of different energy and wavelength. The radiation which is used involves the discrete wavelengths of visible light and ultraviolet radiation. [78] The detector of the equipment, then can identify the transmitted or absorbed intensity of these radiation waves. In this way, the information that is recovered from the procedure can identify numerous molecules or structures in the material. [78] Furthermore, because of the usage of visible light this setup can be also used to measure light transmittance and quantify the material's transparency. Uv/vis spectroscopy is very popular in numerous sectors, like the food industry or DNA/RNA analysis. [78]

B.3. Scanning Electron Microscopy/Optical Microscopy

Scanning Electron Microscopy (SEM) and *Optical Microscopy (OM)* are visualization techniques that are occasionally used in depicting surfaces of solid specimens. The major difference between those two techniques lies in the higher resolution which is acquired during the SEM process in comparison to typical optical microscopes. [79] The magnification that SEM can reach up to is on the level of X10.000-30.000, in contrast to lower magnifications of OM. [79]

SEM is a technique that uses an electron beam which hits the sample under a vacuum with high kinetic energy and generates various signals that depict the surface of a solid material. [80] The information that can be acquired from this methodology can be about the texture, chemical composition, crystalline structure, etc. [80] It works with a focused electron beam that hits the sample and produces signals of secondary electrons, backscattered electrons or photons etc. [80] The first two are the most important and are used for visualizing purposes, with secondary electrons being significant for morphology imaging and backscattered electrons being crucial for composition purposes. The high resolution of SEM equipment is probably the biggest advantage in imaging materials, as it can reach up to very high magnification, depending on the equipment.

On the other hand, optical microscopes are certainly setups with lower resolution and magnification than SEM, however, they can be handled easier, quicker and can allow larger specimens to be analyzed. [79] They use visible light as a tool and many optical glass lenses which can work as a system to maximize the magnification of the image. CCD cameras are used within a digital OM to capture images for analysis. [81] There are many variations for OM like the polarized light optical microscope, darkfield microscope, etc.

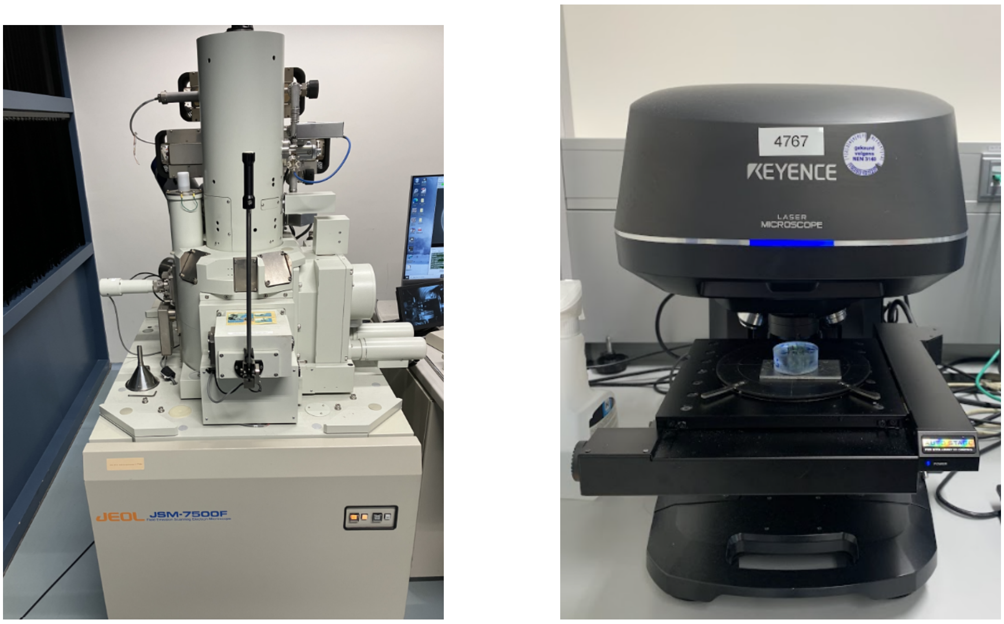

Figure B.2: Left: JSM-7500F Scanning Electron Microscope setup., Right: Keyence Laser Scanning Confocal Optical Microscope

Figure B.3: Left: Abbe's Refractometer setup, Right: Joos Press 1000 kN setup.

B.4. Mechanical Testing

For mechanical properties, a 3-point bending test was conducted, to investigate the flexural strength and flexural modulus. The test was performed on a *Zwick Roell 10 kN Tensile Testing Machine*, with a 1 kN load cell. The support span was set at 30 mm and each cylindrical support's diameter was 10 mm. The samples which were generated from the production techniques, were cut into (LXW) 65X17 ($\pm$3X3) mm. The thickness varied between the samples due to the variation of plies between the specimens but overall stayed around 0.8-1.3 mm. The span-to-thickness ratio stayed around 32:1 levels, as ASTM D7264/D7264M denotes. [59] The crosshead velocity was defined at 1 mm/min. Three specimens were created from each composite sample, to be tested. Below, the setup of the testing procedure is depicted, together with the cylindrical supports. After testing the sample, the load-displacement curve was generated and it was transformed into a stress-strain curve, via the following equations.

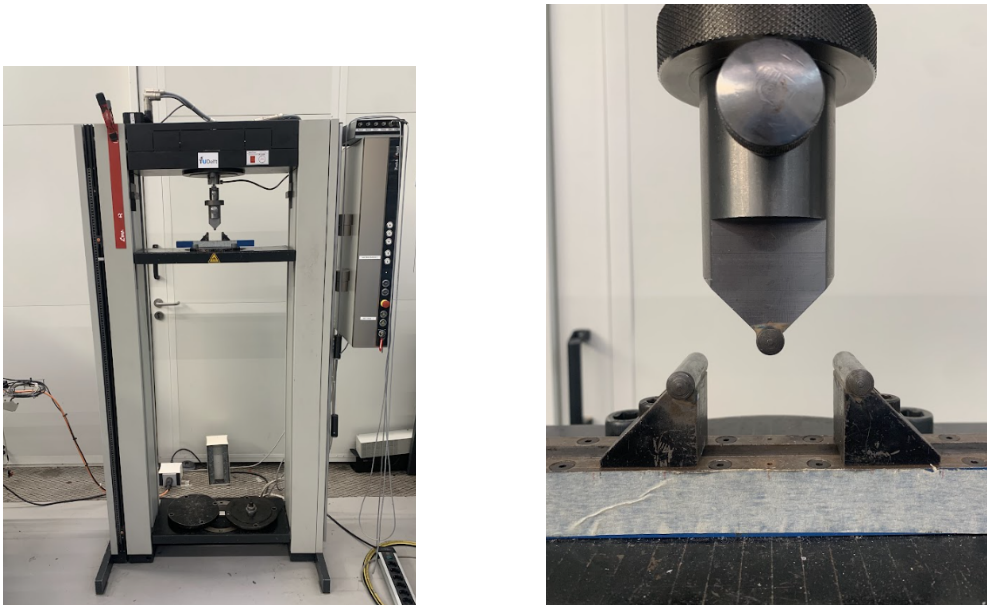

Figure B.4: Left: Zwick Roell 10 kN Tensile Tesing Machine, Right: 3-point bending setup.

The flexural stress is given by the following equation: [59]

$$\sigma_f = \frac{3FS}{2bt^2} \tag{B.1}$$

where F is the load in (N), S is the outer span of the supports in (mm), b is the width of the specimen in (mm) and t is the thickness of the specimen in (mm).

The flexural strain is given by the following equation: [59]

$$\epsilon_f = \frac{6dt}{S^2} \tag{B.2}$$

where d is the deflection of the specimen from its initial middle point in (mm), S is the outer span of the supports in (mm) and t is the thickness of the specimen in (mm).

The flexural stiffness is given by the following equation: [59]

$$E_f = \frac{\Delta\sigma}{\Delta\epsilon} \tag{B.3}$$

where $\Delta\epsilon$ is the difference in strain between two middle points, $\Delta\sigma$ is the difference in stress between two points (MPa). The two points that are selected for the calculation of the modulus are for the strain range of 0.001 and 0.003 with a difference of 0.002, according to the Standard. [59]

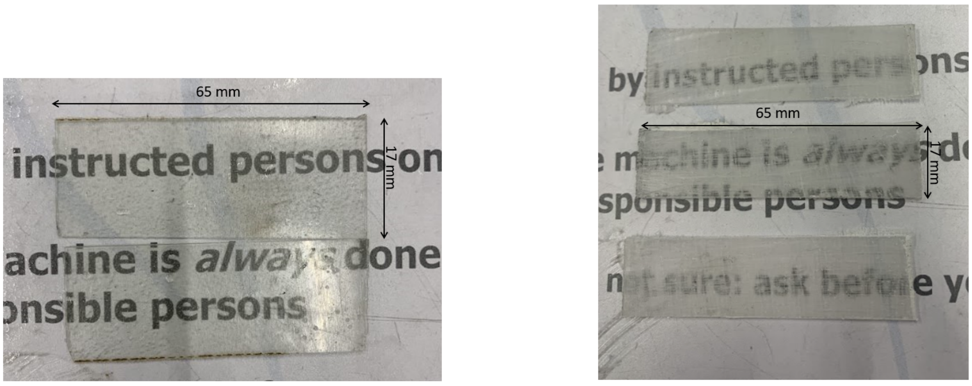

Figure B.5: Three-point bending specimens that were tested to investigate the flexural properties of the GFRP (left) and FFCM (right) materials. Length: 65 mm, Width: 17 mm.

B.5. ImageJ Analysis

In this section, the analysis and calculation of the fiber volume fraction of each material is explained. This calculation was implemented by measuring the area that is covered for each constituent by toggling the color of the pixels of the image. Figure B.6 is an example of this type of analysis. The software checks how many pixels are colored on this image and divides them by the total, calculating an area fraction. This was implemented two times, due to the darker color for the longitudinal flax fiber and the lighter color for the perpendicular fibers. Then these two area fractions were added together to result in the fiber volume fraction which covers the material. This result is a rough estimation of the fiber vf% because it measures the fiber volume fraction only on one image of the cross-section of the material (does not cover the entire material's area, definitely important for the inhomogenous flax fiber composites in which the cross-section are of the composite might change through the length of the material), and also some errors are introduced from the software (neglecting some pixels that might be fibers but they are presenting like resin-different color), due to the imperfect handling or not fully clear OM images.

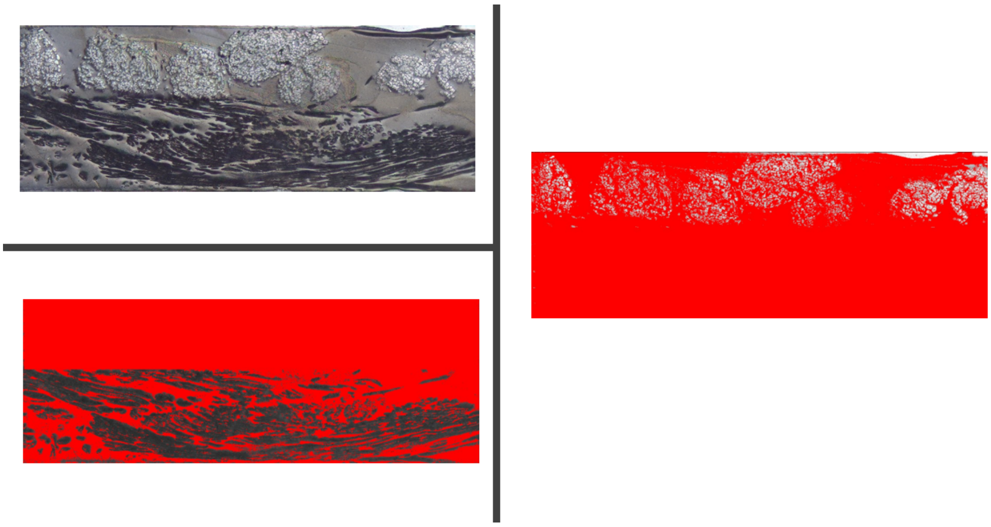

Figure B.6: Imagej analysis for the cross-section of the WC/W300 FFCM which was treated with NaOH/TEMPO-oxidation/Acetylation. Top Image: Original cross-section of the material, Bottom-Left Image: Area covered by the longitudinal flax fiber in the cross-section, Bottom-Right Image: Area covered by the perpendicular flax fibers in the cross-section of the material.

C

Glass Fiber Reinforced Composites

C.1. Production Technique

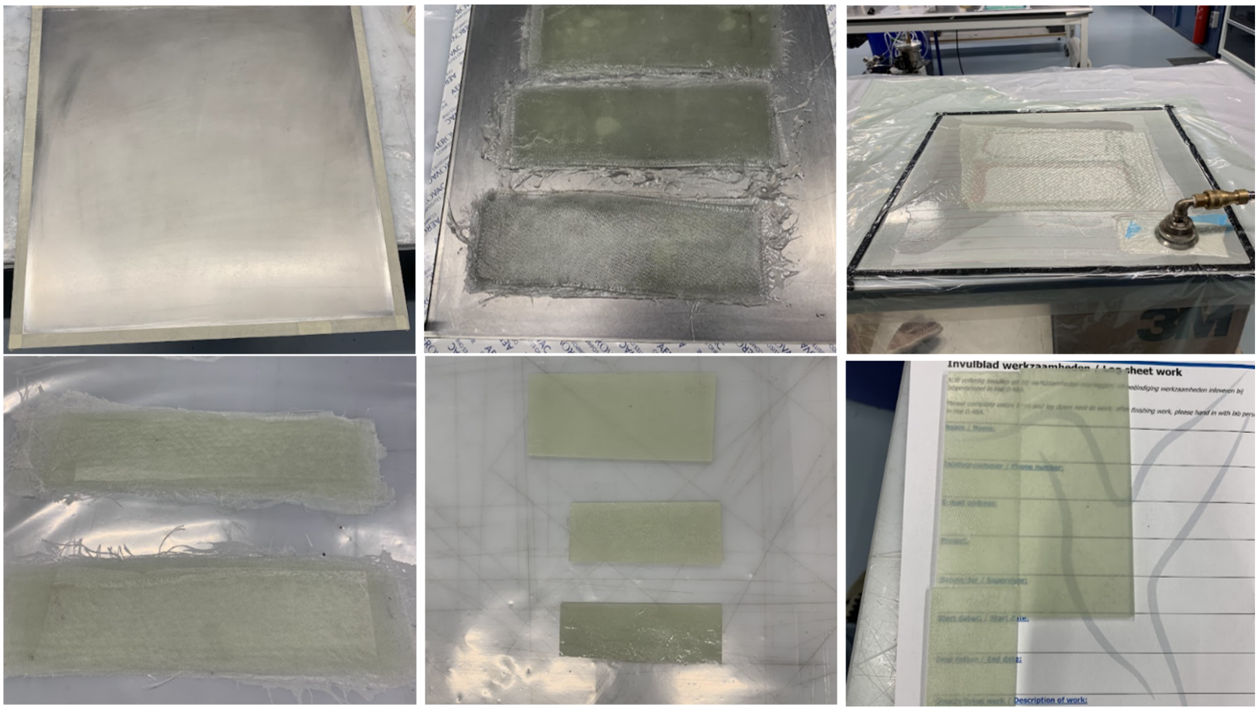

Figure C.1: GFRP production steps based on wet lamination and vacuum pressing with 100 kPa (1 bar).

The detailed process of the GFRP production is presented in Figure C.1. In this image, the aluminum mold, pre-impregnated glass fiber fabric plies with the polymer, and the vacuum bag together with all the appropriate equipment like the breather material and vacuum pump are depicted. The result is depicted on the lower row of images, with the initial material extracted from the mold to be wavy and with excessive fibers coming out from the polymer from the sides. This material was cut into a rectangular shape to mold a specimen. In the figure below, the dry areas which are created from the ”squeeze-out” phenomenon are presented on a WC 8-layer laminate. The ”squeeze-out” phenomenon pushes out resin from the glass fibers due to excessive pressure, leaving poorly impregnated glass fibers.

C.2. Flexural Properties

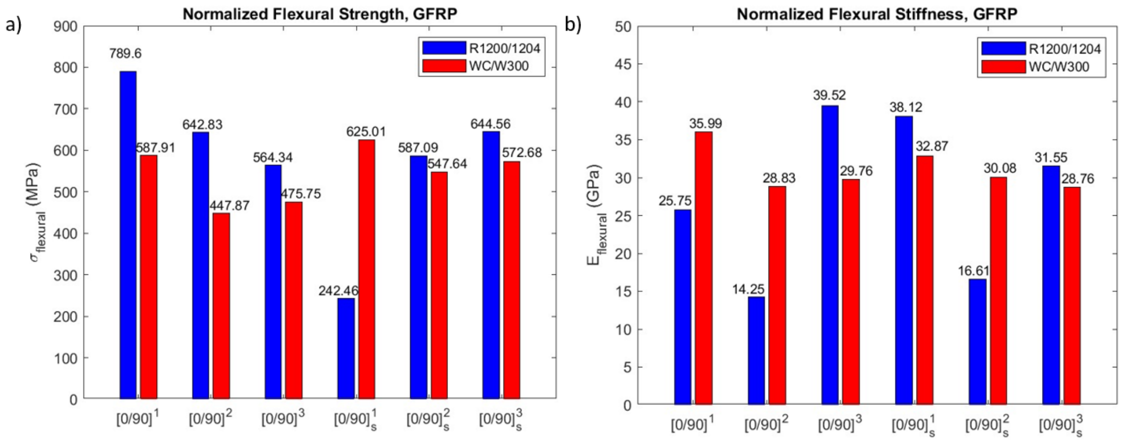

Figure C.2: Flexural properties of the materials produced with glass fiber woven fabric as reinforcement and the aforementioned polymers as matrix. a) Flexural strength b) Flexural stiffness.

D

Flax Fiber Reinforced Composites

D.1. Delignified Flax Fiber Composites

Figure D.1 demonstrates the FFCMs that were created with delignified flax fiber coupons as reinforcement.

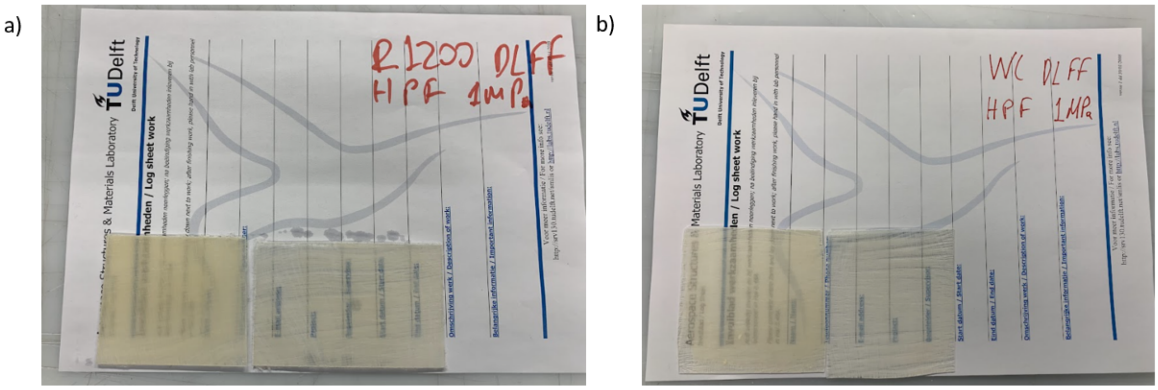

Figure D.1: Flax Fiber Reinforced Composite Materials. The flax fibers which are used are plain delignified flax fiber coupons. In every sub-figure: Left: $[0/90]_s$, Right: $[0/90]$ a) Resoltech 1200/1204 as a resin with wet lamination/hot press forming, b) Water Clear/W300 epoxy casting resin system as a resin with wet lamination/hot press forming.

	Thickness (t) of sample in mm and maximum light transmittance in each location (T) in %			
Resin system	**Resoltech 1200/1204**	**Resoltech 1200/1204**	**Water-Clear/W300**	**Water-Clear/W300**
Reinforcement	**DL Flax Fiber UD Coupon**	**DL Flax Fiber UD Coupon**	**DL Flax Fiber UD Coupon**	**DL Flax Fiber UD Coupon**
Hot Press Forming	[0/90]	$[0/90]_s$	[0/90]	$[0/90]_s$
Thickness (mm)	0.93	1.03	0.82	0.99
Fiber Volume Fraction (%)	39.91	38.46	42.47	44.57
Location 1 (%)	72.64	55.05	67.59	49.70
Location 2 (%)	70.50	60.00	67.21	49.16
Location 3 (%)	67.92	56.90	67.52	51.31
Location 4 (%)	69.92	55.42	70.48	48.60
Location 5 (%)	70.58	57.61	69.34	50.01
Average	**70.31**	**56.99**	**68.43**	**49.90**
Standard Deviation	**1.68**	**1.77**	**1.41**	**0.96**

Table D.1: Thicknesses and maximum light transmittance in each of the five random locations for all the FFCM materials which were produced with delignified flax fibers as reinforcement. The average value and standard deviation of maximum light transmittance for each sample are also depicted.

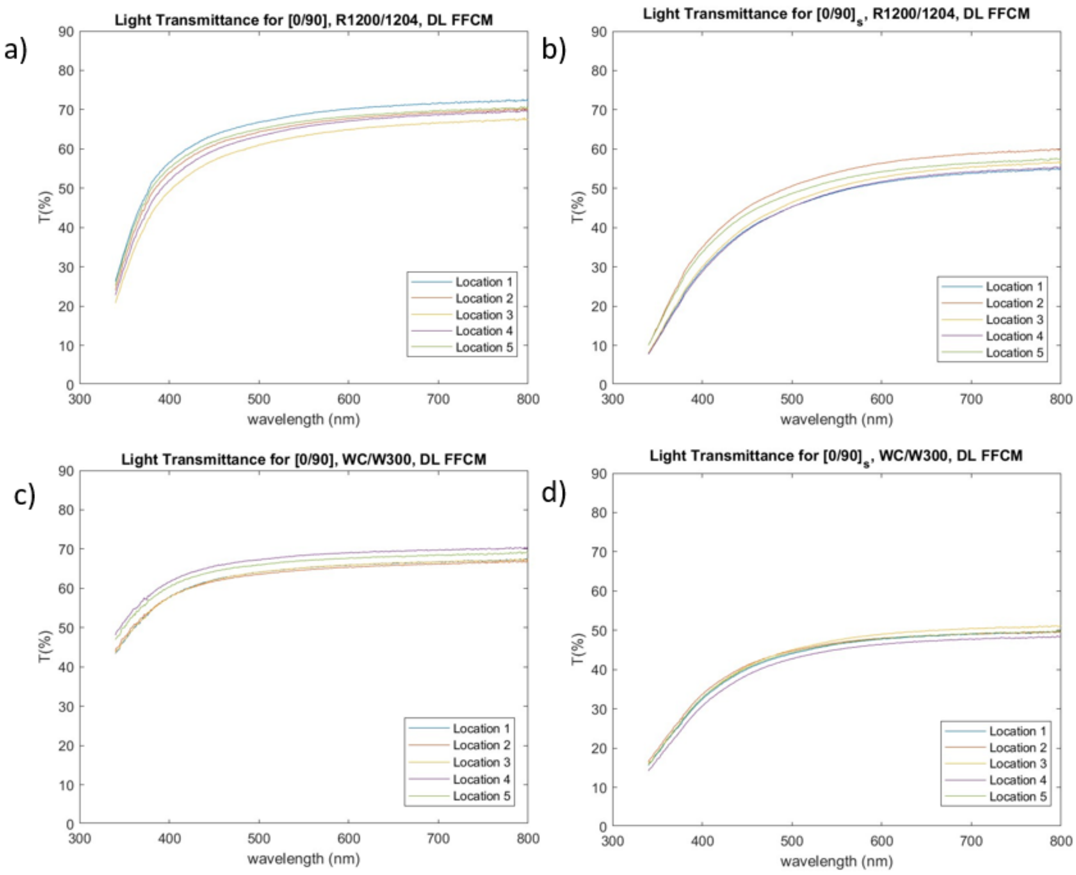

Figure D.2: Light Transmittance of the FFCMs which were presented in Figure D.1. All the composites have plain delignified flax fibers as reinforcement. a) $[0/90]$ FFCMs that have Resoltech 1200/1204 polymer system as a matrix, b) $[0/90]_s$ FFCMs that have Resoltech 1200/1204 epoxy casting polymer system as a matrix, c) $[0/90]$ FFCMs that have "Water-Clear"/W300 polymer system as a matrix, d) $[0/90]_s$ FFCMs that have "Water Clear"/W300 epoxy casting polymer system as a matrix.

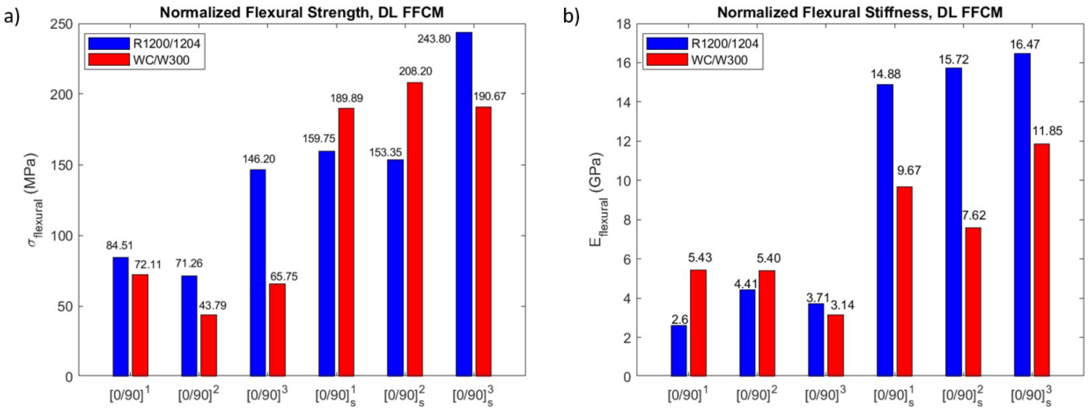

Figure D.3: Flexural properties of the materials produced with delignified flax fiber as reinforcement and the aforementioned polymers as matrix. a) Flexural strength b) Flexural stiffness.

D.2. Nitric Acid/Probe Sonication + Delignified Flax Fiber Reinforced Composites

Figure D.4 shows the treated $[0/90]$ and $[0/90]_s$ flax fiber reinforced composites with nitric acid and probe sonication treatment.

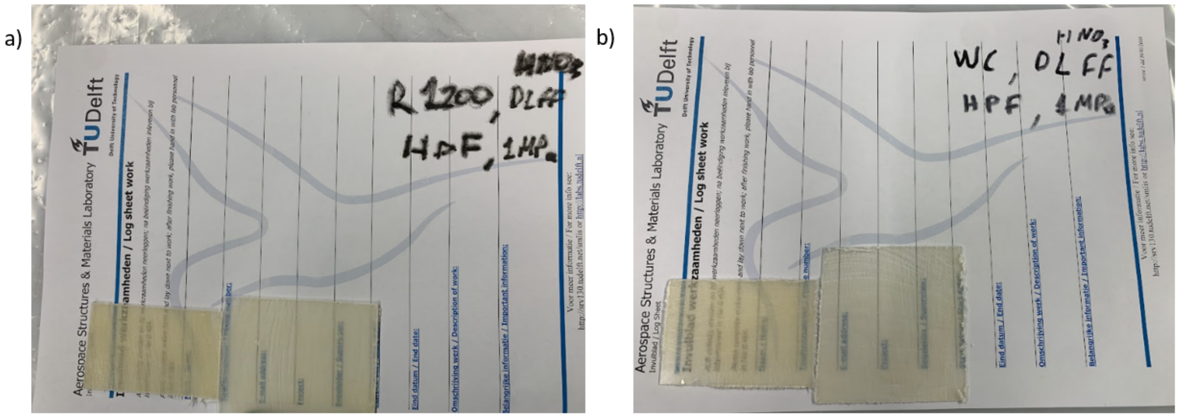

Figure D.4: Flax Fiber Reinforced Composite Materials. The flax fibers that are used are delignified flax fiber coupons which have been subjected to nitric acid and probe sonication treatment. In every sub-figure: Left: $[0/90]_s$, Right: $[0/90]$ a) Resoltech 1200/1204 as a resin with wet lamination/hot press forming, b) Water Clear/W300 epoxy casting resin system as a resin with wet lamination/hot press forming technique.

	Thickness (t) of sample in mm and maximum light transmittance in each location (T) in %			
Resin system	Resoltech 1200/1204	Resoltech 1200/1204	Water-Clear/W300	Water-Clear/W300
Reinforcement	HNO_3/Probe sonication DL Flax Fiber UD Coupon	HNO_3/Probe sonication DL Flax Fiber UD Coupon	HNO_3/Probe sonication DL Flax Fiber UD Coupon	HNO_3/Probe sonication DL Flax Fiber UD Coupon
Hot Press Forming	[0/90]	[0/90]$_s$	[0/90]	[0/90]$_s$
Thickness (mm)	0.83	1.10	0.86	1.17
Fiber Volume Fraction (%)	37.08	43.42	34.40	39.26
Location 1 (%)	72.01	54.77	70.36	55.50
Location 2 (%)	69.23	56.79	68.22	50.11
Location 3 (%)	75.32	57.46	67.46	57.43
Location 4 (%)	67.77	57.06	71.10	58.74
Location 5 (%)	69.89	57.14	69.33	58.72
Average	**70.84**	**56.65**	**69.29**	**56.10**
Standard Deviation	**2.93**	**1.07**	**1.49**	**3.60**

Table D.2: Thicknesses and maximum light transmittance in each of the five random locations for all the FFCM materials which were produced with HNO_3/probe sonication treated delignified flax fibers as reinforcement. The average value and standard deviation of maximum light transmittance for each sample are also depicted.

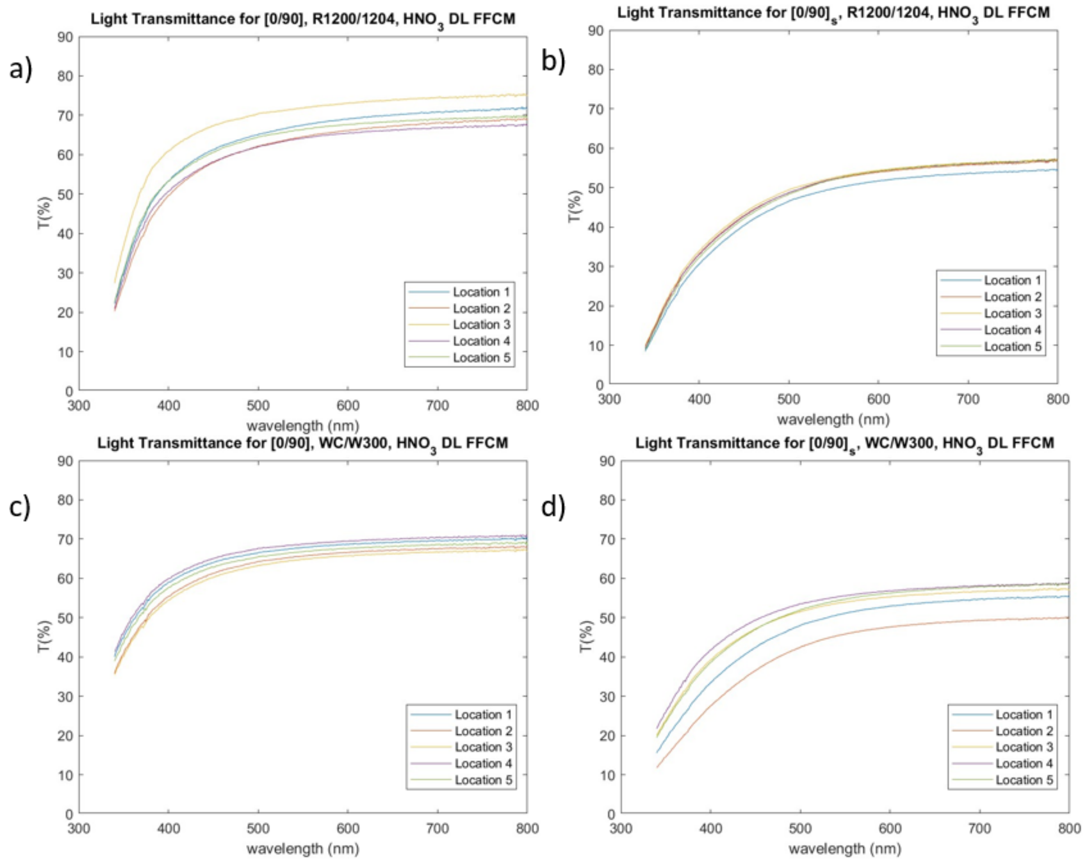

Figure D.5: Light Transmittance of the FFCMs which were presented in Figure D.4 All the composites have delignified flax fibers which were treated by HNO_3/probe sonication, as reinforcement. a) $[0/90]$ FFCMs that have Resoltech 1200/1204 polymer system as a matrix, b) $[0/90]_s$ FFCMs that have Resoltech 1200/1204 epoxy casting polymer system as a matrix, c) $[0/90]$ FFCMs that have ”Water-Clear”/W300 polymer system as a matrix, d) $[0/90]_s$ FFCMs that have ”Water Clear”/W300 epoxy casting polymer system as a matrix.

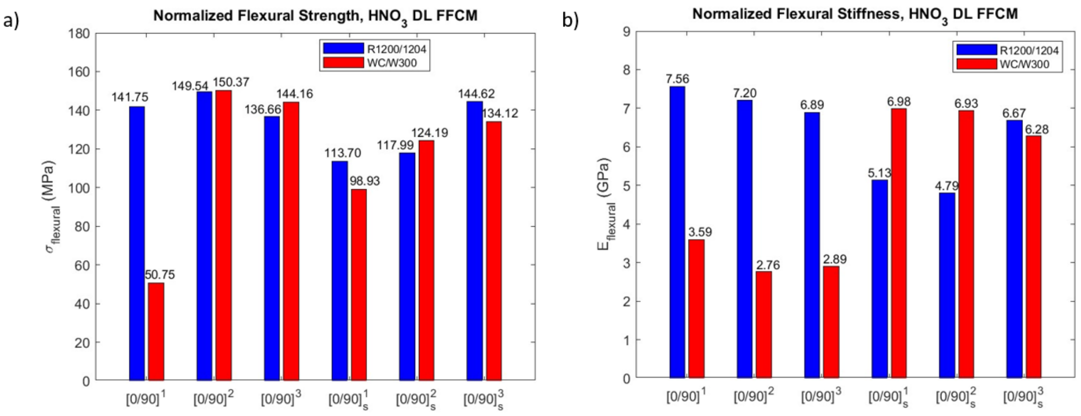

Figure D.6: Flexural properties of the materials produced with HNO_3/PB treated delignified flax fiber as reinforcement and the aforementioned polymers as matrix. a) Flexural strength b) Flexural stiffness.

D.3. NaOH/TEMPO Oxidation/Acetylation + Delignified Flax Fiber Reinforced Composites

Figure D.4 shows the treated $[0/90]$ and $[0/90]_s$ flax fiber reinforced composites with NaOH/TEMPO-oxidation/Acetylation.

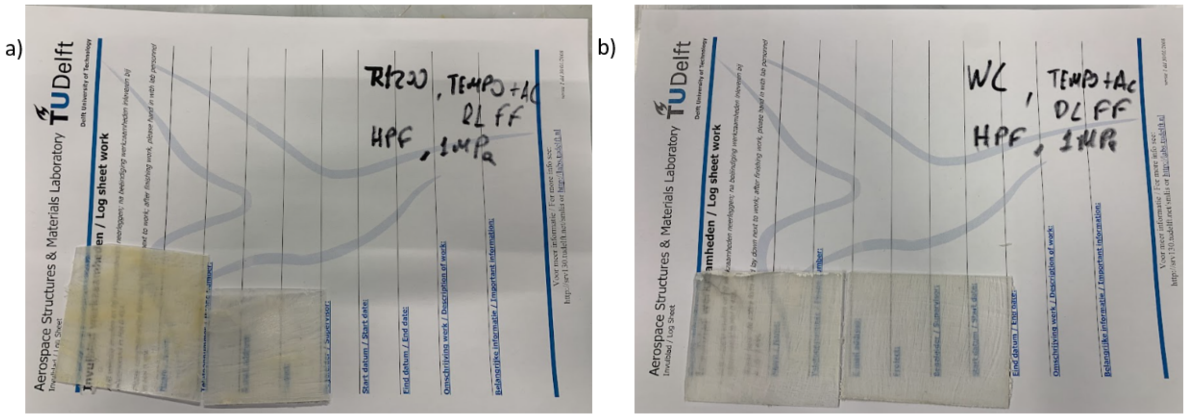

Figure D.7: Flax Fiber Reinforced Composite Materials. The flax fibers that are used are delignified flax fiber coupons which have been subjected to NaOH swelling, TEMPO oxidation, and acetylation. In every sub-figure: Left: $[0/90]_s$, Right: $[0/90]$ a) Resoltech 1200/1204 as a resin with wet lamination/hot press forming, b) Water Clear/W300 epoxy casting resin system as a resin with wet lamination/hot press forming technique.

	Thickness (t) of sample in mm and maximum light transmittance in each location (T) in %			
Resin system	**Resoltech 1200/1204**	**Resoltech 1200/1204**	**Water-Clear/W300**	**Water-Clear/W300**
Reinforcement	**TEMPO/Acetylation DL Flax Fiber UD Coupon**	**TEMPO/Acetylation DL Flax Fiber UD Coupon**	**TEMPO/Acetylation DL Flax Fiber UD Coupon**	**TEMPO/Acetylation DL Flax Fiber UD Coupon**
Hot Press Forming	[0/90]	[0/90]$_s$	[0/90]	[0/90]$_s$
Thickness (mm)	0.74	0.84	1.01	1.18
Fiber Volume Fraction (%)	36.89	42.44	40.42	32.52
Location 1 (%)	69.34	53.58	70.13	58.40
Location 2 (%)	67.24	63.19	69.74	58.35
Location 3 (%)	63.55	61.51	69.74	58.35
Location 4 (%)	61.68	55.23	69.65	59.88
Location 5 (%)	68.11	56.78	69.61	54.69
Average	**65.98**	**58.08**	**69.78**	**57.93**
Standard Deviation	**3.23**	**4.12**	**0.20**	**1.92**

Table D.3: Thicknesses and maximum light transmittance in the five random locations for all the FFCM materials which were produced with NaOH/TEMPO-oxidation/acetylation treated delignified flax fibers as reinforcement. The average value and standard deviation of maximum light transmittance are depicted.

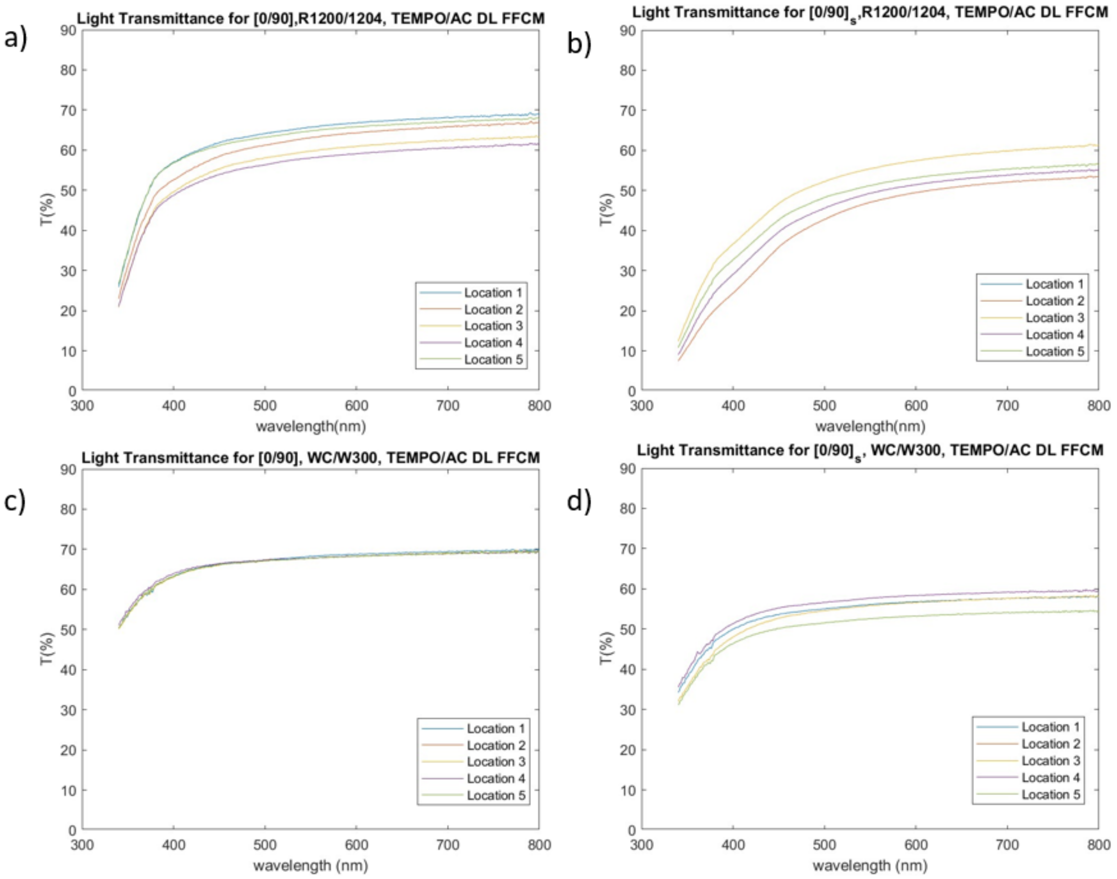

Figure D.8: Light Transmittance of the FFCMs which were presented in Figure D.7. All the composites have delignified flax fibers which were treated by NaOH swelling, TEMPO oxidation, and acetylation, as reinforcement. a) $[0/90]$ FFCMs that have Resoltech 1200/1204 polymer system as a matrix, b) $[0/90]_s$ FFCMs that have Resoltech 1200/1204 epoxy casting polymer system as a matrix, c) $[0/90]$ FFCMs that have ”Water-Clear”/W300 polymer system as a matrix, d) $[0/90]_s$ FFCMs that have ”Water Clear”/W300 epoxy casting polymer system as a matrix.

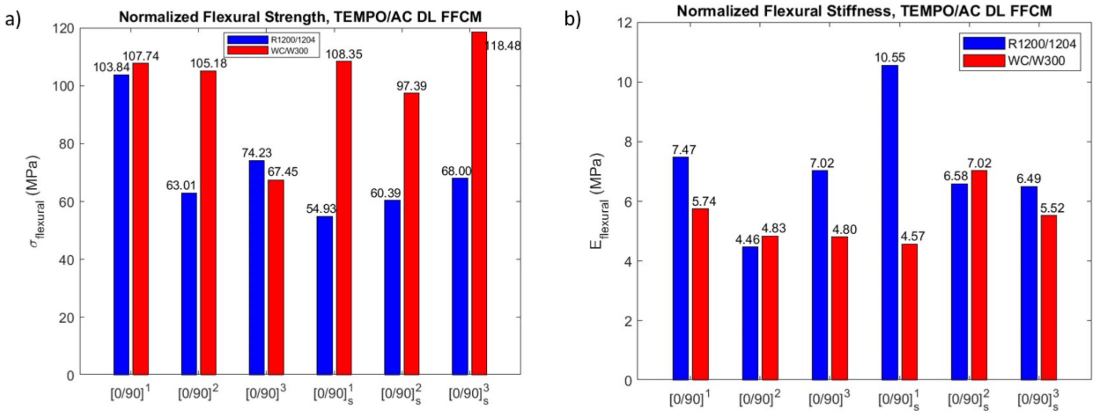

Figure D.9: Flexural properties of the materials produced with NaOH/TEMPO-oxidation/Acetylation treated delignified flax fiber as reinforcement and the aforementioned polymers as matrix. a) Flexural strength b) Flexural stiffness.